

24875532



This is to certify that the
dissertation entitled
Kinetics of Porcine Carotid Artery Brain Isoform
Creatine Kinase In Situ and In Vitro

presented by

Joseph F. Clark

has been accepted towards fulfillment
of the requirements for

Ph.D. degree in Physiology


Major professor

Date Jan. 9, 1990

PLACE IN RETURN BOX to remove this checkout from your record.
TO AVOID FINES return on or before date due.

DATE DUE	DATE DUE	DATE DUE
JUL 21 2005	_____	_____
JUL 03 2005	_____	_____
_____	_____	_____
_____	_____	_____
_____	_____	_____
_____	_____	_____
_____	_____	_____

MSU is An Affirmative Action/Equal Opportunity Institution

**KINETICS OF PORCINE CAROTID ARTERY BRAIN ISOFORM
CREATINE KINASE IN SITU AND IN VITRO**

By

Joseph Floyd Clark

A DISSERTATION

**Submitted to
Michigan State University
in partial fulfillment of the requirements
for the degree of**

DOCTOR OF PHILOSOPHY

Department of Physiology

1990

6051005

ABSTRACT

**KINETICS OF PORCINE CAROTID ARTERY BRAIN ISOFORM
CREATINE KINASE IN SITU AND IN VITRO**

By

Joseph Floyd Clark

This thesis contains two major parts. The first part consists of the development of a purification procedure for the BB isoenzyme of creatine kinase (CK) from porcine carotid arteries and determination of its kinetics in solution. The second part involves performing saturation transfer experiments on perfused carotid arteries to determine the kinetics of CK in the tissue.

The purification of BBCK was accomplished using the procedure described by Wang and Cushman for human brain. Using the Cardiotrac method from Corning the activity of CK was determined for the samples and isoenzyme fractionation. The purification produced 97% BBCK with less than 3% MMCK and no detectable MBCK. During the purification it was found that porcine carotid artery contains approximately a 1:1:1 activity ratio of the CK isoenzymes BB, MB, and MM. This isoenzyme ratio had not been reported in other smooth muscle tissues studied to date.

BBCK had an activity of 84 units per milligram of protein. SDS-PAGE electrophoresis showed one band demonstrating no significant protein impurities and a monomeric molecular weight of 42,500 Daltons for the BB isoenzyme.

Saturation transfer was done on resting, isolated porcine carotid arteries which were perfused with physiological salt solution with 0.1 mM Pi. ^{31}P NMR spectra were taken for all measurements. Exchange was observed between the phosphate peak of phosphocreatine and γATP . Results indicate (n=6), $k_f = 0.19 \pm 0.04$ and $k_r = 0.12 \pm 0.03$. These results were used to determine that the reaction was near equilibrium (0.71 ± 0.11 as compared to one for equilibrium) as determined by the net flux ratio (the ratio of forward and reverse flux). The ATPase rate was found to be significantly less than the CK rate.

I would like to dedicate this thesis to each and every member of my family. They have been my foundation, my strength, and support through all the long years it has taken for me to achieve this degree. To my mother and father who got me started and kept me going. It is by their example of hard work and dedication that I have been able to persevere and finally succeed. To my brother Jim, who is always there when I need him and always will be. To Kathy and Pete for always keeping me on my toes and a smile on my face. To Mommom and Poppop who have been there and always will be there with smiling faces and friendly advice. They are the people who have set the foundation for a strong family background and support. And to all my relatives who are all such a large part of my life, offering love and friendship and support. It is to my entire family network that I dedicate this thesis, because it is from their support and kindness that I have found the strength and pride to continue and to succeed. This work is just as much a product of their labor as it is a labor of mine, because without them, I would have been lost long ago. To all of you, thank you.

ACKNOWLEDGEMENTS

I'd like to take this opportunity to thank all of the people who have helped me through the years in preparing this thesis. I'd like to thank Dr. Dillon, my mentor and advisor, for his patience, understanding, and wealth of knowledge that I have gained from him. It is through his guidance and open-mindedness that has allowed me to grow and develop as a scientist. I would like to thank the members of my guidance committee for their assistance and expertise in the development of my thesis project and writing of my thesis. Thanks too, go to Dr. Gale Harris for his many hours of assistance in the development of the DANTE pulse sequence. I would like to thank Dr. Seth Hootman for his expert tutelage on electrophoresis and Dr. Steve Heidemann for the use and instruction of the densitometer. I would like to thank everyone at Banes Packing for their friendly and helpful services in obtaining the tissue samples from the hogs. Finally, I would like to thank Deborah Murphy for her moral support through all the trying times, and for her patience and understanding during the critical and emotional periods which she has endured with the preparation of this thesis. Also, I would like to express my deepest gratitude for her assistance in the typing and preparation of the thesis. I couldn't have done it without her.

TABLE OF CONTENTS

LIST OF TABLES	ix
LIST OF ABBREVIATIONS	xi
INTRODUCTION	1
Background and Rationale	1
Objectives	5
BACKGROUND AND LITERATURE REVIEW	8
Creatine Kinase Introduction	8
Phosphocreatine Background	9
Creatine Kinase	14
CK Background	14
CK Functional Background	18
Metabolic and Energetic Background for CK	20
CK Physical Characteristics	23
Creatine Kinase Shuttle	26
Physicochemical Action of PC and CK	31
Smooth Muscle Background	33
Skinned Smooth Muscle Studies	36
NMR And Creatine Kinase Background	37
NMR Background	39
DANTE Background	41
BBCK Clinical Background	43
Summary	45

METHODS	47
Tissue Collection	47
Pouring Chromatographic Column	47
Purification of BBCK	48
Electrophoresis Methods	53
Molecular Weight Determination	57
Isoenzyme Determination	57
Methods For Kinetic Activity In Solution	59
Determination of Solution Kinetics	60
Kinetic Calculations	61
NMR Methods	62
DANTE Methods	63
NMR solution Methods	68
Methods for T1 Collection	70
Calculation of T1 in the Absence of Exchange	74
NMR Kinetic Experiments	76
NMR Peak Integration	77
CST Methods	77
MST Methods	80
RESULTS	84
Purification Results	84
Solution Kinetics Results	97
NMR Results	112
CST Results	112
MST Results	116
DISCUSSION	126
Purification	126

Multiple Isoenzymes	127
CK Elution Profile	128
Electrophoresis	132
Possible Protein Impurities	132
Activity of the Purified BBCK	133
Solution Kinetics	135
CST Experiments	136
MST Experiments	137
DANTE Discussion	140
Rate Constant Introduction	142
Kinetics Summary	143
Conclusions	144
Future Directions	145
APPENDICIES	147
Appendix I	147
Appendix II	148
Appendix III	149
LIST OF REFERENCES	150

LIST OF TABLES

1.	CK Kinetics Comparison with β GPA	13
2.	Comparison of Kinetic Constants	17
3.	CK Tissue Activity Table	25
4.	Enzyme Purification Procedure	51
5.	Biorad High Molecular Weight Standard	55
6.	Delays for Progressive Saturation Experiments	72
7.	MST Saturation Protocol	82
8.	Purification Steps of BBCK	96
9.	Summary of Solution Kinetics	110
10.	Magnitization Changes from CST Experiments	113
11.	Rate Constants for CK Reaction Determined by CST Experiments	114
12.	Ratios of CST Results	115
13.	Kinetic Data from MST Experiments on Porcine Carotid Arteries	118

LIST OF FIGURES

1.	Creatine Phosphate Shuttle	27
2.	Electrical Analog Model	32
3.	Nuclear Spin	40
4.	Trajectories of Magnetization with DANTE	42
5.	Chromatographic Column	49
6.	Fluorometric Measurement of CK Control and Purified	86
7.	Fluorometric Measurement of CK Fraction from Homogenate	87
8.	Fluorometric Measurement of CK Ethanol Precipitation	88
9.	Elution Profile	90
10.	Electrophoresis Gel	93
11.	Densitometer Trace	95
12.	Progress of Reaction	99
13.	Kinetics Plots with PC Added	103
14.	Kinetics Plots with ATP Added	107
15.	T1 Experiment Graph	111
16.	CST Experiment Spectra Stack Plot	121
17.	MST Experiment Solution Control	123
18.	MST Experiment Spectra Stack Plot	124
19.	Creatine Loading	125

LIST OF ABBREVIATIONS

CK	creatine kinase
PC	phosphocreatine
ATP	adenosine triphosphate
ADP	adenosine diphosphate
AMP	adenosine monophosphate
MMCK	muscle CK homodimer
BBCK	brain CK homodimer
MBCK	muscle brain CK heterodimer
Cr	creatine
k_f	pseudo first order rate constant in forward direction
k_r	pseudo first order rate constant in reverse direction
CKM	muscle CK monomer
CKB	brain CK monomer
mito CK	mitochondrial CK
β GPA	β -guanidinopropionate
β GPAP	β -guanidinopropionate phosphate
FDNB	1-fluoro-2,4-dinitrobenzene
ATPase	adenosine triphosphatase
NMR	nuclear magnetic resonance
CST	conventional saturation transfer
MST	multisite saturation transfer
T1	spin lattice relaxation time

T₂	spin spin relaxation time
P_i	inorganic phosphate
γATP	gamma phosphate of ATP
M_z	magnetization along the Z axis
M_y	magnetization along the Y axis
M_x	magnetization along the X axis
M_{xy}	magnetization in the xy plane
M₀	magnetization along the Z axis of the magnetic field
B₀	local magnetic field strength
Hz	hertz
U	units (μ mole/min.)
DANTE	delays alternating with nutations for tailored excitation
PW	pulse width
CW	continuous wave
EDTA	ethylene diamine tetra-acetic acid
ME	2-mercapto ethanol
TA	tris acetate
tris	tris-(hydroxymethyl) amino methane
MOPS	3-[N-morpholino]propane sulfonic acid
MES	2-(N morpholino) ethane sulfonic acid
ETOH	ethanol
SDS-PAGE	sodium dodecyl sulfate polyacrylamide gel electrophoresis
TEMED	N,N,N',N',-tetramethylethylenediamine
TCA	tricarboxylic acid
G-6-P	glucose-6-phosphate
NADP	nicotinamide adenine dinucleotide phosphate
NADPH	nicotinamide adenine dinucleotide phosphate reduced form

BSA	bovine serum albumin
HPLC	high performance liquid chromatography
FID	free induction decay
PSS	physiological saline solution
D	daltons (atomic mass unit)
mM	milimoles per liter
M	moles per liter
TEA	triethanolamine
G6PDH	glucose-6-phosphate dehydrogenase

INTRODUCTION

Background and Rationale

Creatine kinase (CK) exists in four different forms; three cytosolic and one mitochondrial isoenzyme. The three cytosolic isoenzymes are dimers of the CKM and CKB monomers, producing MMCK, MBCK, and BBCK. The mitochondrial isoenzyme of CK is an octomer found on the outside of the inner mitochondrial membrane (56,70). The molecular weight of the cytosolic CK has a range of 80-85 kD in the dimeric form. Cytosolic MMCK is a homodimer composed of two CKM monomers and is found predominantly in skeletal muscle. BBCK is a homodimer composed of two CKB monomers and is found in brain and smooth muscle. MBCK is a heterodimer composed of a CKM and a CKB monomer. It is found predominantly in the heart.

CK catalyzes the reaction of:



The reaction going from phosphocreatine (PC) to ATP will be referred to in this thesis as the forward reaction. The reaction of ATP to PC will be referred to as the reverse reaction. It is via this reaction that CK has an important role in buffering the concentration of ATP in

the cell, by phosphorylating ADP with PC.

Studies by Walliman and Eppenberger (170,171,173) have shown that CK is bound to the myofibrils in the heart and skeletal muscle. This binding was predominantly at the M and Z lines of the myofibrils. They found that 5-10% of the activity of CK can be bound to the myofibrils of heart and skeletal muscle.

Studies by Ventura-Clapier et al have determined that CK may play a role in the contractility of skinned heart myofibrils (161,162,163, 164,165). In the skinned heart myofibrils they found that CK can be rinsed off the myofibrils and that the rinsing of CK from the myofibrils is accompanied by a decrease in contractility. They defined this decrease in contractility as a decrease in twitch tension associated with an increase in rest tension. The increase in rest tension is reported to be caused by an increase in the number of rigor bridges. They have also found that after rinsing CK off, it can be reapplied to the myofibrils with a significant return of function. The return of function is seen as an increase in twitch tension and decrease in rest tension. Their conclusion from these studies is that CK plays a significant role in maintaining the normal contractile function of the heart myofibrils.

In studies performed by Seradarian et al, cultured heart muscle cells incubated with exogenous creatine have an increase in PC content (138,139,140,141,142). They also found that the increase in PC content is significantly less if oxidative phosphorylation is

inhibited by addition of oligomycin. Conversely, increased ATP concentration is seen if cultured heart muscle is incubated with adenosine. This increase in ATP was significantly less if CK was inhibited by the addition of FDNB. Their conclusion from these studies was that PC synthesis is linked to oxidative phosphorylation and that ATP synthesis is linked to the activity of CK.

Clinically CK is used as a diagnostic indicator of heart attack, stroke, trauma, ischemia and muscular dystrophy (3,50,66,147). The cytosolic CK is released from the tissue via an unknown mechanism and is found, with kinetic activity, in the blood stream of patients. Jacobus et al have found a decrease in activity for the heart mitochondrial CK during ischemia (68). It has not yet been determined what, if any, correlation there is between the release of cytosolic CK and a decrease in mitochondrial CK activity.

Cytosolic CK released into the blood stream may be due to some controlled release or a general permeabilization of the membrane to allow the leakage of cellular contents. When CK is found in the blood stream however, other cell products are not always found (178). On the other hand, ischemia associated with a heart attack generally produces cell death and is associated with significant increase in serum CK activity (124,125). Thus there is conflicting evidence on the possibility of leakage of cellular contents producing the rise in serum CK activity as well as experimental evidence refuting that claim. The mechanism or stimuli for CK release from tissue is not known and is an area of active study.

The role of the mitochondrial CK (found on the outside of the inner mitochondrial membrane) is to synthesize PC from ATP which has been produced by oxidative phosphorylation. PC is then hypothesized to diffuse out of the mitochondria and across the cytoplasm to sites of ATP hydrolysis and buffer the ATP concentration in the cytoplasm via cytosolic CK. After donating its phosphate to ATP, creatine then will diffuse back to the mitochondria to get rephosphorylated by mitochondrial CK from ATP (8,9). Jacobus and Saks have found that when coupled to oxidative phosphorylation, mitochondrial CK has an increased affinity for the $ATP \cdot E \cdot Cr$ complex of up to 10 fold (69). They conclude that this increased affinity may increase the propensity for the release of PC which will then diffuse to other sites in the cell to help buffer the ATP concentration. This communication of PC between the mitochondria and the myofilaments is referred to as the creatine phosphate shuttle. The creatine phosphate shuttle hypothesis is supported by Bessman et al (9) but is ascribed to a physical-chemical mechanism by Meyer et al (96,97). These differences are discussed in greater detail in the Background Section of this thesis. However, when addressing the energetics of a cell the creatine phosphate shuttle and possible subcellular localization of cytosolic CK (which may be independent processes) are important considerations.

Mitochondrial CK is found in varying amounts in tissues depending upon the mitochondrial content and oxidative capacity of the tissue. Iyengar et al have hypothesized that the total PC concentration is proportional to the total CK activity in the tissue (64,65). The dialogue between mitochondrial CK and cytosolic CK has drawn much

attention in the heart and skeletal muscle but is poorly studied in vascular smooth muscle due to the very low mitochondrial content of vascular smooth muscle and reduced diffusion distance due to a relatively small cell diameter.

The conclusion to be drawn from the discussion above is that CK plays a significant role in the buffering of the ATP concentration in the cell as demonstrated by studies in the heart and skeletal muscle. CK is also important in the contractility of the tissue, and as a clinical diagnostic indicator. The studies discussed above have focused predominantly on the skeletal and heart muscle and thus on the MM and MB cytosolic isoenzymes of CK. To date, there are few studies of BBCK and its role in the buffering of ATP in smooth muscle or its role in contractility or other normative functions of the smooth muscle tissue. The question being asked in this thesis is what are the kinetics of porcine carotid artery CK *in situ* and BBCK *in vitro*. This question can be addressed by determining the kinetics of CK in the porcine carotid artery under resting conditions, to purify BBCK from the carotid artery, and to characterize that purified CK to determine its kinetics. This study will further the knowledge and understanding of CK and vascular smooth muscle energetics which have been sparse compared to those of heart and skeletal muscle.

Objectives

The questions being asked in this thesis are: what are the kinetics of CK observable in the porcine carotid artery, using the NMR

technique of saturation transfer, and what are they for BBCK which has been purified from porcine carotid artery? To be able to answer these questions, several objectives must be obtained. First, BBCK must be purified from the porcine carotid artery. Second, the purified BBCK must be characterized to obtain the enzyme kinetics. Third, the CK kinetics of the porcine carotid artery must be determined in the NMR using saturation transfer.

Objective 1. To be able to study the kinetics of an enzyme it should be isolated to an adequate degree of purity for the studies to be performed. The first objective of this thesis is to purify the representative CK from porcine carotid artery. BBCK was assumed to be the predominant form of CK in smooth muscle; thus the purification procedure used in this thesis utilizes a technique for isolating the BBCK from the porcine carotid artery.

Objective 2. After purification of the enzyme, the kinetics are measured in solution focusing on the NMR visible substrates of PC and ATP. The kinetics are measured under steady state, pseudo-first order conditions to determine K_m and V_{max} .

Objective 3. NMR saturation transfer is performed to determine the kinetics of the CK reaction in the tissue. Saturation transfer can determine the pseudo first order rate constant of the NMR visible nuclei undergoing exchange. This assumes that all of the measurable ATP and PC are available for the CK reaction. Conversely, if metabolites are sequestered around or away from exchange sites (e.g.,

shuttling between mitochondria and myofilaments) errors in calculating the pseudo first order rate constants may occur.

Each of the objectives above are designed to provide information regarding the physiology and/or biochemistry of vascular smooth muscle CK. The purification and characterization of BBCK from vascular smooth muscle has not been reported prior to this thesis. These are the focus of Objectives One and Two. There have been few reports on the kinetics of CK in smooth muscle using NMR saturation transfer, and none using vascular smooth muscle. This is the focus of Objective Three. The results of these three objectives will contribute to a better understanding of BBCK in vascular smooth muscle.

BACKGROUND AND LITERATURE REVIEW

Creatine Kinase Introduction

Creatine kinase kinetics have been studied extensively in solution over the years (102,107,108,109). Creatine kinase catalyzes the reaction:



The reaction of PC to ATP will be referred to as forward and ATP to PC as reverse. PC participates in no other known reactions and can only make ATP from ADP, and thus is considered an ATP buffer (28,169). When a tissue (e.g., skeletal or cardiac muscle) is stimulated, PC falls first to very low levels before ATP begins to fall (98,120, 122,146). Qualitatively, the same phenomenon is observed in smooth muscle but is poorly understood due to the limited extent of study (20,63,114). CK is found in many tissues (31,37,64,71,85,95,118, 122,155,158,175). It exists in four forms: BB, MM, MB and mitochondrial. BB is CK found in brain. MM is CK found in skeletal muscle. MB is CK found in the heart. Porcine carotid arteries, like other smooth muscles, contains a large BB isoform concentration (174). The MM, MB, and BB isoenzymes are found in the cell cytosol. They are dimers with a molecular weight between 80 and 85 kD. The

mitochondrial CK is an octomer found on the outside of the inner mitochondrial membrane. In general, the specific activity of CK in heart and skeletal muscle is greater than in smooth muscle or brain (31,65,172,179).

Phosphocreatine Background

Phosphocreatine (PC) is intimately involved in energy metabolism (96,98) and contains a phosphate with a high free energy of hydrolysis (84,108). It is present in mammalian cells and in amphibians (30). Arginine phosphate is found in lower life forms and is considered PC's evolutionary precursor (1,2,30). Arginine kinase also has a 10 fold lower activity than CK (98). PC was once thought to be the energy source for muscle contraction (67). Later studies (22) found that ATP was the true energy currency for the muscle contraction.

The role of PC was found to be as a buffer for ATP. As ATP is used to supply energy for muscle contraction and other cell functions, PC is used to rephosphorylate ADP to ATP. This reaction is accomplished enzymatically by creatine kinase. As discussed above, creatine kinase (CK) catalyzes the reaction:



PC is not known to be involved in any other reactions except

degradation to creatinine. This degradation is a constant non-enzymatic conversion of PC to creatinine, and is not considered to significantly effect the kinetics of PC to ATP (145,169).

The buffering of ATP via the CK reaction has been demonstrated by several researchers using various techniques (14,19,22,38,48,64,77,97, 131,132,141,146,162,179). Both solution techniques and NMR have been employed to examine CK kinetics. CK buffering has been demonstrated by substituting PC with analogs like β -guanidinopropionate phosphate (β GPAP) (26,40,41,42,43). The buffering of ATP by CK has been observed *in vivo* as well as in cell cultures (138,139,140,141). Several of these techniques will be discussed in greater detail below.

Cain and Davies (22) first demonstrated the buffering of ATP by PC by inhibiting CK with 1-fluoro-2,4-dinitrobenzene (FDNB). When the CK in muscles was inhibited the muscle failed to contract after 3 to 4 twitches. Meyer (96) described the CK system as having energy storage capacitance for rat skeletal muscle. This capacitance was described as being directly proportional to the total creatine level.

Fisher and Dillon (38) used NMR to measure the high energy phosphate in porcine carotid artery. They found that during hypoxia PC decreased to 16% of control while ATP only decreased to 81% of control. Initial changes in PC concentration is seen well before the change in ATP concentration.

As the above studies have determined, PC serves as an energy

reservoir in muscle. In an effort to identify biochemical and pathological changes due to deficiencies in either of these compounds, Fitch (26,40,41,42,43) has fed rats a creatine analog β -guanidinopropionate. It has been shown that β -guanidinopropionate (β GPA) will competitively compete with creatine for entry into skeletal muscle (43). As the β GPA is taken into the skeletal muscle it will get phosphorylated to β -guanidinopropionate phosphate (β GPAP) by CK. This process of uptake and phosphorylation produces a decrease in cell creatine concentration from 15 to 8 μ moles/g as well as a decrease in cell PC from 22.5 to 1.6 μ moles/g (63). In these experiments the rats are fed a diet of 1% β GPA for 6 weeks. It was also found that the β GPA diet will produce a decrease in ATP and glucose-6-phosphate concentrations of 6.77 to 3.22 and 0.74 to 0.34 μ moles/g respectively.

It might be predicted that β GPAP would have the same high energy phosphate bond as PC and be used as a source of energy in the muscle. However, β GPAP does not behave as efficiently as PC to buffer the concentration of ATP. From *in vitro* studies on skeletal muscle CK, β GPAP has a V_{max} which is 0.18% of PC (26). The low affinity of CK for β GPAP seen *in vitro* supports observations, *in vivo*, of decreased tension and rapid fall in tension for rat skeletal muscle which was loaded with β GPAP (40). Meyer et al (96a) found in β GPA fed rats that force did not decline with stimulation. They report that PC is not essential for energy production under steady-state conditions but that Pi from PC hydrolysis may be important for maximally activating glycolysis and/or glycogenolysis.

Pathological changes have also been seen in β GPA fed animals such as retarded growth, abnormal muscle contractions and a decrease in the size of white skeletal muscle fibers (26,40). The physiological implications (if any) of these pathological changes have not been determined.

β GPA as a creatine analog can thus be used to effectively substitute β GPAP for PC in the cell. However, β GPAP cannot be used by the cell to buffer ATP as efficiently as PC because CK has a much lower V_{\max} for β GPAP. Also, the K_m for β GPAP is lower than PC further compromising CK efficiency. (see Table 1) (26).

TABLE 1

CK KINETICS COMPARISON WITH β GPA

substrate	K_m^*	V_{max}^*
β GPA	50 mM	0.21 μ M/min/mg
β GPAP	4.9	0.22
Cr	16.7	75.1
PC	2.2	231

*Ref. Chevali and Fitch 1979, (26) experiments done with rabbit skeletal muscle MMCK.

As can be seen in Table 1, CK favors the hydrolysis of PC and would not be able to utilize β GPAP as an effective substitute for PC. Thus β GPAP cannot buffer the ATP concentration as efficiently as PC. When PC is replaced with β GPAP the muscle fatigues quickly as well as demonstrates a decrease in twitch tension. Conclusions drawn from β GPAP data should be analyzed carefully because a finite amount of buffering will still be available via the residual PC in the cells as well as slow transfer from the β GPAP.

Creatine Kinase

CK Background

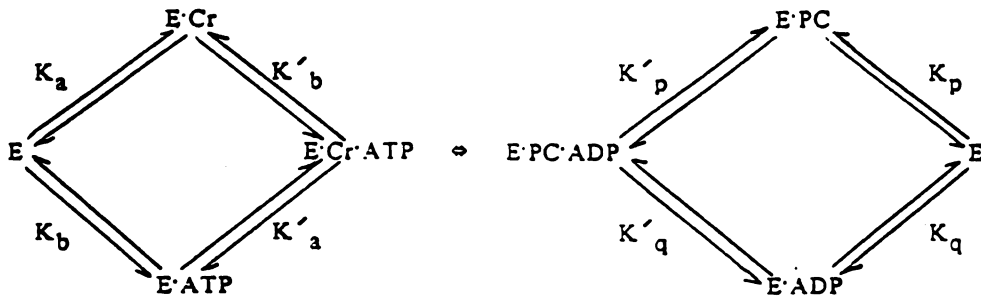
Phosphocreatine is made by the phosphorylation of creatine by creatine kinase using up 1 mole of ATP per mole of PC produced. This reaction also produces one proton. Therefore, the reaction can be written:



In mammals this reaction is catalyzed by the enzyme creatine kinase. CK exists as one of four isoenzymes. The form of CK found in the mitochondria is an octomer on the outside of the inner mitochondrial membrane of all tissues containing the CK system (69,89,129) and is referred to as mitochondrial CK. The other three isoforms are dimers. The BB isoenzyme is a homodimer of two CKB monomers. The BBCK form is the isoform found in brain (52,53,88,174). There is also an MM isoenzyme. This is a homodimer of the CKM monomer. The MM isoenzyme is the major form of CK found in skeletal muscle. There are small amounts of BB and MB present in the skeletal muscle of humans. BB and MB are also found in larger amounts early in skeletal muscle development (71,154). The MBCK isoenzyme is a heterodimer of the M and B monomers. This isoenzyme is found predominantly in the heart muscle. The two other cytosolic isoenzymes are also

present in the heart (71).

Chegwidden and Watts (25) compared the kinetic constants of CK from various sources and species. They found that the kinetics of CK varied from species to species and tissue to tissue (see Table 2).



Kinetic formula for two substrates, two products, on enzyme kinetics model discussed by Chegwiddden (25). In this model K_a is the binding of creatine (Cr) to CK (E), K_b is the binding of ATP to E, K'_b is the binding of ATP to the E·Cr complex, K'_a is the binding of Cr to the E·ATP complex, K'_p is the binding of ADP to the E·PC complex, K'_q is the binding of PC to the E·ADP complex, K_p is the binding of PC to E and K_q is the binding of ADP to E. Using this model, Chegwiddden examined the details of the enzyme substrate and enzyme product interactions of CK from various sources (Table 2).

TABLE 2

Comparison of Kinetic Constants

Reaction	Kinetic Constant	Monkey Skeletal Muscle	Calf Skeletal Muscle	Rabbit Skeletal Muscle	Calf Brain	Calf Smooth Muscle
*Cr+E	K_a	154	53	15.6	29	2.20
ATP+E	K_b	1.79	0.97	1.2	0.93	0.75
Cr+E • ATP	K'_a	12.75	21	6.1	3.7	0.58
ATP+E • Cr	K'_b	0.147	0.78	0.48	0.13	0.20
E+PC	K_p	16.7	45	8.6	20	ND [#]
E+ADP	K_g	0.177	0.17	0.17	0.12	ND
E • ADP+PC	K'_p	3.5	23	2.9	2.0	ND
E • PC+ADP	K'_g	0.039	0.094	0.05	0.01	ND

*Cr: Creatine

[#]ND: Not Determined

Ref. #25

From the data presented in Table 2 it can be seen that the CK kinetics from different species vary. There are also differences in the kinetics of BBCK from calf depending upon whether the isoenzyme is from brain or smooth muscle. These data appear to support the hypothesis of Vaidya (158) in which the CK is modified post

translationally depending upon the tissue or species which they believe may alter the role of the CK.

Focant (44,45,46) examined CK from smooth muscle. Smooth muscle BBCK had differing amino acid content, differing kinetics, and differing physical characteristics than the BBCK from the brain. It was demonstrated that the ox stomach BBCK had a molecular weight of 83,500 Daltons while the ox brain had a molecular weight of 80,000 Daltons (44). However, an examination of the amino acid content demonstrated that the differences between the two enzymes could not be simply explained by post translation modification of the protein. In another study (46) it was found that the kinetics of the smooth muscle BBCK was significantly different than the brain BBCK.

CK Functional Background

As mentioned in the Rationale Section, Wallimann found CK bound to the M line of myofibrils, while Ventura-Clapier et al (160,162,163) found that a large part of the MBCK activity is reversibly bound to heart myofibrils. Their results suggest that there are specific binding sites of CK in the myofibrils other than at the M line. These binding sites may have a lower affinity and thus may have been rinsed off the myofibrils during Wallimann's experiments. However, these experiments were not able to localize the binding sites in the myofilaments. In similar experiments using chicken heart, Ventura-Clapier et al found that the MM isoenzyme will also reversibly bind to the myofilaments (163). The heart is the only tissue where MBCK is

found in any significant quantities. The ratio in the heart of MM and MB can vary from species to species (154) (Table 3). The role of the various CK isoenzymes or their localization is not known.

Vaidya et al (158) determined that human heart contained 5 variants of the MM isoenzyme. This was accomplished by use of isoelectric focusing to determine the individual pI's of MMCK. Five variants with five distinct isoelectric points were found in the human heart. They also described different kinetic activities and attributed these observations to post translational modification of the MMCK.

Mechanical and chemical skinning techniques have been employed to evaluate the binding and activity of CK in the heart (94,132,159,160, 162). These studies showed that the relaxation of rigor tension in skinned heart muscle fiber was intimately dependent upon the kinetic activity of CK. Ventura-Clapier et al (162) demonstrated that in the absence of ATP, at high (12mM) PC and low (250 μ M) MgADP, the relaxation of skinned papillary muscle could be maintained in the presence of active CK. In the absence of CK, rigor tension would develop under identical conditions. Ventura-Clapier (163) also found that the addition of CK will relax rigor tension in myocardial tissue. These results demonstrate that CK plays a role in the mechanical properties of heart muscle by providing ATP as well as removing ADP from the active site of actomyosin ATPase and thus effecting the mechanics.

Metabolic and Energetic Background for CK

Seraydarian (138,140) has examined the correlation between PC and muscle function using cultured neonatal rat heart. It was found that muscle fatigue in frog sartorius correlated with a fall in PC while no significant fall in ATP concentration occurred. A concomitant rise in Pi is observed with the fall in PC. The increased Pi lowers the free energy of ATP hydrolysis within the cell. It is believed that this lower free energy contributes to the decrease in muscle tension. Increasing creatine in the medium produced an increase in PC. However, the increased PC was not maintained if the inhibitor of oxidative phosphorylation, oligomycin, was added to the incubation medium (141,142). These data suggest that creatine stimulated PC synthesis is dependent upon oxidative phosphorylation.

Seraydarian et al (139) increased ATP concentration by incubating heart culture cells in 50 μ M adenosine and also observed an increase in the rate of spontaneous contractions. The PC concentration, however, remained unchanged. The concomitant increase in ATP concentration with the increase in contraction rate was considered evidence that membrane excitability and intracellular ATP are correlated in the cultured heart cell. The addition of FDNB, the inhibitor of CK, prevented the net synthesis of ATP in the presence of adenosine. These results suggest a possible role of CK in the increase of the ATP concentration in the presence of adenosine.

Bessman (8,10) used labeled Pi to study mitochondrial CK. It was

found that if ^{32}P labeled Pi was added to mitochondrial suspensions, the Pi was preferentially incorporated into PC. They found that the specific activity of mitochondrial CK was less than the specific activity of the labeled γ phosphate of the total pool of ATP. ATP generated by mitochondria was not labeled and must have been used to produce the unlabeled fraction of the PC. It was suggested from these data that oxidative phosphorylation supplies ATP to CK in the mitochondria without the ATP mixing with the extra mitochondrial pool of ATP.

In a parallel set of experiments, Bessman inhibited ATPase and ATPsynthase activity with carbonylcyanide chlorophenylhydrazone and atractyloside respectively and used exogenous ^{32}P labeled γATP to observe the exchange of ^{32}P from ATP to form PC. Quantitatively there was a decrease in PC formation and all the PC formed was from exogenous ATP. Bessman concluded from these studies that mitochondrial compartmentation of CK allows the formation of significantly more PC in the presence of oxidative phosphorylation than the bound CK can produce in the presence of exogenous ATP alone.

Jacobus and Saks (68,69) described the coupling of mitochondrial CK to oxidative phosphorylation. This study demonstrated that when mitochondrial CK is coupled to oxidative phosphorylation the dissociation constant of MgATP for CK decreased 10 fold for the ternary complex, $\text{E} \cdot \text{MgATP} \cdot \text{creatine}$. Thus, oxidative phosphorylation increases the apparent stability of the $\text{E} \cdot \text{MgATP} \cdot \text{creatine}$ complex and will decrease the release of MgATP into the cellular medium and

concomitantly increase the release of PC into the cellular medium.

Iyengar (64) describes a general correlation between the amount of CK activity in a tissue to the PC content in the brain and skeletal muscle. Fisher and Dillon (38,39) found 0.5 mM PC in porcine carotid artery. This is much less than the 15 mM PC (14) found in heart muscle. Lang found human carotid artery to contain less than 1% of the heart CK activity. In spite of this relatively low concentration of PC and CK activity, the porcine carotid artery is able to maintain sustained contraction and efficiently buffer its ATP concentration (4,11,20,39,104,167).

Reiss and Kaye (123) described an increase in uterus CK induced by estrogen treatment. Estrogen will subsequently increase the phosphogen content in the uterus as well as other well established anabolic effects. This lends support to Iyengar's finding of a relationship between CK content and PC concentration.

As can be seen in Table 3, smooth muscle predominantly contains the isoenzyme BBCK (64,65,71,154). The purified BBCK generally has lower activity than the MM and MB forms (64,66,83). NMR experiments done with bullfrog stomach muscle (179) showed CK to have a forward rate constant of 0.16 s^{-1} . This value is about half the 0.3 s^{-1} that Ugurbil (155,157) found in the rat heart. Carotid arteries contain approximately 0.5-1% the cytosolic CK activity that heart contains (71,88,154). There is also a lower PC concentration (38,86). It might be expected from these observations that the smooth muscle would

not exhibit good buffering capacity for ATP. However, it has been demonstrated that smooth muscle can buffer its ATP concentration similar to the buffering found in other muscles (4,11,20,38,39,86, 104,167).

CK Physical Characteristics

Grossman (52) used monkey brain to purify BBCK and described conformational modifications in the enzyme using fluorescence and fluorescence polarization. Polarization changes of labeled BBCK due to ADP binding were measured to determine structural distances and conformation. Grossman's experiments found a propensity for conformational changes and concluded that the brain BBCK is a more flexible protein than muscle CK. Also it was observed that the active site is more open than the muscle CK and that the binding of ADP produces a more compact CK. This more compact CK changes the conformation of BBCK such that it resembles muscle CK, and from these data conformational modification was implicated in the regulation of monkey brain BBCK (52). In this way, the neurobiochemical role of BBCK was thought to be distinct from the metabolic functions of muscle CK.

Grossman (53) suggested isoenzyme specific compartmentation which could be the result of different subunit arrangements. In these experiments rabbit brain and skeletal muscle was used to isolate the BB and MM isoenzymes respectively. These two homodimers were used to produce the MB heterodimer. In this study the energy transfer from one subunit to the next subunit between the reactive thiols of MMCK

was measured. The reactive thiols were found to be separated by a distance of 48.6-60.4 Å, such that energy transfer between thiols had a low efficiency. The heterodimers were found to have a shorter site-site distance of 27-52 Å. It was this difference in active site distance and energy transfer between the two isoenzymes which led to the suggestion of isoenzyme compartmentation. The difference in the conformation of the two isoenzymes, suggested by the observed difference in active site distance, might explain the lack of binding of the MB form to the M line.

As discussed above there are different isoenzymes of CK and differences within isoenzymes. Several studies have identified multiple variants of the MM isoenzyme (36,149,150,151,158). It was found that skeletal muscle has multiple forms of MMCK and that these forms have differing pIs. The different isoenzymes also demonstrated differing kinetics. Such heterogeneities within the isoenzymes of CK was attributed to post translational modification (158), but it is unclear if these physical characteristics have physiological significance.

Table 3

CK TISSUE ACTIVITY TABLE

<u>Tissue Sample</u>	<u>U/g</u>	<u>%MMCK</u>	<u>%MBCK</u>	<u>%BBCK</u>	<u>Ref.#</u>
Skeletal Muscle	3281	100			154
	860	96	3	1	71
Tongue	225	90	5	5	71
Diaphragm	140	94	4	2	71
Heart	800	52	46		88
Right Atrium	402	78	22		154
Brain					
Cerebrum	90			100	88
Cerebellum	87			100	88
Hypophysis	11			100	88
Spinal Cord	27			100	88
Stomach	23	3	6	91	71
Gastrointestinal Tract	140		3	97	88
Colon	125	4		96	154
Ileum	161	3	1	96	154
Bladder	35	2-7	3-5	89-93	71
Aorta	1	39	7	54	71
Carotid	2	56	2	42	88

Creatine Kinase Shuttle

A transport mechanism has been proposed by which PC from the mitochondria is transported to the cytoplasm (8,9,10,94,98,133). The method by which PC is transported from the mitochondria to energy utilizing structures in the cell has been referred to as the PC shuttle. The PC shuttle hypothesis is not, however, universally accepted. A discussion of the literature regarding the shuttle hypothesis should be examined with attention to the controversy involved with this proposed shuttle mechanism. However, due to the nature of this thesis consideration of the experimental observations and theories pertinent to the PC shuttle hypothesis is warranted and will be discussed.

In muscle cells, as well as many other cells, the PC synthesized by mitochondrial CK is utilized by the cytosolic CK elsewhere in the cell (e.g., myofilaments). The mechanism by which PC gets to the myofilaments is called the phosphocreatine shuttle. This shuttle also may act to signal an energy demand as well as delivering energy to the organelles as PC. The phosphocreatine shuttle acts as an intercommunication process to signal demand for energy and the transport of energy produced as a response to that signal to the sites utilizing

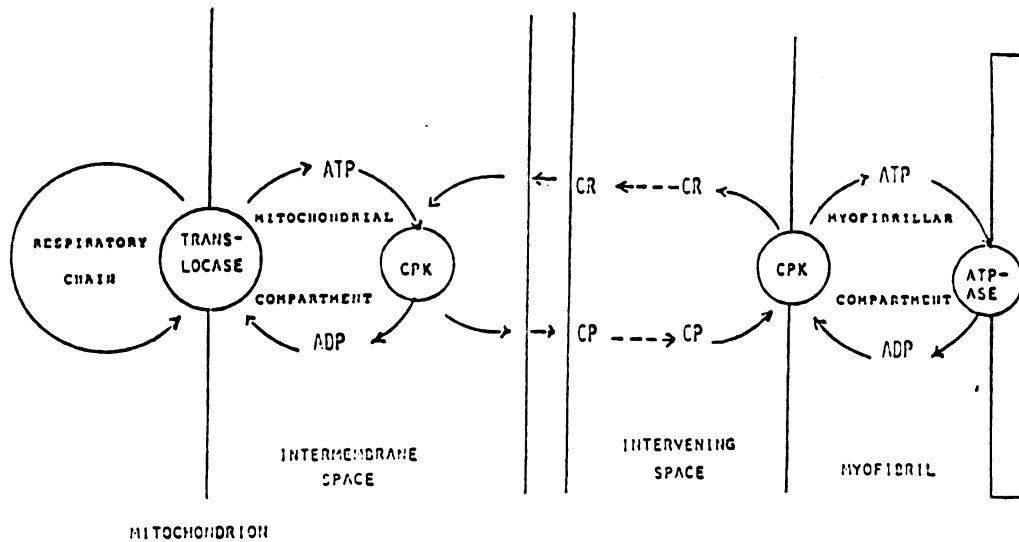


Figure 1. Creatine phosphate shuttle showing the site of synthesis at the inner mitochondrial membrane. CK resides on the outer surface of the inner mitochondrial membrane. The intervening space is the space within the cell between the mitochondria and the myofilaments. At the myofilaments, the CK is depicted as being bound to the A band of the myofibril. In this model the mitochondrial energy is transported as phosphocreatine (Bessman). CPK: creatine phosphate, CP: phosphocreatine.

energy (10,112,133,152). ADP could be the signal for energy demand, but Jacobus and Saks (69) determined that creatine as a signal for energy demand would have a parallel effect as that of ADP to signal energy demand (Figure 1).

During the contraction of a muscle, ATP is hydrolyzed and ADP is produced by CK phosphorylating ADP with PC, producing creatine. Creatine can then act at the mitochondria to stimulate oxidative phosphorylation (69,70, 129). This production of creatine, concomitant with ADP, occurs at or near the site of contraction. The creatine has its signaling action at the mitochondria. Therefore the creatine must diffuse or be transported away from the myofibrils to the mitochondria. Meyer (98) determined that simple diffusion of the metabolites is an adequate mechanism for transport within cells.

Creatine at the mitochondria gets phosphorylated by mitochondrial CK using ATP synthesized via oxidative phosphorylation (69). ATP donates its gamma phosphate and ADP is produced. ADP production is an immediate control stimulus at the mitochondria for respiration to produce more ATP (10,127).

PC leaves the mitochondria and diffuses towards the myofilaments (69,98,127). The net flux of creatine is in the reverse direction. PC arrives at the myofilaments as a carrier of energy from the mitochondria. This energy is transferred from PC to ADP via

cytoplasmic CK to produce ATP and creatine as well as consuming one H^+ . The dialogue between the two isoenzymes of CK occurs within brain, heart, skeletal and smooth muscles (8,9). Each tissue contains 2 different isoenzymes (mitochondrial and cytoplasmic CK) to help effect the dialogue in the different locations. The shuttle of creatine and PC are what is exchanged in this dialogue.

The creatine - PC system allows for communication of information and energy between the site of energy synthesis and the site of energy utilization. This system can allow the dialogue to be conducted between certain points in the cell which are capable of transducing the message. The 2 CK isoenzymes act as the transducers in this dialogue. Therefore a cell system such as Na^+K^+ ATPase which is coupled to cytosolic CK (130) would be able to buffer its energy supply with PC. A cell system not physically coupled to a CK isoenzyme would not be able to buffer its energy supply in this way. A cell system like this could use free ATP from the mitochondria or PC buffering from soluble CK to meet its energy demands. Cell systems coupled to CK could then have preferred buffering of their energy supply. Such systems in the cell are the myofilaments (160,161,170) and the Na^+K^+ ATPase (51,130). Peripheral components which utilize ATP, and may have a sudden increase in ATP demand, might be considered as excellent candidates for a coupled CK system.

Meyer et al (98) discussed the PC shuttle in relation to storage of high energy phosphate that buffers changes in ATP levels. It was demonstrated that the properties of the CK reaction permit it to

function as the transporter of high-energy phosphate within cells. The shuttling of CK metabolites is described as being analogous to facilitated diffusion. Applying Fick's law of diffusion, metabolic conditions in the cell, and assuming CK to be at equilibrium, it was determined that by diffusion alone the majority of the diffusive flux of high-energy phosphate from site to site within mammalian muscle is carried by PC. The conclusion drawn here was that the transport and buffer aspects of the CK reaction are features of the same fundamental properties. The transport function and buffer function of CK both were viewed as resulting from the CK reaction being near equilibrium.

Meyer et al (98) discussed the function of CK in muscle. The CK reaction was discussed as tending to lessen the dissipation of free energy by diffusion. The steady state calculations, regarding the spatial buffering of CK, for a hypothetical 30- μm diameter myocardial cell were applied to this system. They found that the free energy drop was less than 1 kJ/mole even without the CK reaction. They concluded that due to the distances typically involved and small energy drop, it would be unlikely that CK would be required to support high-energy phosphate transport into myofibrils. This conclusion assumes that the mitochondria are packed around the myofibrils as in the case for the myofibrils in the rat heart.

The above argument regarding spatial buffering of the CK reaction would be most important for large cells where the mitochondrial distribution could be non-uniform and a significant ATPase rate exists. In small cells (e.g., smooth muscle) the diffusion distances are

sufficiently small such that the buffering by CK would not have a significant effect because no significant diffusion gradients for any of the metabolites would be established. In this case even without the CK reaction there would be little ATP gradient.

Physicochemical Action of PC and CK

Meyer (96) used an electrical analog model to represent respiratory control in muscle during submaximal rates of oxidation. In this model the CK reaction is described as capacitance. The PC concentration is analogous to stored energy charge on the capacitor. Resistance represents the number and properties of the mitochondria while current is analogous to the rate of oxidative phosphorylation (Figure 2).

If this model is correct, the level of PC must be linearly related to the cytosolic free energy of ATP hydrolysis over the observed submaximal oxidative rates in the cell. Also the ATP synthesis by oxidative phosphorylation must be linearly related to the cytosolic free energy of ATP hydrolysis. It was determined that the above relationship was linear over much of the range of phosphorylation which would be observed during moderate work. Thus the free energy of ATP hydrolysis is proportional to the level of PC and the energy storage capacitance of the CK system is linearly proportional to the total level of creatine.

The model can thus make several predictions as long as the above mentioned limitations are observed. The first prediction is that the

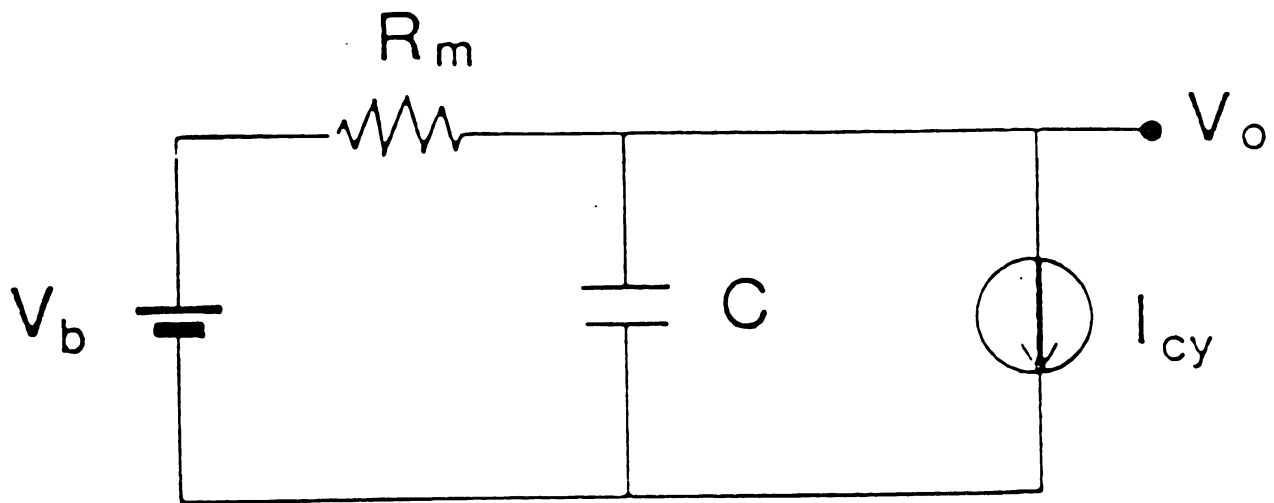


Figure 2. Electrical analog model for respiratory control of the muscle as described by Meyer (1988) for submaximal rates of oxidation. V_b represents the free energy potential in J/mole. R_m is resistance, which is a function of the number and properties of the mitochondria in the cell. V_o represents the cytosolic free energy of ATP hydrolysis. C is capacitance, which is due to the concentration of PC and the CK reaction. I_{cy} represents the current due to the ATPase rate.

time constant for PC changes should be identical at the beginning of and during the recovery from a step change in cytoplasmic ATPase rate. Also, the apparent time constants should be independent of ATPase rate. Finally, steady-state oxygen consumption should be linear at a steady-state level of PC during ATPase rates which are below the maximum aerobic capacity.

These predictions were tested experimentally using NMR measurements in the rat gastrocnemius. The results were consistent with the electrical analog model. It was found that the PC time constants changed independent of work rate and were similar at the onset vs. during recovery after stimulation. Also, the relationship between steady state PC levels and the rate-force product was linear. The final conclusion of the study by Meyer was that the apparent first order behavior of PC concentration changes, observed in the rat gastrocnemius can be modeled using a general linear circuit analog.

Smooth Muscle Background

Paul et al (114,115,116) studied the contractibility of vascular smooth muscle and its coupling to energy metabolism in the cell. Using oxygen consumption as a measure of ATP utilization, the ATP cost of contraction was measured. By measuring O_2 consumption and ATP synthesis it was found that the ratio of ATP synthesis to O utilization (ATP:O ratio) was approximately 3. The time course of energy utilization was measured during steady-state isometric contraction. Oxygen consumption, (ATP synthesis) did not correlate with the development

and maintenance of force. It was found that O_2 consumption closely paralleled the velocity of contraction. This phenomenon was referred to as an increased energy utilization in the pre-steady-state condition and the result is that maintained tension in vascular smooth muscle does not cost as much energetically as tension development. This energetic economy of maintained tension was estimated to be approximately a factor of 2 over tension development. The difference in contractile costs of vascular smooth muscle was related to the differences in smooth muscle contractile protein interaction compared to skeletal muscle.

Dillon et al (34) first described the latch phenomenon in porcine carotid arteries. Latch describes the state of vascular smooth muscle where force is maintained with high energy economy. It was described as a state where the attached crossbridge is dephosphorylated but remains attached to the actin molecule. It was found that the shortening velocity was correlated to the level of myosin light chain phosphorylation. The phosphorylation of myosin light chains are Ca^{+2} dependant. Therefore, Ca^{+2} dependent myosin phosphorylation generates actomyosin activity and crossbridge cycling, while myosin light chain phosphatase can dephosphorylate attached crossbridges and reduce the rate of crossbridge detachment. The attached but noncycling cross bridge can maintain tension and is referred to as a latch bridge. This latch bridge can thus maintain tension with low energy cost to the tissue. The release of the latch bridge is reported to occur with a time constant greater than that seen in cycling crossbridges (24,54,55).

Hai and Murphy (54,55) discussed the phosphorylation of myosin light chains and the energetics of contraction. Their model is intrinsically dependent upon the latch bridges having the same force generating capacity but a 5-fold slower rate of detachment than the phosphorylated and cycling crossbridges. Estimates of ATP turnover determined that the tension maintenance is very economical. In contrast, the efficiency of the work done is considerably lower when compared to skeletal muscle. The low efficiency was due to a high ATP consumption rate for crossbridge phosphorylation. Therefore, the energetics of smooth muscle is economical for the maintenance of tension while not very efficient in generating tension.

Butler et al (21) using rabbit portal vein performed pulse chase experiments to determine the nucleotide bound to myosin and the release rate under relaxed and activated conditions. The results suggested that the myosin exists primarily complexed with ADP. This complex predominates between ADP and myosin during active and relaxed states. The release of ADP in the relaxed smooth muscle was biexponential. The first exponential of ADP release contained approximately 1/3 of the total ADP and was 5-10 times faster than the other release component. It was suggested that these data indicate that there may be a 5 to 10 fold difference in the rates of cycling for different attached crossbridges in smooth muscle. This, they proposed may also account for the variable energy costs for force output.

Skinned Smooth Muscle Studies

Skinned skeletal and heart muscle has been used to study muscle metabolic and biochemical function as well as CK action (4,15,21,23, 95,130,132,159,160,161,162,163,164). Skinning techniques have been used to study smooth muscle (58,61,72,75,106,111, 119,126,168) but the study of CK in smooth muscle is limited. Bose (15) using canine tracheal smooth muscle found that rigor tension was induced when the CK inhibitor FDNB was added in the presence of iodoacetic acid. It was also noted that this change in tension was not significantly different in the presence or absence of Ca^{+2} .

Kargacin and Fay (73) determined that after saponin skinning smooth muscle will retain its ability to contract and that the Ca^{+2} regulatory mechanism is still required (i.e., calmodulin action is still needed to induce shortening) (76). It was also found that the shortening velocity is decreased if ATP concentration is decreased. If CK and PC are added to the medium in the presence of a low ATP concentration the rate of shortening is significantly increased. Similar findings have been found in the heart by Ventura-Clapier et al (162,165). Coupled with the observations of Bose (15), the results may be considered as evidence for CK having a role in the contractile mechanism of smooth muscle.

Kossmann et al (81) examined the effect of skinning on smooth muscle preparations. They found that studies on skinned smooth muscle can be regarded with confidence because the act of demembration does

not grossly disturb the composition and organization of the contractile apparatus. However, the storage and handling of the skinned smooth muscle preparation can alter the contractile response. It was observed that there can be significant protein loss from the muscle during sequential contraction and relaxation cycles. Storage in glycerol will also lead to a significant loss of contractile proteins and contractility. These studies described a means for controlling and monitoring the integrity of skinned smooth muscle preparations. Kossmann et al believe that the skinning model is a valid research model, but that the results of skinning experiments need to be carefully examined and interpreted (81).

NMR and Creatine Kinase Background

NMR has been used in chemistry, physiology and medicine as an analytical tool. NMR spectra give data on molecular structure, concentration, orientation and interaction (5,27,47,57,62,101). The NMR technique of saturation transfer has been used to measure molecular exchange of the CK reaction in living tissue (16,47,93,97,120,144, 155). NMR is a non-invasive technique which makes it well suited for biological and medical applications.

Saturation transfer can be used to determine the CK kinetics in living tissue and has been used to do so in several experiments (14,16,17,19,179). The technique itself is discussed in greater detail in the Methods Section. One advantage of the technique is that it can be used to determine the kinetics of CK in the living tissue

and be able to alter conditions of the experiments and repeat experiments in the same tissue. Thus, each tissue is its own control (144,146,157,179). It is also possible to make measurements on functioning organs while in the living organism (17).

Bittl et al (14) found that the CK flux increased with oxygen consumption and cardiac performance. This relationship held over a wide range of cardiac performance. They suggested that the CK reaction was controlled by a substrate that also controlled oxidative phosphorylation. This prediction is consistent with the discussion previously regarding creatine's effect on oxidative phosphorylation (8,69).

Ugurbil's (156) treatment of the CK reaction as a three site exchange takes into account ATPase effects on ATP degradation (the reverse rate constant). It was determined experimentally that the CK reaction was in fact at equilibrium in heart, and that the continuous wave saturation transfer experiments, assuming a two site exchange, are prone to underestimating k_r .

Using a technique similar to Ugurbil's MST, Spencer et al in 1988 (146) repeated experiments by Bittl et al (14). Spencer found that the fluxes were erroneous if a two site exchange is assumed. The results showed that CK was at equilibrium during conditions where previous results gave significant differences in the net flux. These experiments also showed that the discrepancy resided in the determination of the rate of ATP degradation or k_r . The value of k_r had been reported as being lower than it was when measured with MST. To date

there are no studies examining the MST and CST techniques in the CK kinetics of smooth muscle.

NMR Background

The longitudinal relaxation time (T1) of the exchanging nuclei effect the calculation of the kinetic rate constant. Therefore the T1 for each nuclei must be determined and taken into account when calculating the rate constant (18).

To generate T1 the nuclei must first be in a low energy state dictated by the magnetic field. When atoms are in the presence of a strong homogeneous magnetic field, some of the nuclei align themselves with parallel and anti-parallel spins to the field. As long as the magnetic field is applied, the sum of the spins will form a net vector along with the Z axis of the magnetic field (M_0). The nuclear spins will precess at the Larmor frequency ω^0 . Once the nuclei are so arranged a radio frequency pulse is applied at the Larmor frequency along the X axis. This causes the magnetization vector, M_0 , to tip away from the Z axis (Figure 3). The frequency of transmission for the nuclei is determined by the formula:

$$\nu = \gamma B_0 / 2\pi.$$

1

Where: ν = the resonance frequency, γ = the gyromagnetic ratio, B_0 = the local magnetic field strength. After a radiofrequency pulse, the nuclear spin is in a high energy state. This energy state is

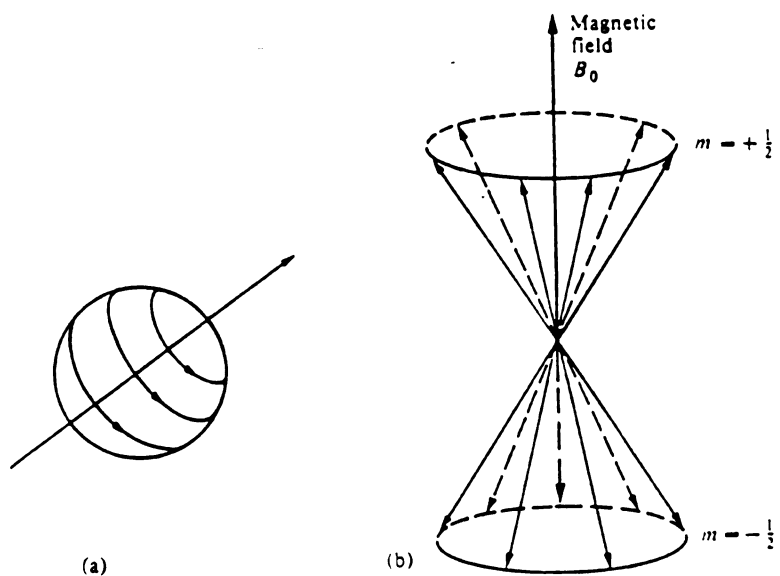


Figure 3. Modified from Gadian 1982 (47). A representation of the magnetic moment generated by the spin of a nucleus is seen in (a). The orientation that can be formed by the nucleus when in an applied magnetic field B_0 is seen in (b).

represented by a net vector in the x-y plane given by the formula:

$$M_{xy} = M_0 \sin \theta.$$

2

Where: M_{xy} is the magnetization in the x-y plane and θ is the angle away from M_0 . The 90 degree pulse width is a pulse long enough to flip the net spin 90 degrees away from M_0 . In this way, the flipping of the nuclei can continue through 360 degrees. As the nuclei begins to recover back towards the Z axis they recover with an exponential time constant referred to as the longitudinal or spin lattice relaxation time. During the recovery, nuclei emit energy which can be received by rf coils tuned to that frequency (5,47,101).

DANTE Background

To be able to perform multisite saturation transfer (MST) two tailored pulse sequences must be applied simultaneously in the time excitations domain so as to result in two different saturating excitations in the frequency domain. Bittl et al (13) and Spencer et al (146) performed MST by using a synthesizer and harmonic oscillator. Ugurbil (156) generated MST using two computer-controlled synthesizers. The synthesizer generates saturation with a continuous pulse applied in the time domain to excite a specified resonance in the frequency domain. The continuous wave (CW) saturation (soft pulse) will have the effect of exciting a single resonance peak in the frequency domain without exciting neighboring resonances (Figure 4). In contrast a "hard pulse" is

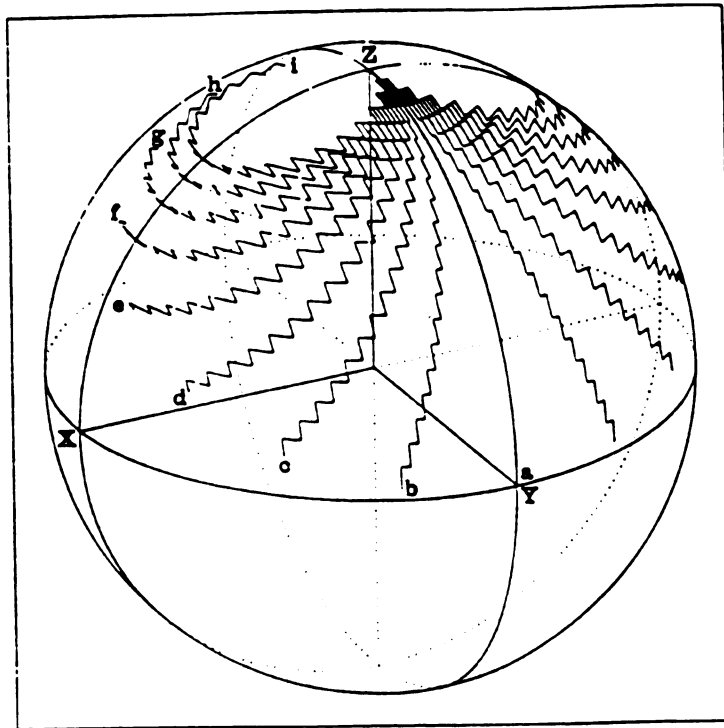


Figure 4. Trajectories of magnetization vectors computed by the Bloch equations as described by Morris and Freeman (1978). In this example the excitation train of twenty pulses were spaced two milliseconds apart and their sum totaled the 90° pulse. Trajectory [a] represents the magnetization changes which occur on resonance for this pulse train. Trajectories [b] through [i] represent trajectories which reside off resonance of trajectory [a] by increments of 2.5 Hz. The unlabeled trajectories opposite of trajectory [a] represents vector effects with equidistant offset to the labeled trajectories. As can be seen from the [h] and [i] trajectories, an extended train of pulses would cause the off resonance trajectories to achieve a steady state approaching the Z axis.

used to excite a region in the frequency domain. Morris and Freeman (100) described a pulse sequence utilizing a train of hard pulses which will generate a tailored excitation called DANTE. The details of this technique are discussed in the Methods Section.

BBCK Clinical Background

BBCK has been used clinically as a biomarker of neurological disease or damage and is used as a parameter for the diagnosis of certain cerebral carcinomas (29,166). It has been found in the blood stream during parturition, Caesarian section, and coronary bypass surgery (158,166). Normal serum BBCK values are below 1 U/liter. Vladutin et al (158), however, found that during bypass surgery BBCK increased to as much as 43 U/liter with a concomitant increase in MBCK. They found that the clearance of BBCK is faster than the clearance of MBCK. This study also noted that the isoenzymes can dissociate into monomers *in vivo* and reassociate. However, the possibility of BBCK originating from reassociated B monomers or MBCK originating from M and B monomers was not investigated. The tissue origin of the BBCK was not determined in this study.

BBCK has high activity in brain, uterus (especially during pregnancy), gastrointestinal tract and vascular smooth muscle (33,65,123). Damage to these tissues has been reported to cause increased BBCK activity levels in the serum (29,49,166,180). The release of BBCK from

the brain is believed to be attenuated due to the blood brain barrier. Perturbation of the blood brain barrier, such as from trauma, however, may allow increased release of BBCK from the brain (88).

The potential use of BBCK for clinical diagnostic purposes is confounded by significant inactivation of BBCK while in the bloodstream (113). Thus assays using kinetic activity for BBCK fractionation can be inaccurate. Conversely, immunological assays for CK fractionation which react with the CKB monomer will cross react with MBCK and produce misleading results when determining BBCK (59,134). BBCK has been found bound to IgG's in the human serum (88). Binding to IgG in the human serum will cause a change in the electrophoretic mobility of BBCK and again lead to potentially erroneous results (90). It has been observed that while in the serum, CK dimers will dissociate and reassociate. The monomers can reassociate with either monomer, so CKB may be recombining with CKM to form MBCK (74,134). If this were to occur, MBCK might be more likely to be detected in the serum because of its increased stability.

BBCK is a significant fraction of the heart and skeletal muscle CK activity during early developmental stages (71,88,110). It also persists as a large part of the adult skeletal muscle CK with muscular dystrophy (83,78). In patients with Duchene Muscular Dystrophy, BBCK comprises 10% of the CK activity in the afflicted muscle (83). Therefore, the BBCK which might be found in the serum of young or

muscular dystrophy patients could be originating from tissue normally not associated with BBCK. As discussed above the BBCK can originate from multiple organs, unlike MBCK which is predominantly found in the heart and in only trace amounts in the skeletal muscle (99). Thus BBCK may have clinical relevance as a diagnostic tool, but the results from BBCK measurements should be evaluated cautiously because the tissue of origin may be uncertain (32).

The possibility of BBCK release from smooth muscle becomes increasingly convoluted in light of the multiple CK isoenzymes which are observed in smooth muscle (71,154). CK isoenzymes are known to have differing kinetics and different physical properties (45,46,53,74,83,90, 99). If a tissue contains multiple forms of CK it is not known if these different forms are localized in different places in the cell. *In vitro* studies have demonstrated kinetic differences between CK isoenzymes as well as different physical properties.

Summary

From the discussion above, it appears that much is known about MM and MBCK from heart and skeletal muscle from *in vivo* and *in vitro* studies, and using multiple research techniques. Less attention, however, has been given to the study of BBCK in vascular smooth muscle. The purpose of this thesis is to determine the kinetics of CK observable in the porcine carotid artery using the NMR technique of saturation

transfer, and the kinetics of BBCK in solution which has been purified from porcine carotid artery. The purification of a single isoenzyme from the tissue is performed because it has not been determined what, if any, interaction the multiple isoenzymes undergo within a tissue. If multiple forms of cytosolic CK are present in the porcine carotid artery, saturation transfer results will reflect the kinetics of the available isoforms and/or of nuclei which are NMR visible. Performing these experiments contribute to better understanding of vascular smooth muscle energetics and BBCK kinetics.

METHODS

Tissue Collection

Porcine carotid arteries were obtained from pigs at the time of slaughter. Tissue was kept in ice cold physiological salt solution (PSS) after removing clots and flushing the lumen with PSS. PSS contained; 116 mM NaCl, 5.4 mM KCl, 25.3 mM NaHCO₃, 1.1 mM NaH₂PO₄, 2.5 mM CaCl₂, 1.25 mM MgSO₄, 0.1 mM EDTA and 15 mM glucose. Within 2 to 3 hours of collection arteries were randomly divided into two groups. The first group of arteries were placed in fresh PSS and stored overnight at 4°C for NMR kinetic experiments. The second group was put aside to be prepared for purification experiments.

Pouring Chromatographic Column

Several weeks prior to the purification experiments the chromatographic columns were prepared. Six Pyrex columns were purchased from Corning Glass Works (Corning, NY) with dimensions of 20 x 400 mm and fine glass frit at the bottom. Hydroxylapatite for the chromatography was purchased from Biorad (Richmond, CA), pre-suspended in a solution containing 0.01 M sodium phosphate and 0.02% NaN₃. Packing of the columns was accomplished following the methods of Ault (6). The hydroxylapatite solution was thoroughly mixed and approximately 30 ml

of solution was poured quickly into each column. Columns were then allowed to settle over night at 4°C. After settling, excess buffer was siphoned off and the pouring procedure repeated. This sequence was repeated until the columns were packed to a height of 25 cm of hydroxylapatite. During this procedure the columns and solutions were kept at 4°C and the columns were not allowed to dry. After the columns were poured, they were allowed to settle further for several days. The columns were then fitted with disks placed at the top of the column of hydroxylapatite. The disks were made of QZ Filter Paper from Fisher which were cut to fit the internal diameter of the columns. On top of the filter paper was placed glass wool and finally a layer of glass beads (Figure 5). Once the packing was complete the columns were rinsed thoroughly with column buffer. Column buffer contained 10 mM tris acetate, 25 mM ME and 0.5 mM EDTA at a pH of 7.4. Rinsing was accomplished at 4°C and the columns were protected from drying. The columns were kept at all times at 4°C during experiments as well as between experiments.

Purification of BBCK

Freshly collected arteries were stripped of loose connective tissue and adventitia using the technique of Herlihy and Murphy (60). This technique involves removing the bulk of the connective tissue by blunt dissection and scissors leaving the artery and a thin protective sheath of connective tissue surrounding the artery. By anchoring the proximal aspect of the artery and grasping a small section of connective tissue just distal to the anchor the remaining connective tissue

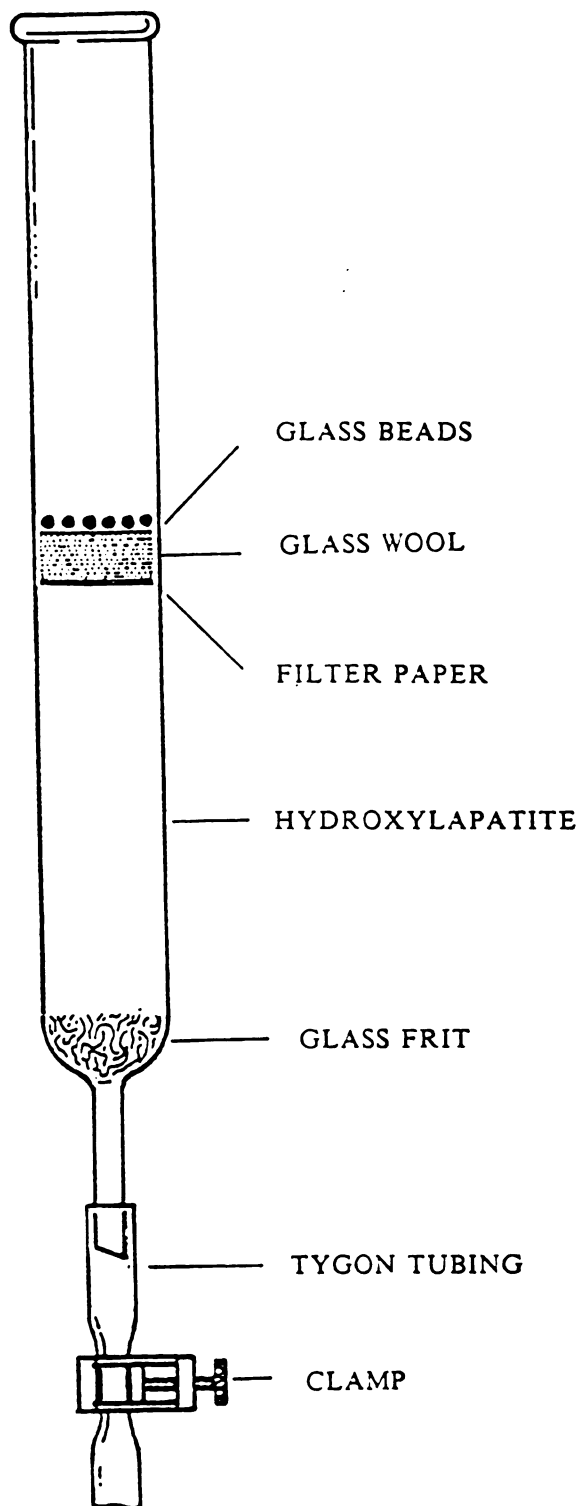


Figure 5. Chromatographic column used for purification of creatine kinase modified from Ault (6). See text for packing instructions and dimensions.

can be peeled off distally. The remaining tissue has 96% vascular smooth muscle cells, the remainder being endothelial cells from the intima (60).

Stripped arteries were fast frozen with clamps precooled in liquid nitrogen. Frozen arteries were stored at -85°C for up to several months to accumulate sufficient tissue mass for purification. On the day of the purification procedure, 100g of frozen tissue was quickly mixed with 400 ml of standard buffer at 4°C . Standard buffer consisted of: 50 mM Tris acetate (TA), 0.5 mM EDTA, 25 mM 2-mercaptoethanol (ME) and 10 mM KCl. The pH was brought up to 7.4 using 1 N NaOH. Unless otherwise stated, all procedures and solutions are at 4°C . The tissue and buffer was homogenized for 30 minutes in a Waring blender. Following the procedure described by Wang and Cushman (174), the homogenate was centrifuged at 37,000 g for 45 minutes. Modifications to Wang and Cushman's method for the purification of BBCK from human brain were obtained from methods of Iyengar et al (65) where 10 mM KCl was used during the homogenization and the duration of homogenization increased to 30 minutes and repeated twice. While saving the pellet, the supernatant was precipitated with 1.57 volumes of 95% ethanol chilled to -10°C . The precipitated supernatant was centrifuged at 8,000 g for 20 minutes. While pooling this pellet with the other pellet from above, the supernatant was precipitated with 1.23 volumes of 95% ethanol. Using 2-3 times the volume of the pooled pellets, standard buffer was used to rehomogenize the pellets for 20 minutes. The rehomogenized pellets were centrifuged at 37,000 g for 45 minutes. The pellet was discarded and the supernatant precipitated

Table 4

Enzyme Purification Procedure

<u>Fraction</u>	<u>Comments</u>
Tissue Collection	At time of slaughter
Clean tissue	Herlihy & Murphy
Freeze & store tissue	-85°C
Homogenize	30 min in standard buffer
Centrifuge @ 37,000g	45 min, Save pellet
Precipitate supernatant	1.57 v/v ETOH -10°C
Centrifuge supernatant @ 8,000g	20 min, Save pellet
Rehomogenize pooled pellets	30 min, in standard buffer
Centrifuge homogenate @37,000g	45 min, Discard pellet
Precipitate supernatant	1.23 v/v ETOH -10°C
Centrifuge @ 8,000g	20 min, Discard pellet
Pool all supernatants	
Precipitate pooled supernatants	Final ETOH content of 70%
Centrifuge pooled supernatants	20 min, Discard pellet
Load column with supernatant	Discard eluent
Rinse column	Discard eluent
Elute protein	Save eluent
Concentrate protein	Fractional Dialysis

with 1.57 volumes of 95% ethanol and centrifuged at 8,000 g for 20 minutes. The pellet was discarded and the resulting supernatant was brought up to 70% ethanol with 1.23 volumes of 95% ethanol. All supernatants were pooled and centrifuged at 8,000 g for 20 minutes and the pellet discarded (Table 4).

The supernatant was loaded on a 40 cm hydroxylapatite column with a diameter of 2 cm packed previously to a height of 25 cm using hydroxylapatite purchased from Biorad (as described above). The column had been rinsed thoroughly with column buffer containing 10 mM TA, 0.5 mM EDTA and 25 mM ME at a pH of 7.4 and kept at 4°C. Once the columns were loaded, they were rinsed with a volume of column buffer equivalent to the total volume of standard buffer used in preparation. Elution was performed with an elution solution of 10 mM KH_2PO_4 , 0.5 mM EDTA and 25 mM ME. The volume of elution solution was the same as that of the column buffer used to rinse the columns. Fractions were collected from the column every 7 mls. Fractions with approximately 17 μg of protein per ml or greater were pooled. Figure 9 (Results Section) shows the elution profile from a purification batch. Protein concentration was determined using the Biorad (Richmond CA) microassay procedure. The eluted enzyme was concentrated by fractional dialysis.

Fractional dialysis consists of dialyzing against 70% ethanol and 25 mM ME. Following ethanol dialysis, the dialysis tubing is tied off at a smaller volume and dialyzed against standard dialysis solution containing 10 mM TA and 25 mM ME solution to remove the ethanol. If further concentration is desired, this process can be repeated. The

final protein concentration obtained by this method was 66 $\mu\text{g/ml}$.

Electrophoresis Methods

SDS-PAGE electrophoresis was performed to determine purity and molecular weight of the enzyme. The method of Lamelli (87) was followed. The plates for the electrophoresis were thoroughly rinsed with distilled water and dried in a drying oven prior to the pouring or assembly of the plates. They were assembled to make a 1 mm thick gel using plastic spacers at the sides, and sealed at the bottom and sides with a silicon tubing gasket. The plates were mounted together using 4 clips at the sides of the plates. Next the lower gel was prepared and poured. This included preparing the lower gel with 8 ml of a solution of 30% acrylamide with 0.8% bisacrylamide, 8 ml of a buffer containing 1.5 M tris and 0.4% SDS, pH 8.8, and 16 ml of distilled water. The above was filtered and polymerization initiated with the addition of 10 μl of TEMED and 365 μl of ammonium persulfate. The pouring of the lower gel was accomplished by quickly adding the gel solution between the plates. This was done using a Pasteur pipette. During the pouring, care was taken to prevent the formation of bubbles and to detect the presence of leaks. If a leak was observed, the plates were disassembled and re-assembled before continuing. To prevent drying of the lower gel an over lay solution of 11.25 ml of water, 3.25 ml of a solution containing 0.5 M tris and 0.4% SDS at pH 6.5, 15 μl TEMED and 45 μl of 10% ammonium persulfate was placed over the lower gel. The upper gel consisted of 8.6 ml water, with 2.25 ml of a solution containing 30% acrylamide and 0.8% bisacrylamide and

3.75 ml of a solution containing 0.5 M Tris and 0.4% SDS at a pH of 6.8. The polymerization was initiated with the addition of 15 μ l TEMED and 45 μ l 10% ammonium persulfate. The overlay was removed by paper absorption and the upper gel poured using a technique similar to that used for the lower gel. A teflon comb was placed in the top of the upper gel solution to form 16 lanes leaving greater than 1 cm of upper gel from the bottom of the lane to the top of the lower gel. The upper gel and comb was cleared of bubbles and allowed to polymerize for a minimum of 60 minutes.

While the gel is polymerizing 1 liter of running buffer is prepared. Running buffer contains 0.025 M tris, 0.192 M glycine and 0.1% SDS. This can be stored as a stock solution at 10 times the above concentration at a pH of 8.3.

To run gels the comb and gasket was removed and the plate placed in the holder. Sufficient running buffer was added to cover the gel's top and bottom chambers. Bubbles were removed from above and below the gel's surface to ensure even resistance across the gel. A total of 20 μ l of sample was loaded into each lane using an Eppendorf pipette. Samples contained 10 μ l of sample buffer composed of: 30 mM tris, 9% SDS, 15% glycerol, 5 mM ME and 0.05% bromphenol blue. Up to 10 μ l of protein solution sample could be added to each well. Molecular weight standards contained the Biorad high molecular weight standard. Table 5 lists the contents of Biorad high molecular weight standard.

TABLE 5

Biorad High Molecular Weight Standard

Protein	Molecular Weight (Daltons)
Myosin (rabbit skeletal muscle)	200,000
β -galactosidase (E. coli)	116,250
Phosphorylase (rabbit muscle)	97,400
Bovine serum albumin	66,200
Ovalbumine (hen egg white)	45,000

Gels were run at 20 milliamps using a Gelmen power supply for 3-4 hours. The power was turned off and the gel removed and placed in a staining solution containing 0.05% coomassie blue and 25% TCA. The gel was stained for 30 minutes with constant shaking. Destaining was accomplished by soaking the gel in a 10% methanol, 10% acetic acid solution for 10 hours. Gel drying was accomplished by using a Slaborel drying unit from Ann Arbor Plastics/Scientific Products (Ann Arbor, MI). This procedure used cellophane sheets which were soaked in the destaining solution and placed on either side of the gel. This sandwich setup is allowed to dry for 6-8 hours in a well ventilated warm and dry area. After drying the excess cellophane was cut away leaving the dried gel.

Silver staining of the SDS-PAGE gels was performed using the

Gelcode silver stain kit from Pierce Chemical Company (Rockford, IL). The kit comes complete with 4 bottles containing the concentrated reagents. Reagent one contained the silver stain reagent. Reagent two contained the reducer aldehyde. Reagent three contained the reducer base. Reagent four contained the stabilizer base. The specific contents and concentrations of these reagents are proprietary. Reagent one was diluted 1:15 (v/v) with deionized water for use. Reagents two and three were diluted 1:7.5 and reagent four 1:45 for use.

Prior to silver staining the gel was fixed with 50% ethanol and 5% acetic acid. This can be done to rehydrate a dried gel with a rehydration time of 12 hours. The gel was washed with deionized water for three hours and stained with diluted reagent one for one hour. Reagents two and three were mixed immediately prior to use and the gel soaked for 10 minutes in them. The gel is rinsed 3 times, for 60 minutes each time, in the diluted reagent four and dried using the technique described above.

Following electrophoresis the stained gel was analyzed with a densitometer to determine the relative purity of the enzyme. Each lane was scanned for the length of the lane over a width of 3.2 mm. Figure 11A (Results Section) is a scan taken from the lane containing the fraction taken from the crude homogenate. Figure 11B is taken from the lane containing purified BBCK. Figure 11C is taken from BBCK purchased from Sigma Chemical Company.

Molecular Weight Determination

Molecular weight of the monomeric BB creatine kinase was determined by plotting the molecular weight vs. migration distance on 3 cycle semi log paper. The migration distance of the purified protein can thus be used to determine the monomeric molecular weight using interpolation. See Appendix III.

Isoenzyme Determination

Fractionation of the three cytosolic CK isoenzymes was performed using the Cardiotrac Fluorometric method by Corning (Corning NY). This method involves separation of the isoenzyme by agarose electrophoresis. Using agarose film supplied in the kit approximately 1 μ l of sample is applied to the film in the preformed well. Electrophoresis is performed after each chamber is filled with running buffer which contains the Barbital buffer supplied in the cardiotrac kit containing a final concentration of 0.05 M sodium barbital with a pH of 8.6.

The film is placed in a horizontal chamber with the sample well closest to the cathode. Power was turned on and ran for 20 minutes at 90 volts using a dedicated Corning Power supply (Corning, NY). When electrophoresis was complete the excess buffer was removed and pre-soaked substrate paper placed over the gel. The substrate paper was soaked for 30 minutes in a solution containing 1 ml of MES buffer added to 1 vial of substrate reagent. The MES contained a proprietary

concentration of morpholino ethane sulfonic acid at pH of 6.2. The lyophilized reagent vial contained; PC, ADP, glucose, hexokinase, NADP, glucose-6-phosphate dehydrogenase and AMP. Following the mixing procedures described the final concentrations of the reagents will be: 90mM PC, 12 mM ADP, 60 mM glucose, 9000 IU/liter hexokinase, 6 mM NADP, 7500 IU/liter glucose-6-phosphate dehydrogenase, and 15 mM AMP. The agarose gel and substrate paper were incubated for 30 minutes. Activity of CK was measured by the production of NADPH using the following series of reactions:



After drying, the production of NADPH is measured by a Beckmen Apprase Densitometer (Beckmen Instruments) which will scan the gel for fluorescent changes occurring at 365 nanometers from the NADPH produced during the incubation. This procedure will give total CK for a given lane and activity vs. distance migrated. The fractional distances migrated are divided into 3 regions according to the migration characteristics of the isoenzymes to give the ratios of activity for CK isoenzymes in the sample.

Methods For Kinetic Activity In Solution

Protein concentrations of purified enzyme was determined using the Biorad dye binding assay. See Appendix I. This assay uses the principal of the Bradford assay (147), a colorimetric measurement of Coomassie Brilliant blue. This method has preferential binding of protein and dye to form a blue complex with an extinction coefficient much greater than the free dye. The advantages of this technique are that few impurities or solvents effect the results and measurements can be made immediately.

Specific activity of the enzyme was calculated by determining the rate of ATP production. Where one unit of activity is defined as the amount of enzyme which will convert 1 μ mole of ADP to ATP per minute under standard conditions. The standard conditions are 37°C and saturating conditions of substrate.

The stock solution for kinetic experiments consisted of 50 mM tris, 10 mM $MgCl_2$, 25 mM ME 0.1% BSA at a pH of 7.5. The reaction was started at time zero by addition of substrate. If the forward reaction was being examined, PC was added to a solution containing 1 mM ADP in the presence of 33 μ g/ml enzyme. To examine the reverse reaction the reaction was started by the addition of ATP to a solution of 20 mM Cr. All kinetic experiments were carried out at 23°C with a total volume of 1 ml. The reaction was stopped by addition of 0.5 ml of 3 N perchloric acid. One minute later, the pH was brought back up to approximately 8.0 with 0.5 ml of 3 N KOH and 1 M TEA.

The curve seen in Figure 12 (Results Section) is representative of the progress of the reaction under saturating conditions of substrate versus time. The time points seen in this curve are 0, 5, 20, 60 and 180 seconds. This reaction was started by the addition of 10 mM PC to a solution of 1 mM ADP and measuring ATP production. This curve was used to determine that the appropriate time to stop the reaction for the kinetic experiments was 20 seconds.

ATP production was used to measure the forward reaction while disappearance of ATP was used to measure the reverse reaction. ATP was measured spectrophotometrically using the coupled enzyme assay described above to produce NADPH. NADPH production was measured by combining 2 mls of assay stock solution, 0.5 ml of sample, 25 ml of 50 mM NADP and 10 ml of a solution containing 0.1 U/ml G6PDH and 0.1 U/ml of Hexokinase. The assay stock solution contained 50 mM tris, 1 mM $MgCl_2$, 1 mM glucose, 0.5 mM ME at a pH of 8.0. This reaction was allowed to come to equilibrium for 30 minutes and spectrophotometric measurements made at 340 nm. See Appendix II.

Determination of Solution Kinetics

Kinetics experiments on purified BBCK were performed in 1 ml of solution and stopped with 3N perchloric acid after 20 seconds. The determination of the forward kinetics was performed in a reaction solution containing 1 mM ADP, kinetic stock solution, and 33 $\mu\text{g/ml}$ of BBCK. The reaction was initiated with the addition of varying amounts of PC. The PC concentrations used produced a final concentration in

the reaction system of 20, 10, 5, 2, and 1 mM and were all performed in duplicate. Following the additions of acid and base the solution was kept at 4°C until ATP measurements. ATP measurements were accomplished within 24 hours of the kinetic experiments.

The reverse kinetics were determined by using a solution containing the kinetic stock solution and 20 mM creatine as well as 33 µg/ml of enzyme. The reaction was started with the addition of varying concentrations of ATP. The final concentrations of ATP were 60, 20, 10, 5, and 2 mM. The progress of the reaction was determined by measuring the ATP concentration present in the kinetic solution and calculating the disappearance of ATP.

Kinetic Calculations

K_m and V_{max} were determined from the Lineweaver-Burke, Hanes-Woolf, and Hofstee plots. To accomplish this, forward and reverse data were plotted by $1/v$ vs $1/[S]$, $[S]/v$ vs $[S]$, and v vs $v/[S]$ respectively. A multiple determination of the K_m and V_{max} as described above produces a range of values for K_m and V_{max} which are reported in the Results Section.

NMR Methods

The arteries were kept at 4°C in PSS until the time of the experiment the following day. Two to three arteries, containing a total tissue weight of 2 grams, were cleaned, cut horizontally into rings, and placed into a 10 mm NMR tube. Arteries were superfused from the bottom of the NMR tube and the solution removed from above the tissue and recirculated at 37° C. The solution contained regular PSS except for the following changes: 0.1 mM NH_2PO_4 and 19 mM NaHCO_3 . The low NaH_2PO_4 concentration decreases the contribution of perfusion Pi to the Pi signal observed from the tissue. The NaHCO_3 concentration is decreased because the experiments were performed at 37°C using a bicarbonate buffered solution with continuous bubbling by 95% O_2 , 5% CO_2 .

Perfusion was accomplished by a Harvard peristaltic pump with a flow rate of 10 ml/min. The Tygon tubing used was approximately 3 meters long because the perfusion apparatus will not operate in close proximity to the magnet due to the strong magnetic field. To prevent solution cooling while in the perfusion lines the Tygon tubing was jacketed with silastic tubing perfused with 37°C water from a Haake constant temperature pump. The infusion line was jacketed in this manner up to the bore of the magnet. The bore temperature was maintained at 37°C with forced warm air. Siphoned solution was returned via unjacketed tubing to a 1 liter flask of PSS. PSS was continuously bubbled at 37°C with 95% O_2 , 5% CO_2 .

The field was optimized by shimming on the ^1H resonance at 400.131 MHz. The perfused tissue was allowed to equilibrate for 2-3 hours before any experimental measurements were obtained. During the equilibration period pre-control spectra were continuously taken to ensure tissue stability and viability. Control spectra consisted of 200 summed scans collected 15 seconds apart using a 18 μsecond pulse width (PW).

DANTE Methods

The specific methods described by Ugurbil and Ingwall were not available for these experiments. Therefore, a different technique was used which employed both CW and DANTE saturation. Both hard (DANTE) and soft (CW) pulses are utilized simultaneously to generate the two tailored excitations.

The DANTE pulse sequence described by Freeman and Morris generates selective excitation by a regular sequence of identical, short radio-frequency pulses. The pulse width (α) is very short and the nutation time (t) between the pulses is also short. This pulse sequence will produce excitation which is offset from the transmitter frequency by an amount:

$$\Delta\nu = 1/(\alpha+t), \quad 3$$

where α is the pulse width and t is the nutation time between pulses and $\Delta\nu$ is in Hz. The elicited excitation will occur at the center

frequency and at intervals of $\Delta\nu$.

The excitation produced by DANTE at the offset frequencies described by $\Delta\nu$ occurs by a cumulative effect of the short hard pulses. Before the first pulse, the net nuclear magnetization vector M is at its Boltzman equilibrium value, M_0 . During the first pulse the magnetic moment vectors of the nuclei are tipped away from their equilibrium value along a particular trajectory. The next pulse tips vectors of those nuclei at the $\Delta\nu$ resonance farther away from M_0 along the same trajectory on the unit sphere of the nuclei. Vectors of nuclei which are not at the $\Delta\nu$ frequency are tipped away from M_0 but along different trajectories. The differences in the trajectories depend upon the value of $\Delta\nu$. Subsequent pulses cause the vectors for nuclei at the $\Delta\nu$ frequency to be tipped again along the same trajectory away from M_0 while other vectors are tipped along their shifted trajectories (Figure 4 in Background Section). The continued application of the short, hard pulses will flip the on-resonance vectors along the same trajectory. Off-resonance magnetization vectors will continue to have their trajectories shifted such that they will reach a steady state with their resultant vector near M_0 . In this way, nuclei which resonate at frequency $\Delta\nu$ will have their magnetization vectors flipped by the cumulative effect of the pulses, while off-resonance magnetization will remain near M_0 -thus producing a selective saturation at the on-resonance frequency.

Because the DANTE sequence was developed to selectively excite a spin vector such that the net effect approximates a 90° or 180° pulse,

it had to be modified to produce a continuous-wave type of saturation. This was accomplished by making the number of pulses (n) very large such that the on-resonance vector is continuously saturated. The objective of the MST experiment was to saturate one resonance of interest with DANTE while saturating another resonance with CW, and to do it such that the times required for equivalent saturation be equal. To demonstrate that the small alteration in the pulse train did not alter the magnetization effects shown to occur by Freeman and Morris, the Bloch equations were solved incorporating the changes discussed above.

It is assumed that the magnetization can be represented by M_x , M_y and M_z where M_z is along the M_0 axis. Initially the magnetization vectors will be along M_z .

The net magnetization is represented by its components in the x, y and z coordinate system as follows:

$$M_z(t) = M_z^- \cos\alpha - M_y^- \sin\alpha + M_0[1 - \exp(-t/T_1)] \quad 4$$

$$M_y(t) = (M_y^- \cos\alpha \cos\Delta\omega t + M_z^- \sin\alpha \cos\Delta\omega t - M_x^- \sin\Delta\omega t)\exp(-t/T_2) \quad 5$$

$$M_x(t) = (M_x^- \cos\Delta\omega t + M_y^- \cos\alpha \sin\Delta\omega t + M_z^- \sin\alpha \sin\Delta\omega t)\exp(-t/T_2). \quad 6$$

Suppose α is applied and is small such that $\cos\alpha \approx 1$, $\sin\alpha \approx \alpha$, and $M_z^- \approx M_0$. Then,

$$M_z(t) = M_0, \quad 7$$

$$M_y(t) = (M_y^- \cos \Delta \omega t + M_0 \alpha \cos \Delta \omega t - M_x^- \sin \Delta \omega t) \exp(-t/T_2), \quad 8$$

and

$$M_x(t) = (M_x^- \cos \Delta \omega t + M_y^- \sin \Delta \omega t + M_0 \alpha \sin \Delta \omega t) \exp(-t/T_2). \quad 9$$

Combine the terms M_x and M_y as follows:

$$\begin{aligned} M_{xy}(t) = M_x(t) + iM_y(t) &= (M_x^- \cos \Delta \omega t + M_y^- \sin \Delta \omega t \\ &+ M_0 \alpha \sin \Delta \omega t) \exp(-t/T_2) + i(M_y^- \cos \Delta \omega t + M_0 \alpha \cos \Delta \omega t \\ &- M_x^- \sin \Delta \omega t) \exp(-t/T_2) \end{aligned} \quad 10$$

Which simplifies to:

$$\begin{aligned} M_{xy}(t) &= M_x^- (\cos \Delta \omega t - i \sin \Delta \omega t) \exp(-t/T_2) \\ &+ iM_y^- (\cos \Delta \omega t - i \sin \Delta \omega t) \exp(-t/T_2) \\ &+ iM_0 \alpha (\cos \Delta \omega t - i \sin \Delta \omega t) \exp(-t/T_2), \end{aligned} \quad 11$$

$$= (M_x^- + iM_y^- + iM_0 \alpha) (\cos \Delta \omega t - i \sin \Delta \omega t) \exp(-t/T_2). \quad 12$$

Then by identifying M_{xy}^- , and by the definition of $\exp(-i \Delta \omega t)$,

$$M_{xy}(t) = (M_{xy}^- + iM_0 \alpha) \exp(-i \Delta \omega t) \exp(-t/T_2). \quad 13$$

In a departure from the reasoning followed by Morris and Freeman (100)

which applied a cumulative 90° or 180° pulse, an extended series of small α pulses is applied. The sum of these pulses is greater than the 90° or 180° and is applied over an extended period of time similar to a CW saturating pulse. M_{xy} will be expressed by:

$$\begin{aligned}
 M_{xy}(t) = & iM_0 \exp[-(t-t_m)/T_2] \exp[-i\Delta\omega(t-t_m)] \\
 & \{(\alpha_1 \exp[-(t_m-t_1)/T_2] \exp[-i\Delta\omega(t_m-t_1)])\} \\
 & + \dots (\alpha_{m-1} \exp[-(t_m-t_{m-1})/T_2] \exp[-i\Delta\omega(t_m-t_{m-1})]) \\
 & + (\alpha_m \exp[-(t_m-t_m)/T_2] \exp[-i\Delta\omega(t_m-t_m)])
 \end{aligned} \tag{14}$$

Expression 14 can be simplified to

$$M_{xy}(t) = iM_0 \sum \alpha_n [\exp-(t_m-t_n)/T_2] \exp[-i\Delta\omega(t_m-t_n)] \tag{15}$$

Remembering that α is constant and small,

$$M_{xy}(t) = iM_0 \sum \alpha_n \exp[-(t_m-t_n)/T_2] \exp[-i\Delta\omega(t_m-t_n)], \tag{16}$$

where \sum is from $n=1$ to m .

Assume $t > t_m$, and that t is large, then

$$\begin{aligned}
 \alpha_m \exp[-(t-t_m)/T_2] \exp[-i\Delta\omega(t-t_m)] & \cong \\
 \alpha \exp[-(t_m-t_n)/T_2] \exp[-i\Delta\omega(t_m-t_n)], &
 \end{aligned} \tag{17}$$

which upon insertion into equation 16, yields

$$M_{xy}(t) = iM_0 \sum \alpha_n [\exp(-(t-t_n)/T_2)] \exp[-i\Delta\omega(t-t_n)].$$

18

Equation 18 demonstrates that the modified DANTE pulse sequence will saturate a resonance of interest with the same results as those obtained by Freeman and Morris (100). The modifications to the DANTE pulse sequence used in this thesis thus do not alter the results demonstrated by Freeman and Morris. Therefore, when this modified sequence is applied to a resonance for an extended period of time, the resonance will be saturated, as explained by the above solution of the Bloch equations. A two site saturation experiment, which applies the above pulse sequence in conjunction with CW saturation, is thus possible. Therefore, Ugurbil's MST experiments may be performed by using a modified DANTE pulse sequence instead of dual CW saturation.

NMR Solution Methods

Control experiments to demonstrate DANTE were performed on a solution containing 2.5 mM ATP, 5.0 mM PC, 0.6 mM ADP, and 30.0 mM Mg⁺ at pH 7.6 with 10 mM MOPS (Figure 17 in Results Section). These concentrations are supra-normal for smooth muscle but higher phosphate concentrations allow rapid collection of spectra which also allows for quick interpretation of spectra and facilitates the process of optimizing pulse conditions. For all solution spectra 4 dummy scans were used and 16 scans for collection with 15 second cycle time between transients. For complete saturation, the DANTE pulse was generated by applying

50,000 (n) pulses with a pulse width (α) of 0.7 μ seconds. The delay between pulses (t) was 0.00029 seconds or 290 μ seconds. This cycle time would generate a saturation at the center frequency and at a frequency 3440 Hz (18.78 ppm) away and continue to repeat at this frequency ($\Delta\nu$)

$$\Delta\nu = 1/(\alpha+t)$$

19

The pulse sequence described above will generate a train of pulses which will last 14.6 seconds in duration. During the pulse train the CW saturation can be accomplished. The duration of the entire saturation including DANTE and CW saturation is 15 seconds. The DANTE pulse sequence was applied to the PC peak with CW saturation to the γ ATP (Figure 17B). This was done to demonstrate that DANTE and CW could be applied simultaneously and compared to Figure 17A where no saturation was applied to any resonance. To determine if the DANTE and CW saturation had similar effects, both DANTE and CW were applied to PC for 3 seconds. The 3 second saturation was applied at the end of a 15 second saturation of γ ATP. To accomplish DANTE saturation for 3 seconds, a saturation was applied to the PC peak with 10,000 pulses using a pulse width of 0.7 μ seconds and a 290 mili second interpulse delay (Figure 17 E and F). The 3 second saturation from CW was accomplished by starting the CW saturation of PC after 40,000 pulses of DANTE saturation of γ ATP and then completing 10,000 pulses of DANTE for the remaining 3 seconds (Figure 17E) producing incomplete saturation. In both spectra with the short

duration of saturation the saturation is incomplete to a similar extent. In Figure 17D PC is completely saturated with DANTE and γ ATP is not saturated. In this spectrum CW saturation was applied 410 Hz upfield of γ ATP (γ ATP and PC are 410 Hz apart). In Figure 17E γ ATP is completely saturated with DANTE saturation while PC remains unsaturated. CW saturation was applied 410 Hz down field of PC. Figures 17 C and D were performed to demonstrate that DANTE saturation could be selectively applied to either peak of interest and completely saturate said peak.

Methods for T1 Collection

For T1 experiments the arteries were positioned in the magnet as described above. They were unstimulated at 37°C, and perfused with regular PSS for the entire experiment. The tissue was allowed to equilibrate in the NMR for 2 to 3 hours. During this time control spectra were collected. After tissue stability was confirmed from the control spectra, the 90 degree pulse was determined.

The 90 degree pulse was determined by estimating a 180 degree pulse and pulsing the tissue using pulses approximately one half the 180. By systematically changing the pulse width the 90 degree pulse was chosen by being the pulse width which generated the spectrum with the greatest peak height for γ ATP. Once the 90 degree pulse was found the T1 experiments could be performed on the tissue using the technique of progressive saturation.

Progressive saturation was performed to determine the spin lattice relaxation time (T1) of the phosphorus nuclei in the presence of exchange. This technique is frequently used for the measurement of T1 in biological systems because T1 can be determined quickly (47). The disadvantage to this technique is it requires a very accurate 90 degree pulse. The progressive saturation technique involves giving a series of five pulses and collecting the signal after the train of pulses. The duration between the pulses is kept constant until the desired signal to noise is obtained. Then the period of time between the pulses is changed and the process is repeated. The series of time intervals or delays used to obtain the T1s in this thesis is shown in Table 6.

TABLE 6

Delays for Progressive Saturation Experiments.

Series Number	Delay sec.*
1	.0001
2	.001
3	.01
4	.1
5	1.0
6	2.0
7	5.0
8	10.0
9	15.0

* An acquisition delay of 0.204 seconds is added to each of these times.

As the delay is increased the recovery of the nucleus will become more complete. The extent of the recovery can be plotted as delay vs. peak intensity (Figure 15 in Results Section). This plot can be fit to the formula

$$I = A + B \exp (-t/T1)$$

Where t stands for the delay and I is the peak intensity and A and B are constants which are fit to the data. This three parameter fit helps correct for small errors in the 90 degree pulse which would otherwise cause errors in T_1 .

The T_1 for each of the phosphorus nuclei can be determined from a single progressive saturation experiment. However, because of time constraints when using a living tissue, the saturation transfer experiments must be performed on another tissue. Therefore, for rate constant calculations an average T_1 value must be used and not the T_1 of the individual rate constant calculation.

Using an averaged T_1 for all the kinetic experiments assumes that T_1 doesn't change from experiment to experiment. T_1 can be effected by several parameters. To reduce changes in T_1 from experiment to experiment, several precautions have been observed in this thesis. Because field strength can effect T_1 (57,101), the same NMR spectrometer was used for all T_1 calculations and saturation transfer experimtns. Changes in peak position and intensity can also effect T_1 , so unsaturated spectra were obtained at the end of the T_1 experiments to demonstrate no significant changes in the tissues' spectra. If a decrease in peak area of 10% or more was observed in PC peak area, the experiment was discarded. An inaccurate 90 degree pulse is known to cause changes in T_1 , so for every T_1 experiment a 90 degree pulse was determined. Spectra for T_1 experiments were transformed using line broadening

corresponding to 20 Hz. It is assumed that these precautions will decrease changes in T1.

The T1 experiments consisted of 360 summed FIDs collected over a spectral window of 10,000 Hz. The last spectrum collected had a delay of 15 seconds. This was transformed and compared to the last control spectrum before the experiment commenced. This comparison was needed to ensure there were no metabolic changes during the experiment which might have effected the high energy phosphate content and result in an inaccurate T1. Experiments were discarded if changes of 10% or more in PC peak area were observed.

The series of spectra were all transformed with identical processing. After transformation, the series of spectra could be used to calculate individual T1s of any peak. The calculation of T1 was performed by a best fit method as described in the previous section.

Calculation of T1 in the Absence of Exchange

The T1 in the absence of exchange can be calculated from equations in (97):

$$1/\tau = 1/T1_{PC} + k_1$$

and

$$M_{PC}^* = M_{PC}^{\circ} / (1 + k_1 T1_{PC}).$$

τ is the longitudinal rate constant measured in the presence of exchange, $T1_{PC}$ is the longitudinal rate constant in the absence of exchange, k_1 is the pseudo first-order rate constant for the exchange between PC and γ ATP (k_1 is k_f in this thesis), M_{PC}^* is the steady-state PC magnetization when γ ATP is saturated, and M_{PC}° is the steady-state magnetization of PC when there is no saturation. τ , M_{PC}^* , and M_{PC}° were measured experimentally. k_1 and $T1_{PC}$ can then be calculated from the above independent equations, each having the same two unknowns. Similar equations can be used for γ ATP and Pi. During the estimation of the $T1_{\gamma$ ATP, the exchange with Pi was assumed to be negligible at rest relative to the exchange with PC. This assumption was subsequently found to be experimentally valid, since even under stimulated conditions the exchange between Pi and γ ATP is low relative to the CK exchange. For the Pi measurements, the saturated state occurred when both PC and γ ATP were saturated, while the measurement of Pi magnetization in the absence of γ ATP saturation retained the PC saturation. The more rapid relaxation of γ ATP means it will be least effected by exchange relaxation. Similarly, a low change in magnetization upon saturation results in little change in the T1 estimation from the exchangable condition. The calculated values of the rate constants and T1 values in the absence of exchange are presented in the Results Section.

NMR Kinetic Experiments

All NMR experiments were performed in a Bruker wide bore 9.4 Tesla NMR spectrometer. The signal was optimized by shimming on the ^1H resonance at 400.131 MHz. ^{31}P experiments were performed at 161.97 MHz. The perfused tissue was allowed to equilibrate for 2-3 hours before experiments were started. During this time, control unsaturated spectra were obtained. These spectra consisted of 200 summed scans collected 15 seconds apart using the 90 degree pulse. All data were stored in an Aspect 3000 computer interfaced with the spectrometer. Stored free induction decays (FIDs) were Fourier transformed using exponential line broadening corresponding to 35 Hz.

The transformed spectra from the control experiments were compared to each other with regard to time. These spectra demonstrated the viability and stability of the tissue. The tissue was considered stable if the high energy phosphate spectra remained unchanged for 1 hour. The tissue was considered viable if the PC:ATP ratio was greater than 0.4. The estimated concentrations of ATP and PC present in the porcine carotid artery has been reported as 0.70 and 0.51 $\mu\text{mol/g}$ tissue wet weight (38). If either of these criteria were not met the tissue was removed and replaced with fresh tissue.

NMR Peak Integration

Peak integration was accomplished by utilizing the standard integration routine available on the DISNMR software supplied by Bruker Instruments with the Aspect 3000 computer. Integral regions were demarcated with the cursor using a representative spectrum from the series of experiments. Starting immediately downfield of the peak of interest the cursor position was marked. Next the cursor was moved immediately upfield of that same peak and the position marked. The cursor is then moved downfield of the next upfield peak and the marking process repeated. Once all the desired peaks have been demarcated the areas for the integral of each spectra can be obtained using the same demarcations. Phasing and processing of every spectra within an experiment was repeated in the same fashion. During the experiments there was no significant shifting of any of the peak positions such that a peak of interest would fall outside of the demarcated region. Integrals for the peaks of interest were recorded and used to calculate the rate constants.

CST Methods

Conventional saturation transfer (CST) experiments were performed following procedures detailed by Brown, (18,19), and Meyer (97). The resonant frequency of interest was selected and saturated with a monochromatic radio frequency pulse. This results in absence of signal

at the saturating frequency following a 90 degree pulse. The cause for the absence of signal is a randomization of nuclear spin at that frequency. Saturated nuclei maintain the randomization of spin even if they undergo chemical exchange. Exchanged randomization from one nucleus to another during a chemical reaction will effect net magnetization at that resonance accordingly. The change in magnetization can be observed by a diminution of the second resonance. This decrease in magnetization at the second resonance is used to calculate the pseudo first order rate constants (k_f and k_r) of the CK kinetics between ATP and PC.

When ATP is saturated, the forward rate constant (k_f) is determined using the relaxation time (T1) in the absence of exchange for PC and the ratio of the change in magnetization of PC. In this way the k_f for PC degradation can be determined:

$$k_f = (1/T1m) - (1 - M^*/M^0). \quad 21$$

Where: T1m is the spin lattice relaxation time of PC in the absence of exchange, $T1 = T1m / (M^*/M^0)$, M^0 = magnetization without saturation, M^* = magnetization with saturation of PC. If PC is saturated, then the reverse rate constant (k_r) is determined. Control spectra are obtained by saturating off resonance of PC and γ ATP.

The experimental protocol was to obtain unsaturated control spectra

and determine the chemical shift distance between PC and γ ATP. This chemical shift distance was usually 410 Hz. Therefore, 410 Hz downfield of PC is saturated for the first experimental spectrum. PC and γ ATP are then saturated. Finally, 410 Hz upfield of γ ATP is saturated. The saturation downfield of PC is used for M^o during k_f calculations. The saturation upfield of γ ATP is used for M^o during k_r calculations. The flux can be determined from the product of k and the metabolite concentration. The flux ratio is obtained by the product of the pseudo first order rate constant ratios and the peak area ratios. The flux ratio can be used to determine the equilibrium state of the reaction. A reaction at equilibrium will have a flux ratio of one. Spectra were obtained by saturating with a monochromatic continuous wave pulse from a computer controlled Bruker BSV3 synthesizer (Bruker Instruments, Billerica MA). The saturating resonance was sent through the same coil used for pulsing and collecting. The duration of saturation was 15 seconds. This time is sufficient to produce complete saturation of the peak of interest and full relaxation of other peaks between pulses. Each spectrum consisted of 360 summed FIDs. The saturating pulse remained on at all times during the experiment except during pulse and collection. Saturation consisted of 0.4 Watts, which was sufficient power to saturate the PC and γ ATP peaks. The pulse width for collection was 18 μ seconds which corresponded to the 90 degree pulse over a spectral window of 10,000 Hz.

MST Methods

To determine if the ATPase rate can be observed in the carotid multisite saturation transfer (MST) was performed. The carotids were loaded with creatine to increase the PC concentration in the cells and prevent PC depletion during stimulation. Creatine loading has been demonstrated to produce 300-400% increase in intracellular PC concentration (135). The loading is accomplished by soaking the arteries in 40 mM creatine overnight. The creatine loading solution contained 96 mM NaCl, 5.4 mM KCl, 25.3 mM NaHCO₃, 1.1 mM NaH₂PO₄, 2.5 mM CaCl₂, 1.2 mM MgSO₄, 0.01 mM EDTA, 15 mM glucose, 40 mM creatine at 4°C. Using this loading procedure PC content increased by six fold in the carotids (Figure 19).

To further increase ATPase activity, the arteries were stimulated with 75 mM KCl during the NMR experiments. The arteries were prepared for the experiments as described above. The perfusion solution however consisted of 75 mM KCl along with 40 mM creatine and 19 mM NaCl. The other crystalloid concentrations were the same as listed above.

Because of ATPase activity the CK reaction might be considered as a three site exchange (see Background Section) thus multisite saturation transfer would be necessary to accurately determine CK kinetics. The experimental protocol was to prepare the tissue as described above to increase PC concentration and perfuse with the potassium stimulating

PSS. Control spectra were collected for 2-3 hours to determine a steady state for the tissue with regard to potassium stimulation. Multisite saturation was accomplished using the combined continuous wave and modified DANTE technique described previously. The saturation protocol is listed in Table 7.

TABLE 7

<u>MST SATURATION PROTOCOL</u>		
Collection #	DANTE Saturation	CW Saturation
1	PC	Downfield of PC
2	PC	Pi
3	PC	γ ATP
4	PC	Upfield of γ ATP
5	Downfield of PC	Upfield of γ ATP

To determine k_f from an MST experiment the equation:

$$k_f = (\alpha_\gamma / \sigma) [(M_\gamma^* - M_\gamma^{**}) / M_\gamma^*] \quad 22$$

was used.

In this expression M_γ^* is the magnetization of ATP with PC saturated which is determined from Collection 1, Table 7. The parameter σ is defined by the relationship $M_\gamma^0 / M_{Pi}^0 = \sigma [M_\gamma^* / M_{Pi}^*] = k_f / k_r$. The parameter α_γ is equal to $T1_\gamma^{-1}$ plus the sum of the degradation rate

constants of γ ATP. $T1_{\gamma}^{-1}$ is the spin-lattice relaxation time of γ ATP in the absence of any exchange. α_{γ} is the spin-lattice relaxation time of γ ATP while Pi and PC are saturated and can be calculated as described above for the CST experiments. Collection 2 is used to determine M_{γ}^{**} , the magnetization of γ ATP when Pi and PC are saturated. The T1's in the absence of exchange previously calculated were used for all MST kinetic calculations. To determine k_r , Collection 4 was made to determine the value for M_{γ}^* when PC is saturated, and Collection 3 was used for M_{γ}^{**} when γ ATP and PC are saturated. Collection 5 was obtained to confirm tissue stability by demonstrating less than 10% change in the high-energy phosphate metabolite concentration from pre-control values. These measurements are made by defining $ATP \rightleftharpoons Pi$ as k_f and $Pi \rightleftharpoons ATP$ as k_r .

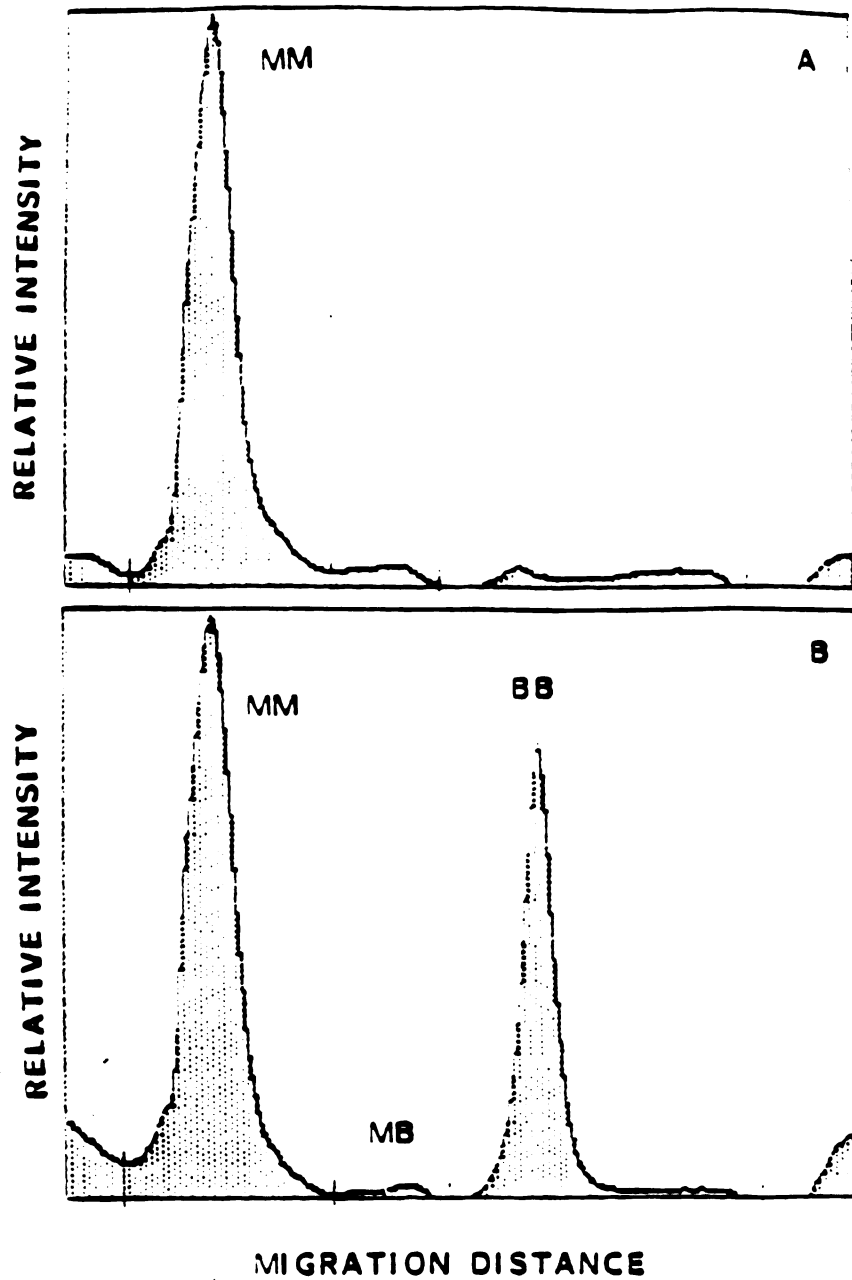
RESULTS

Purification Results

To determine the isoenzyme activities present in the carotid artery, the fluorometric cardiotrac assay method by Corning (Corning, NY) was employed. This method separates the isoenzymes with agarose electrophoresis and measures the activity of the individual isoenzymes using the coupled enzyme assay (discussed in Methods Section) with the production of NADPH measured fluorometrically. The migration by the enzyme closest to the anode is typical of the BB isoenzyme. The MMCK stays closest to origin at the cathode, and MBCK is observed between MM and BB. Figure 6A is a record of the fluorometric absorbance of a control fractionation with known amounts of MM, MB and BBCK. It shows a peak migrating with the characteristics of MMCK and trace amounts of MB and BBCK. Figure 6B is a record of the same control with the purified carotid BBCK added. The specific activity of the enzyme was determined to be 84 units/mg of protein. 96.9% of the activity added to the assay system came from the BBCK isoenzyme. While the remaining 3.1% came from MMCK and no detectable MBCK activity was observed.

Figure 7 is a trace obtained from a fraction of the first homogenate. This represents the distribution of CK isoenzyme activities

Figure 6. Fluorimetric measurement of CK isoenzymes using production of NADPH from the coupled enzyme assay. Figure 6A is a plot of NADPH production vs. migration of agarose (see text). This plot is from a control serum with known MM activity. It contains 86.7% of MM, 4.6% MB, and 8.6% BB respectively. Figure 6B is a plot from purified CK run along with the control. Peak BB demonstrates an increase in CK activity and migrates according to the criteria for BBCK. This plot contains 63.4% MM, 1.5% MB, and 35.2% BB. Subtracting Figure 6A from 6B activity gives 3.1% MM no significant MB and 96.9% BB activity.



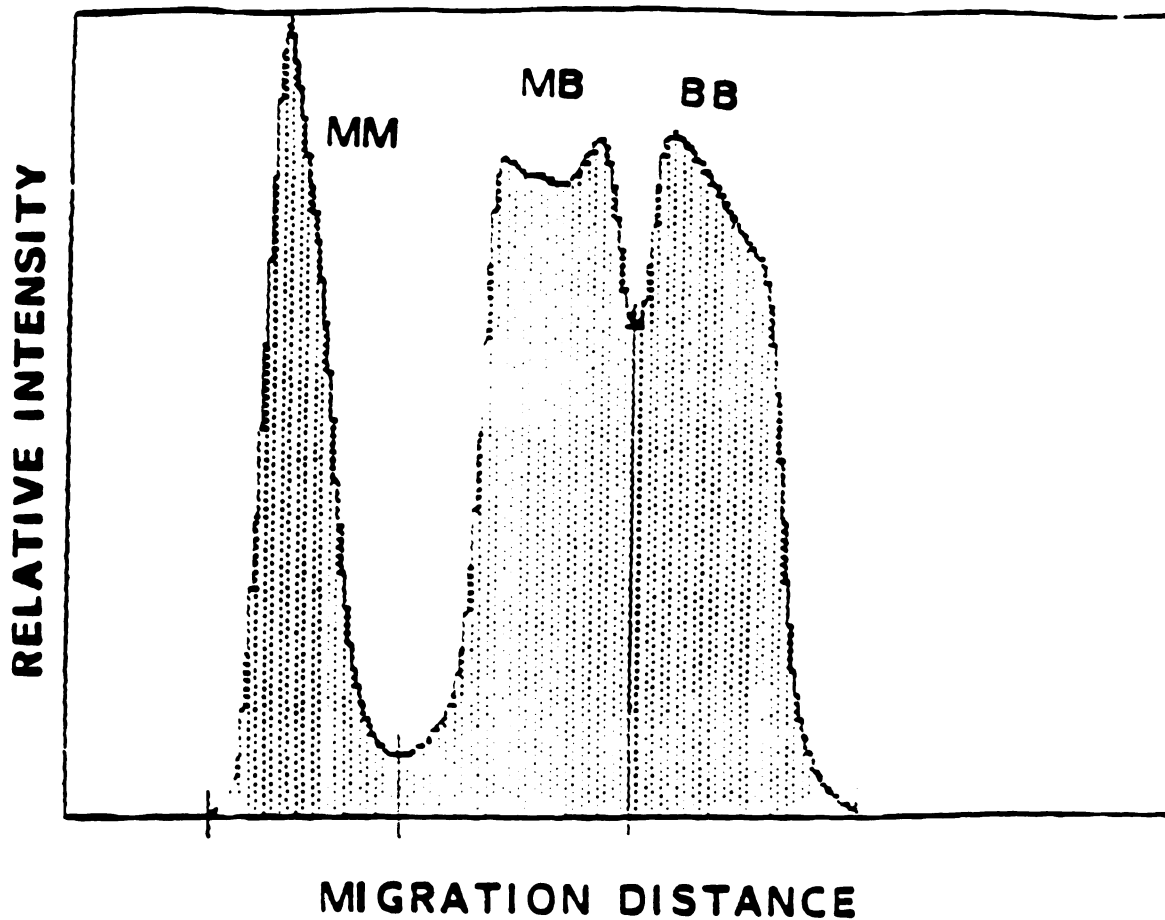


Figure 7. This figure is generated by the same technique used in Figure 6 but is from the crude homogenate without added MMCK. It shows the ratio of isoenzymes coming from the porcine carotid arteries as 23.5% MM, 40.5% MB, and 36% BB. The specific activity for this plot was calculated to be 0.817 U/mg of protein.

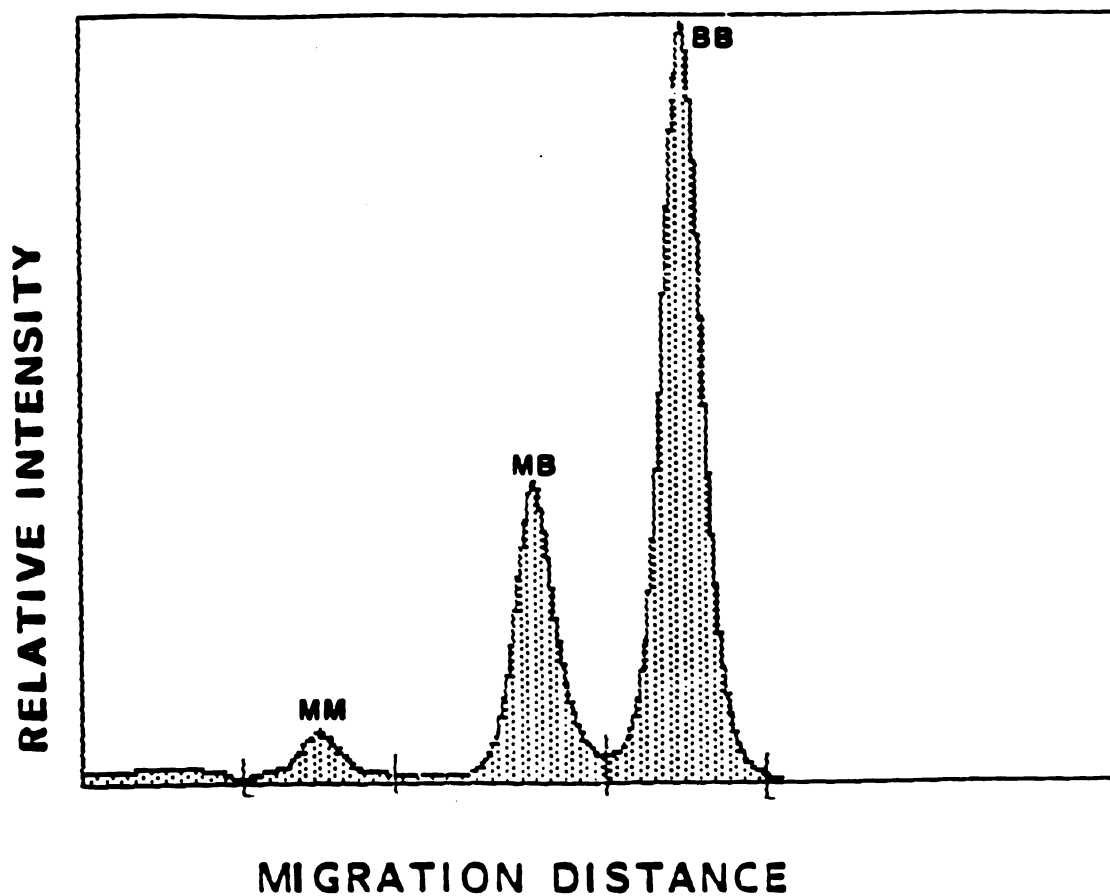
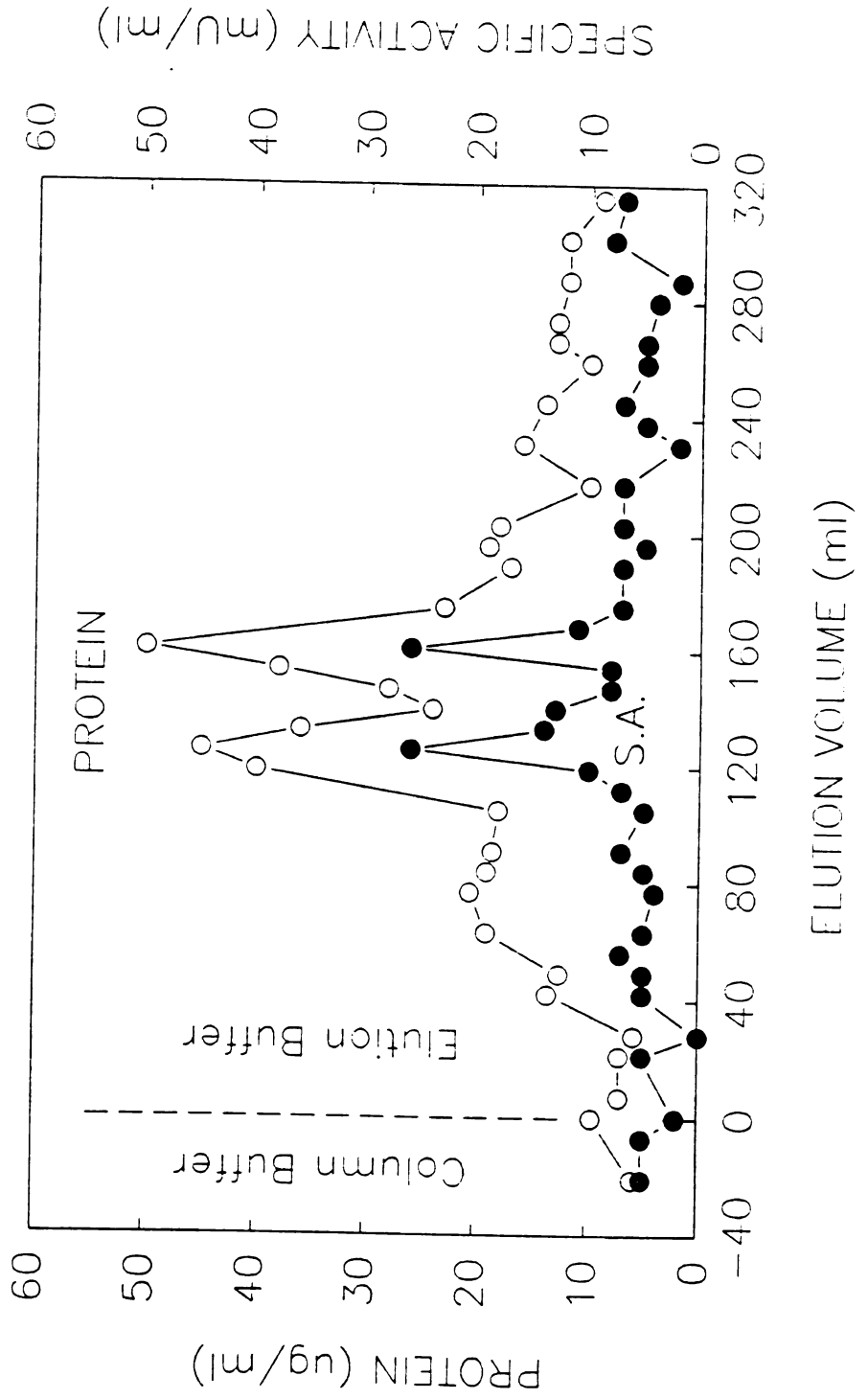


Figure 8. This figure is the isoenzyme fractionation of CK taken after the first alcohol precipitation. This figure was generated using the agarose electrophoresis technique used to obtain Figure 6. The ratio of the peak areas for BB, MB and MMCK was 2:1:0.2 after the second alcohol precipitation.

Figure 9. This figure is the elution profile of protein concentration and kinetic activity taken during the elution of the protein off the hydroxylapatite column. Where: o is protein concentration and ● is specific activity of the enzyme eluted. Samples were taken at 7 ml increments off the column which had a flow rate of about 14 ml/hour.

PORCINE CAROTID ARTERY CK ELUTION PROFILES:
 PROTEIN CONCENTRATION AND SPECIFIC ACTIVITY



present in the carotid artery. It shows that 23.5% of the CK activity comes from MMCK, 40.5% is from MBCK and 36.0% is from BBCK. From these data it can also be determined that the porcine carotid artery has a specific activity 0.81 U/mg of tissue protein.

Figure 8 is a fractionation taken after the first alcohol precipitation. It demonstrates a loss of MM and MB activity while maintaining BB activity. The resulting activity ratio is approximately 2:1:0.2 for BB, MB and MM respectively.

Elution of the essentially purified protein off of the column was accomplished by using 10 mM phosphate buffer solution. This solution contains 10 mM NaH_2PO_4 , 25 mM ME and 0.5 mM EDTA. Figure 9 is a plot of the protein concentration (μg protein/ml) eluted vs. time and specific activity (U/liter) vs. time. Fractions containing 17 $\mu\text{g}/\text{ml}$ protein or greater were pooled for concentration of the protein. The increase in protein concentration and activity paralleled each other. The elevated baseline for protein and activity is indicative of a loss of protein product. Such a loss will decrease the total yield of the procedure. However, no significant loss of specific activity or purity would be predicted.

Figure 10 is an SDS-PAGE of the purified protein stained with silver stain. Lane A contains a fraction from the crude homogenate of the porcine carotid artery. Lane B contains the molecular weight

standard. Lane C contains the purified BBCK. Lane D contains purified BBCK from Sigma Chemical Co.

Table 8 is a table of the results of the activity, yield, and isoenzyme ratio of three different fractions taken during the purification procedure. Fraction one is the crude homogenate. As can be seen, there is an approximately 1:1:1 activity ratio of the three cytosolic isoenzymes. Fraction two is taken after alcohol precipitation and fraction three is taken from the purified enzyme.

Figure 11 was obtained by performing a densitometer analysis on the silver stained gels. Figure 11A is a tracing obtained for the lane containing a fraction taken from the crude homogenate. It demonstrates the presence of many soluble proteins from the carotid artery. Figure 11C was obtained from a fraction of the purified BBCK. It demonstrates one predominating band with two smaller bands of higher molecular weight. Figure 11B is taken from the lane containing BBCK from rabbit brain purchased from Sigma Chemical Company. It demonstrates a similar migration distance for BBCK and also similar migration distances for some impurities. Comparing Figure 11 B and C it can be seen that the BBCK from porcine carotid artery has a greater purification of the BBCK than that of rabbit brain.



Figure 10. This figure is a representation of the electrophoresis of the purified BBCK. Lane 10A contains a fraction of the crude homogenate from the porcine carotid artery. Lane 10B is the Biorad high molecular weight standard. Lane 10C is purified BBCK. Lane 10D is purified BBCK purchased for Sigma Chemical Company.

Figure 11. A, B and C were obtained by an Ultrascan XS scanning densitometer of the silver stained electrophoresis gels. The y axis is the absorbance reading taken from the densitometer. The x axis is the distance along the lane being scanned. The x axis corresponds increasing molecular weight found in the gel. Figure 11A is from the lane containing the crude homogenate of the carotid arteries. Figure 11B is from the lane containing purified BBCK purchased from Sigma Chemical Company. Figure 11C is from the purified BBCK from our experiments.

DENSITOMETER TRACE

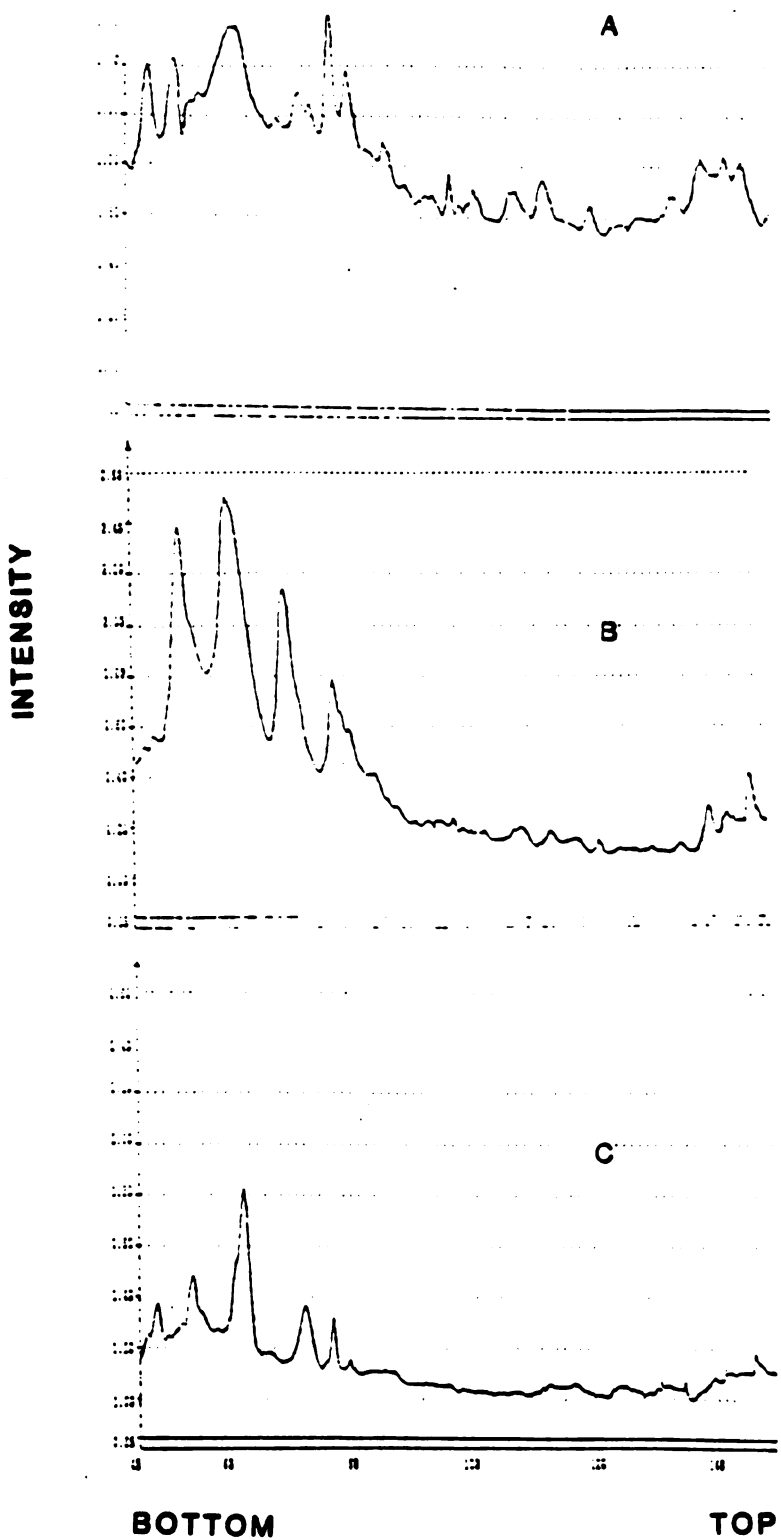


TABLE 8

Purification Steps of BBCK

Fraction #	Activity U/mg protein	Ratio BB:MB:MM	%CK Activity
1	0.8	1:1:1	100
2	11	2:1:0.2	12
3	84	1:0:0	8

Table 8 demonstrates that the alcohol precipitation produces a 88% decrease in total CK activity as can be seen in the differences in the percent CK activity between fraction 1 and 2. This loss of activity is coincident with the loss of MM and MB activity compared to the BB activity demonstrated by the change in the ratios. The specific activity of the purified protein produced in fraction 3 was 84 U/mg protein.

Fluorometric analysis of the electrophoresis demonstrated that the purification procedure produced a significant purification in the BBCK observed and a concomitant decrease in other proteins. A comparison of Figures 11 B and C demonstrates that the purification procedure produces a greater fraction of BBCK than does the BBCK supplied by

Sigma.

Solution Kinetic Results

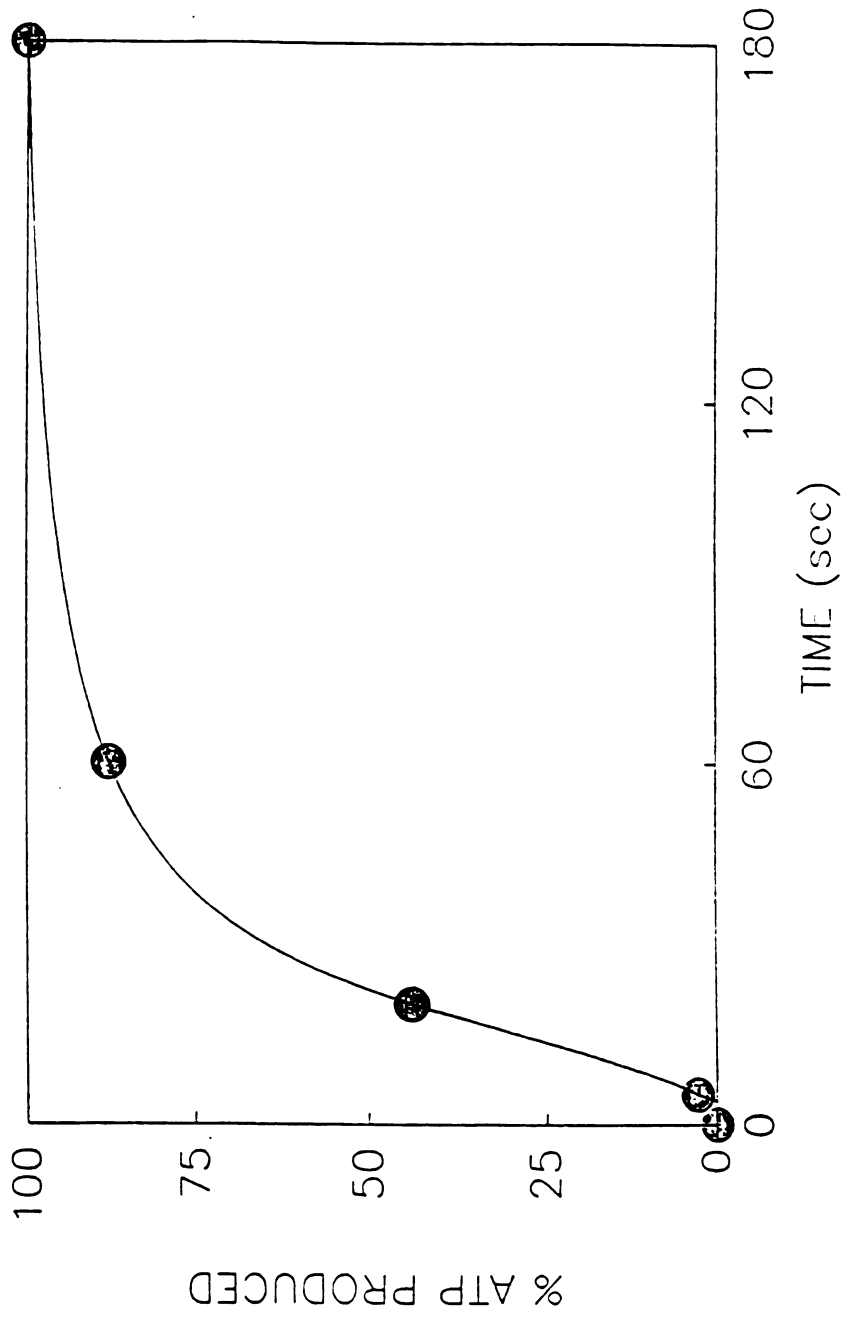
Figure 12A is the progress of the reaction plot determined by measuring percent ATP produced. It demonstrates sigmoidicity of the curve consistent with an allosteric enzyme with a presteady-state interval of about five seconds. Thus, velocity measurements were determined assuming a five second presteady-state interval.

Figure 12 B and C are the velocity plots for the kinetic experiments used to produce Figures 13 and 14. Figure 12B was produced from additions of PC and Figure 12C was produced from additions of ATP.

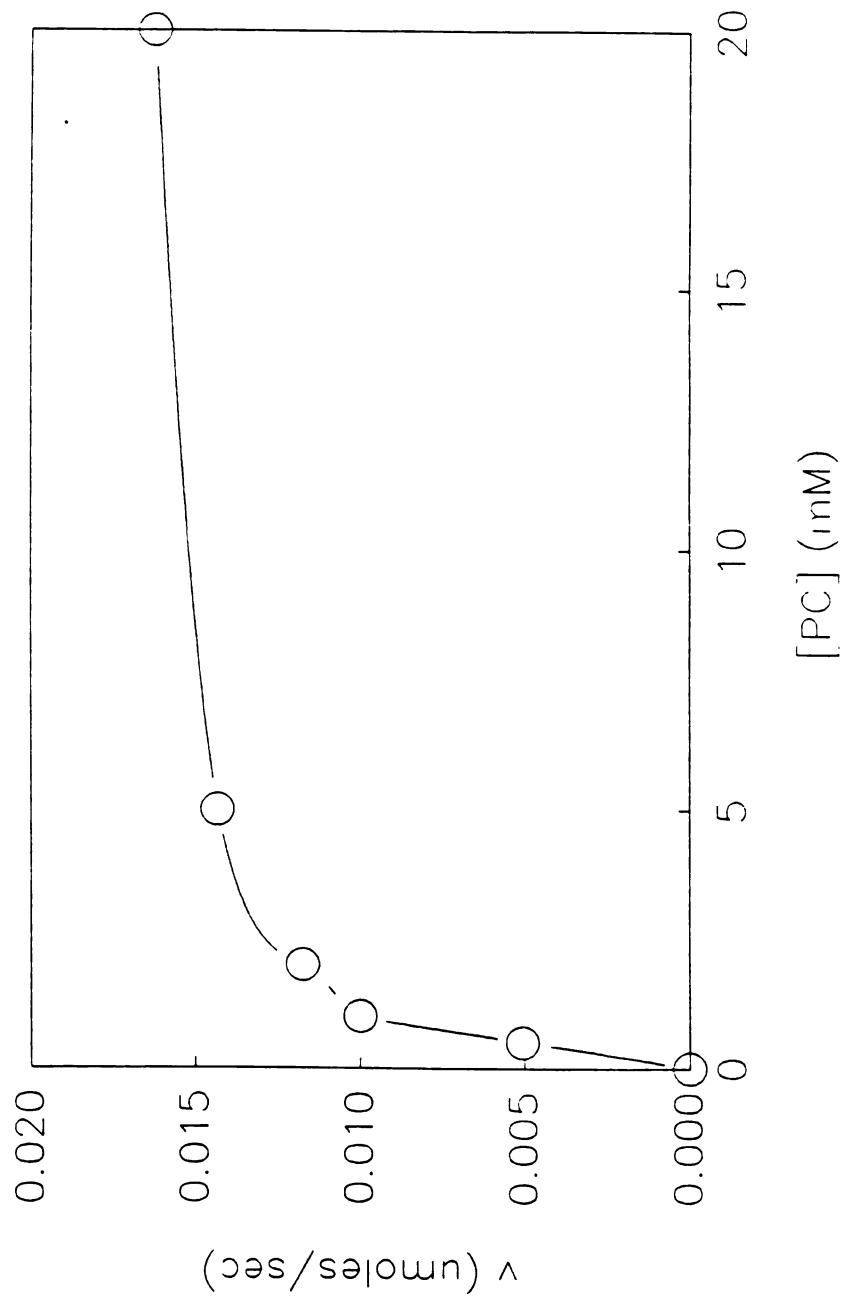
The data obtained from the solution kinetic experiments was used to generate Figures 13 and 14. Figure 13 A, B and C are the Lineweaver-Burke, Hanes-Woolf, and Hofstee plots for PC additions. From these plots V_{max} and K_m can be determined for CK under these solution conditions. It was determined that V_{max} was 0.019, 0.017 and 0.017 $\mu\text{moles/sec}$ respectively. The K_m was found to be 1.32, 0.93, and 0.95 mM respectively. The values for the reverse reaction can be determined from Figures 14 A, B and C. Again these are the Lineweaver-Burke, Hanes-Woolf and Hofstee plots produced by additions of ATP. V_{max} was determined to be 0.29, 0.58 and 0.35 $\mu\text{moles/sec}$ respectively. K_m was found to be 19.4, 42.9 and 16.1 mM respectively (Table 9).

Figure 12A. Progress of the purified BBCK reaction as measured by the % of the ATP produced. Figure 12B is the velocity curve of ATP production from PC additions. Figure 12C is the velocity curve of ATP consumption from ATP additions.

PORCINE CAROTID BB CREATINE KINASE
TIME DEPENDENCE OF ATP PRODUCTION:
PC AND ADP SATURATING



CAROTID BBCK KINETICS: PC ADDITIONS



CAROTID BBCK KINETICS: ATP ADDITIONS

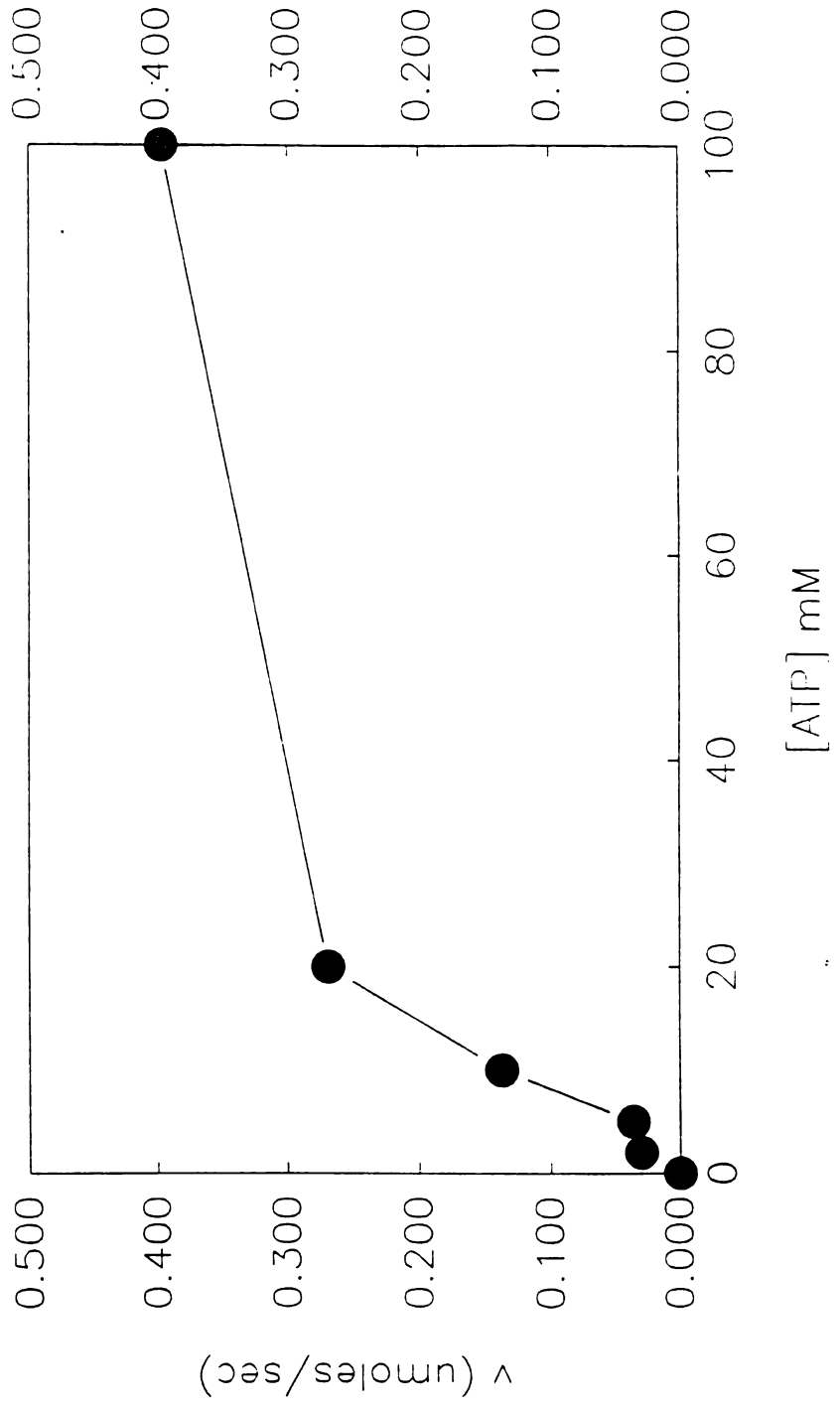
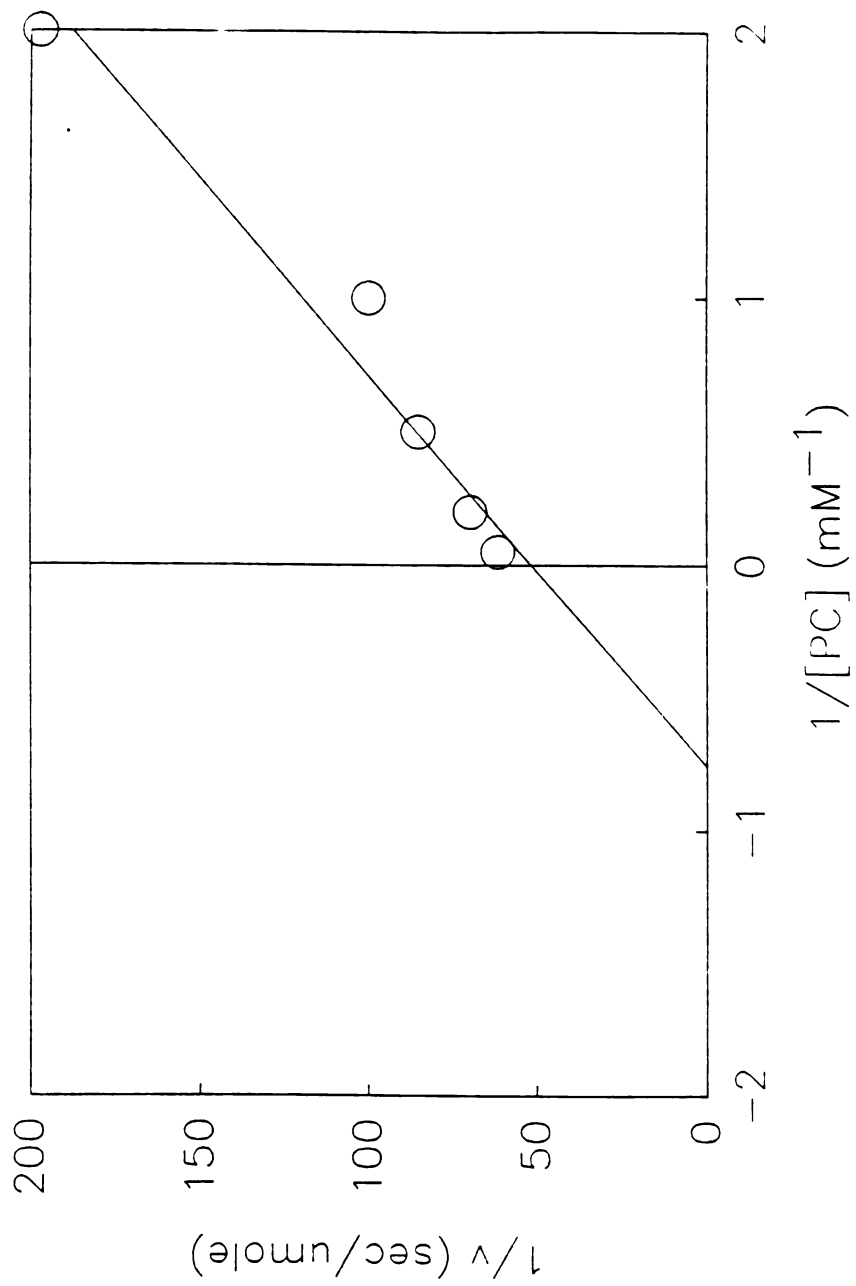
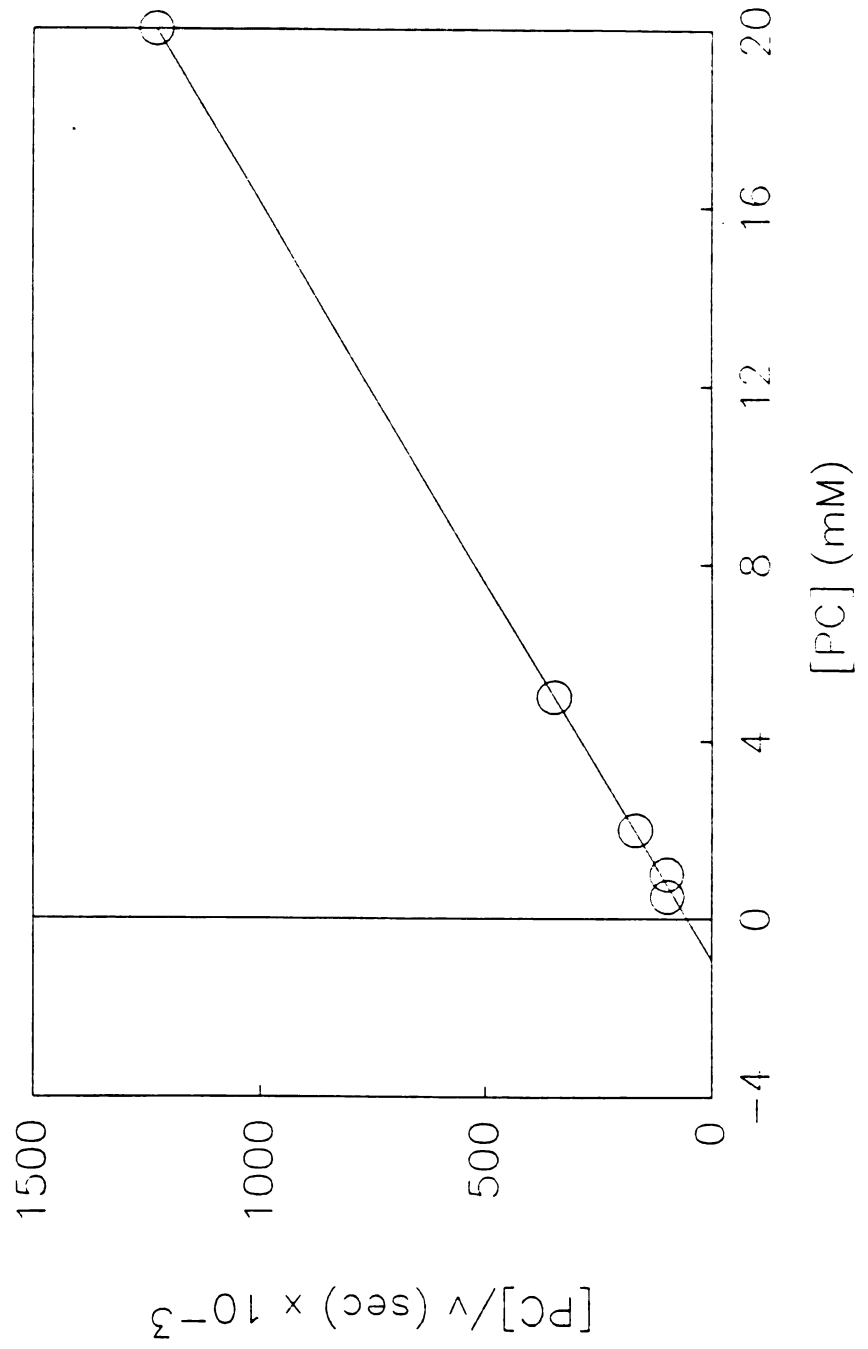


Figure 13 A. This is a Lineweaver Burke plot of the BBCK kinetics with regard to additions of PC. The V_{\max} and K_m for PC determined from this plot is 0.019 mmoles/second 1.32 mM respectively. Figure 13 B is a Hanes-Woolf plot of the BBCK kinetics with regard to additions of PC. The V_{\max} and K_m determined from this plot is 0.017 μ moles/sec and 0.93 mM respectively. Figure 13 C is a Hofstee plot of the kinetics with regard to additions of PC. The V_{\max} and K_m determined from this plot was 0.017 μ moles/sec and 0.95 mM respectively.

L-B PLOT OF CAROTID BBCK: PC ADDITIONS
 $V_{\max} = 0.019$ umoles/sec. $K_m = 1.32$ mM



HI-W PLOT OF CAROTID BBCK: PC ADDITIONS
 $V_{\max} = 0.017$ $\mu\text{moles}/\text{sec}$, $K_m = 0.93$ mM



HOFSTEE PLOT OF CAROTID BBCK: PC ADDITIONS
 $V_{\max} = 0.017$ umoles/sec, $K_m = 0.95$ mM

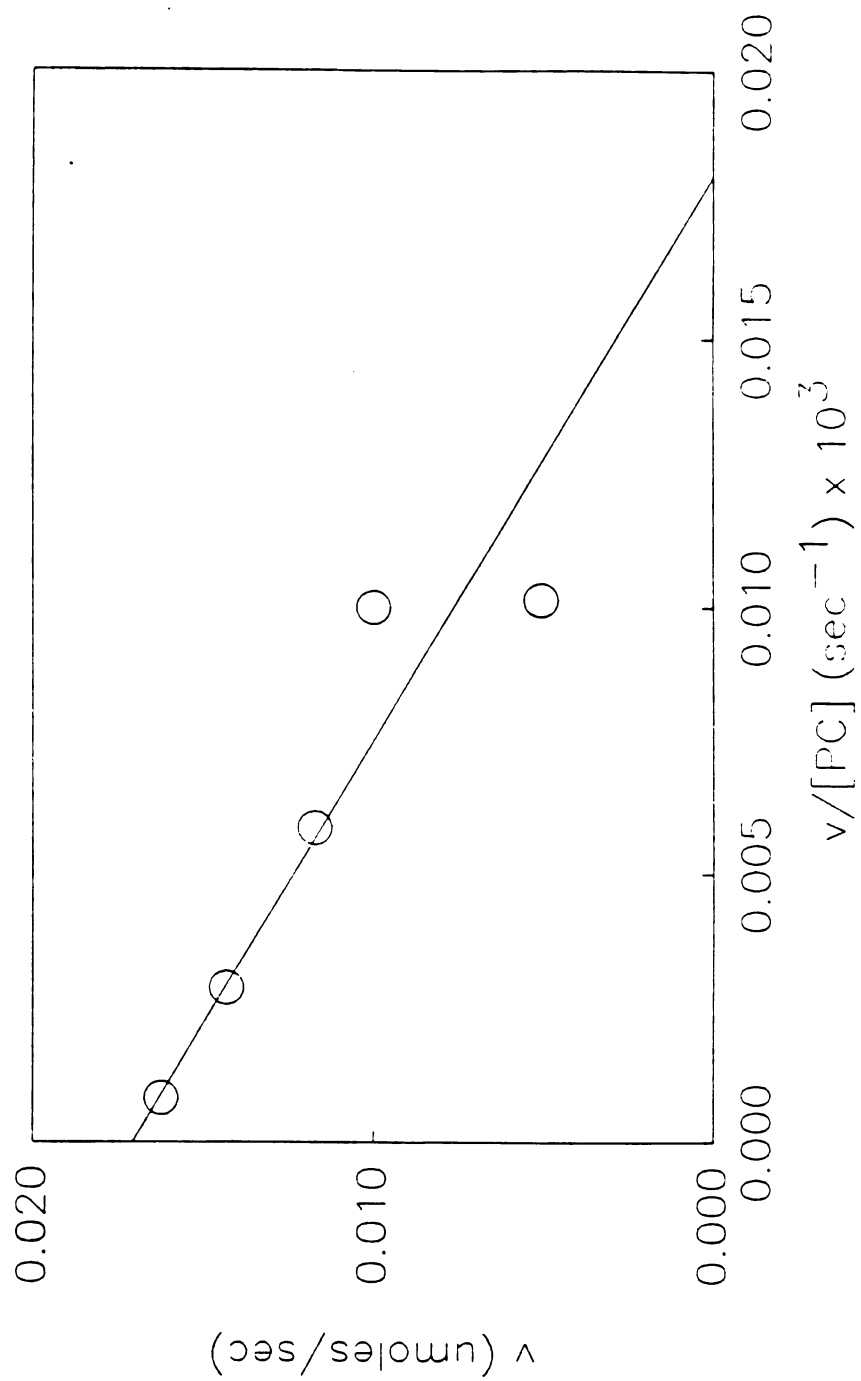
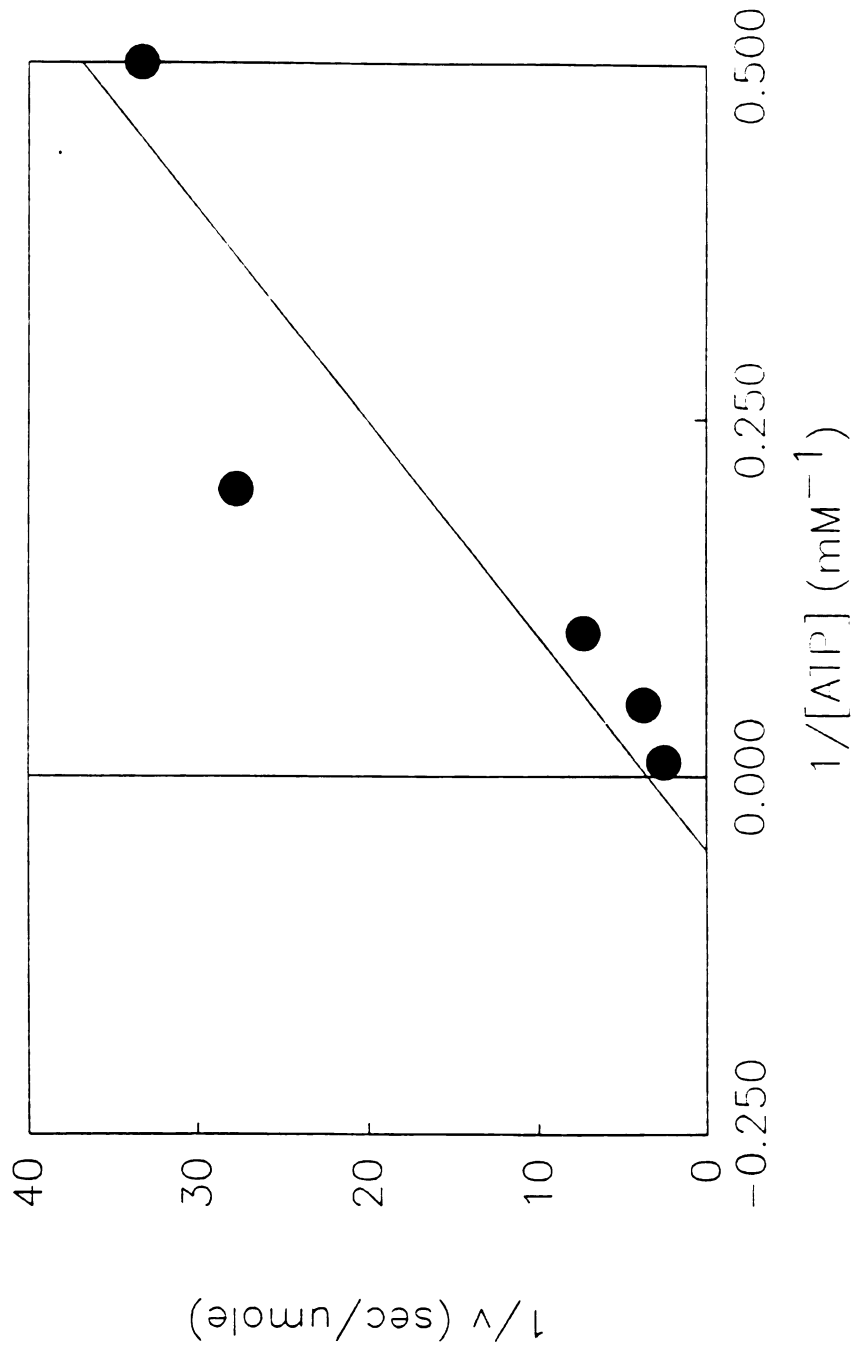
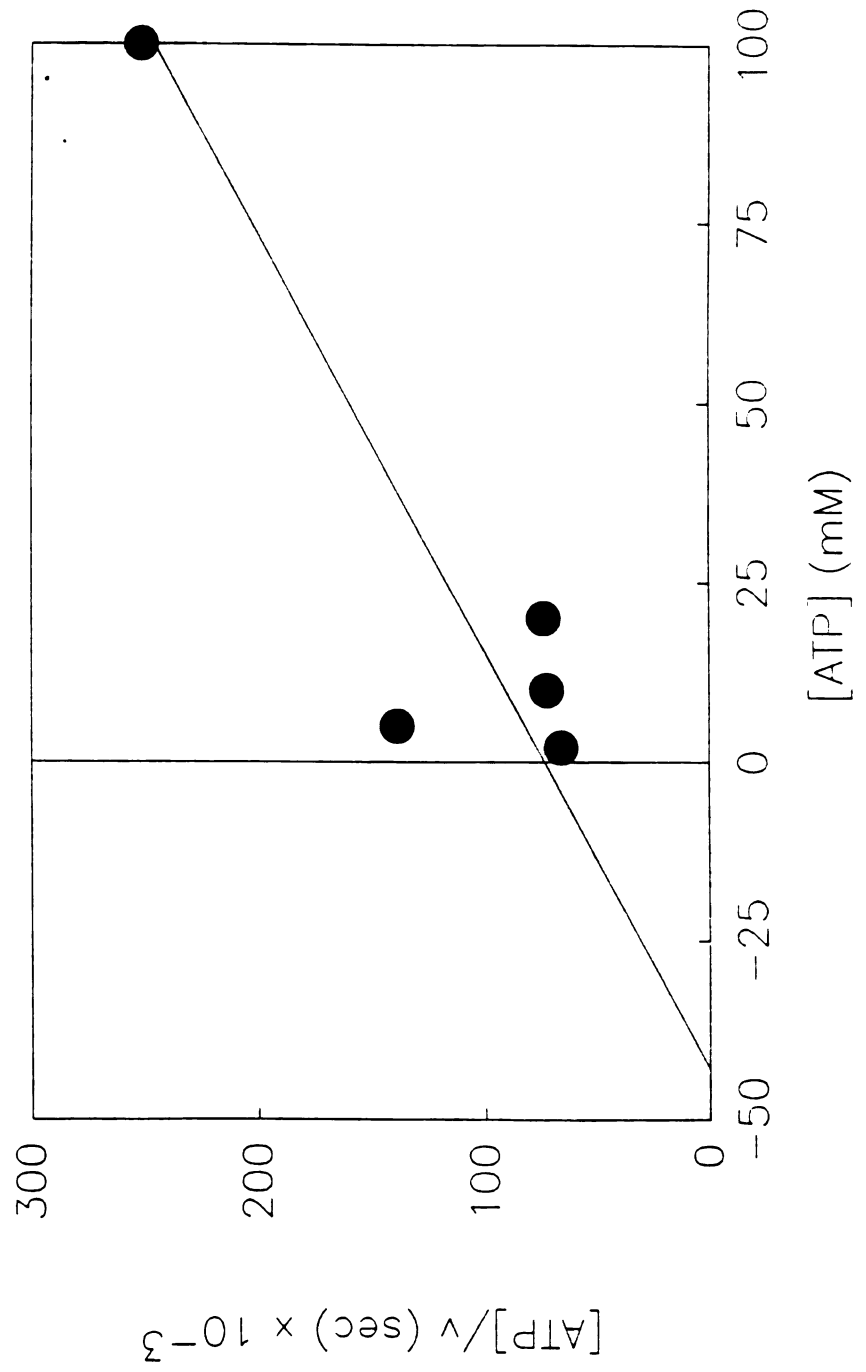


Figure 14 A. This is a Lineweaver Burke plot of the BBCK kinetics with regard to ATP. This plot demonstrated a V_{\max} of 0.29 umoles/second and a K_m of 19.4 mM for ATP. Figure 14 B is a Hanes-Woolf plot of BBCK kinetics with regard to ATP additions. The V_{\max} and K_m determined from this plot was 0.58 μ moles/sec and 42.9 mM respectively. Figure 14 C is an Hofstee plot of BBCK kinetics with regard to ATP additions. The V_{\max} and K_m determined from this plot was 0.34 μ moles/sec and 16.1 mM respectively.

L-B PLOT OF CAROTID BBCK: ATP ADDITIONS
 $V_{\max} = 0.29$ umoles/sec, $K_m = 19.35$ mM



H-W PLOT OF CAROTID BBCK KINETICS: ATP ADDITIONS

 $V_{\max} = 0.58$ umoles/sec, $K_m = 42.88$ mM

HOFSTEE PLOT OF CAROTID BBCK KINETICS: ATP ADDITIONS

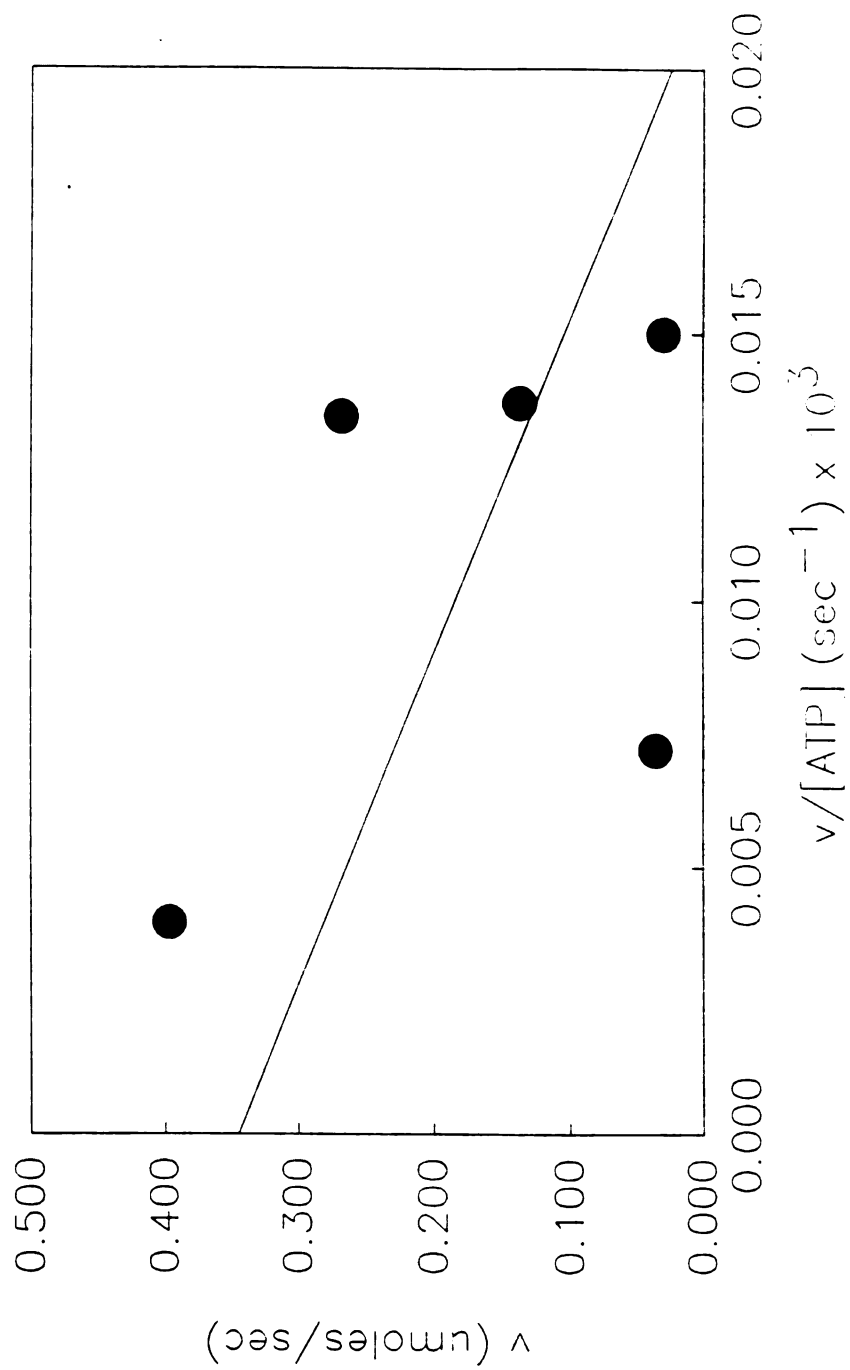
 $V_{\max} = 0.345$ umoles/sec, $K_m = 16.06$ mM

TABLE 9

KINETIC DATA SUMMARY

PC Additions:

	V_{max}^*	K_m^\dagger	R
Lineweaver-Burke	0.019	1.32	0.977
Hanes-Woolf	0.017	0.93	1.000
Hofstee	0.017	0.95	0.919

ATP Additions:

Lineweaver-Burke	0.29	19.3	0.905
Hanes-Woolf	0.58	42.9	0.898
Hofstee	0.35	16.1	0.489

* $\mu\text{moles/sec}$

† mM

Table 9 summarizes the range of values for kinetic data. The resulting K_m values for ATP has a relatively large range of 16.1 to 42.9 mM. It appears that the K_m for ATP is much higher than the concentration of ATP found in carotid artery (0.7 mM). The R values determined for each plot demonstrates values from 0.489 to 0.905 for the ATP additions while PC additions data had R values from 0.919 to 1.000. The low R value observed for the Hofstee plot makes it a questionable

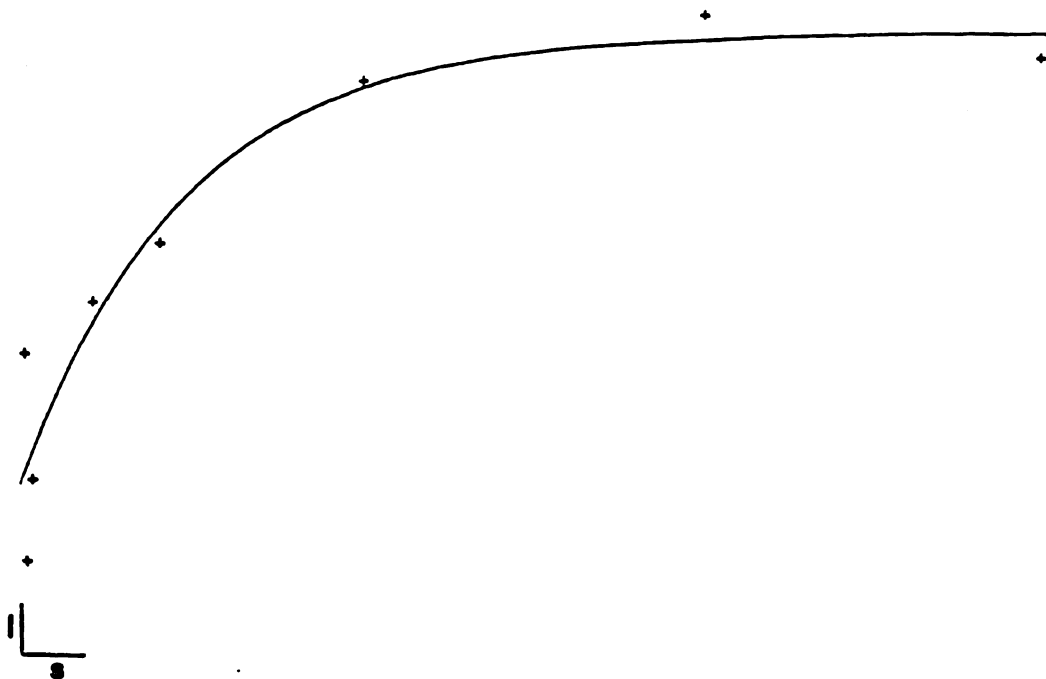


Figure 15. This figure is the computer generated plot of delay vs peak intensity to determine the T_1 of PC. The fitted curve was fit to the formula $I = A + B \exp(-t/T_1)$. Where t stands for the delay between pulses and I is the peak intensity. The values of A and B are constants which are fit to the data. In this particular experiment the calculated value for T_1 was 2.46 seconds.

estimator of K_m and V_{max} . The other methods should still be sufficient for estimating the kinetic data, however. The similar results and higher R values for PC additions produce strong estimates for their K_m and V_{max} values.

NMR Results

The T1 experiments generated T1s for Pi, PC, and γ ATP (Figure 15). Though other peak's T1 is available from the experiments they are not needed for the kinetic calculations, so they were not determined. T1 values in the presence of exchange calculated for Pi, PC and γ ATP were 3.80 ± 0.55 , 2.85 ± 0.53 , and $1.05 \pm 0.11 \text{ s}^{-1}$ respectively (n=5, SE). These values were used for calculating the T1 in absence of exchange and for the calculation of the forward and reverse rate constants for CST and MST experiments.

CST Results

The CST experiments performed produced the changes in magnetization listed in Table 10.

TABLE 10

Magnetization Changes from CST Experiments

	Experiment number					
	1	2	3	4	5	6
PC area	15.5	25.9	34.8	28.9	13.4	21.8
PC* area	10.0	20.9	19.7	10.3	6.8	11.1
γ ATP area	32.9	49.1	79.3	44.8	35.6	80.6
γ ATP** area	31.2	47.3	68.3	34.8	30.6	69.2

* areas of PC when γ ATP is saturated.

** area of γ ATP when PC is saturated.

Values of peak areas seen in Table 10 are relative intensity values. They do not reflect actual units of concentration. The ratios of the peak areas do correspond to the ratio of metabolites in the tissue in these unsaturated spectra. The change in magnetization is indicative of molecular exchange from the saturated species. Table 11 lists the rate constants for each experiment and the mean of $0.17 \pm 0.04 \text{ s}^{-1}$ (SE n=6) for k_f and $0.12 \pm 0.03 \text{ s}^{-1}$ for k_r (SE n=6). The individual values found in Table 11 were calculated using the mean T1 for γ ATP and PC in the absence of exchange of 1.2 and 5.2 seconds respectively. These values were calculated using the solution discussed

in the Methods Section for estimating T1 in the absence of exchange.

TABLE 11

Pseudo First Order Rate Constants* for CK Reaction
Determined by CST Experiments

	Experiment number						
	1	2	3	4	5	6	Mean(SE)
k_f	0.11	0.05	0.15	0.35	0.19	0.19	0.17 ± 0.04
k_r	0.05	0.03	0.14	0.24	0.14	0.14	0.12 ± 0.03

* seconds⁻¹

To determine if the CK reaction was at equilibrium it was necessary to determine whether the flux ratios of the reactants and products were significantly different than one. This was accomplished by calculating the ratio of the rate constants and the ratio of the unsaturated peak areas. The flux ratio is calculated from the expression: $[k_f \times PC]/[k_r \times \gamma ATP]$. Table 12 illustrates these ratios from the individual experiments.

TABLE 12

Ratios of CST Results

Experiment number

	1	2	3	4	5	6	Mean(SE)
Ratio of PC/ γ ATP	0.47	0.53	0.44	0.64	0.38	0.37	0.47 \pm 0.06
Ratio of k_f/k_r	2.28	1.44	1.09	1.45	1.37	1.35	1.50 \pm 0.18
Flux Ratio	1.07	0.76	0.48	0.93	0.52	0.50	0.71 \pm 0.11

The mean flux ratio demonstrated in Table 12 is the product of peak area ratios and rate constant ratios. The value of 0.71 ± 0.11 is less than one. A reaction with a flux ratio away from one is indicative of a reaction not at equilibrium. In the results above this could be due to an underestimation of the PC content in the cell. The small peak height of PC and the signal to noise associated with the spectrometer can produce an underestimation of the integrated area of PC (96b) and thus lead to a flux ratio less than one.

MST Results

Figure 17 shows spectra from the ATP-PC solution with multiple saturation sites. Figure 17A shows the control spectrum. In Figure 17B, the DANTE pulse sequence was applied to the PC peak and CW saturation to the γ ATP. This was done to demonstrate that DANTE and CW can be applied simultaneously. In Figure 17C, γ ATP is saturated using DANTE, while CW is applied 410 Hz downfield of PC. In Figure 17D, PC is saturated by DANTE, and CW is applied 410 HZ upfield of γ ATP. To determine if the DANTE and CW saturation had similar effects, both were used to partially saturate PC during complete γ ATP saturation. CW saturation was applied to PC for three-seconds while DANTE was applied to γ ATP for 15 seconds, and then DANTE was applied to PC for three-seconds while CW was applied to γ ATP saturated for 15 seconds. The three second saturation of PC was applied during the final three seconds of the 15-second saturation of γ ATP. The three second saturation using CW was accomplished by starting the CW saturation of PC after 40,000 pulses of DANTE saturation of γ ATP, and then completing 10,000 pulses of DANTE for the remaining three seconds (Figure 17E). To accomplish the DANTE saturation for three-seconds, 10,000 pulses were applied to PC with a pulse width of 0.7 μ seconds and a 290 millisecond interpulse delay during the final three seconds of the 15-second γ ATP saturation by CW (Figure 17F).

Tissue saturations, of non-creatine loaded unstimulated arteries, are shown in Figure 18 to demonstrate the ability to saturate multiple peaks in a tissue. Figure 18A shows a control spectrum where DANTE

and CW are applied 410 Hz downfield of PC and 410 Hz upfield of γ ATP, respectively. In Figure 18B, PC is completely saturated by DANTE and γ ATP is not saturated. In this spectrum, CW saturation was applied 410 Hz upfield of γ ATP. In Figure 18C, PC is saturated by DANTE and Pi is saturated by CW. The residual peak observed at the Pi resonance may be due to the Pi in the perfusion solution which enters the observable region of the spectrometer without being sufficiently irradiated to effect complete saturation. In Figure 18D, γ ATP is completely saturated by CW saturation while PC remains saturated with DANTE. Figure 18E has CW and DANTE saturation 410 Hz downfield of PC and 410 Hz upfield of γ ATP.

Creatine loading produced an increase in the PC concentration of six fold (Figure 19). The results from the MST experiments, which were performed on the creatine loaded and potassium stimulated arteries, are summarized in Table 13. The data indicate that the reaction of ATP to Pi (k_f) was $0.07 \pm 0.08 \text{ s}^{-1}$ and k_r of $0.005 \pm 0.004 \text{ s}^{-1}$.

Table 13

Kinetic Data from MST Experiments on Porcine Carotid Arteries (n=4)

	Experiment number				Mean (SE)
	1	2	3	4	
k_f^*	0.20	-0.02	-0.07	0.17	0.07 ± 0.08
k_r^*	0.013	-0.002	0.007	0.0	0.005 ± 0.004

* seconds⁻¹

The mean values from Table 12 are not significantly different than zero. Thus no significant ATPase activity is measurable using MST under the described conditions. These data were unable to determine a usable value for the ATPase rate constants. This result is due to low ATPase activity in the porcine carotid artery. The slow ATPase rate may be below the resolution of the NMR spectrometer. MST experiments were not performed to determine the CK kinetics because the PC concentration increases during creatine loading to such a concentration that small changes in the peak area could not be accurately measured.

Absence of observable ATPase under stimulated conditions and the

presence of measurable CK activity under unstimulated conditions may obviate the need for a three site model in vascular smooth muscle.

This concept is discussed in greater detail in the Discussion Section.

Figure 16. The ^{31}P spectra of porcine carotid arteries during a CST experiment. Spectra were collected with 400 summed FID's. Figure 16A is a control spectrum with saturation upfield of γATP . Figure 16B is a spectrum with γATP saturated. Figure 16C is a spectrum with PC saturated. Figure 16D is a control spectrum with saturation downfield of PC.

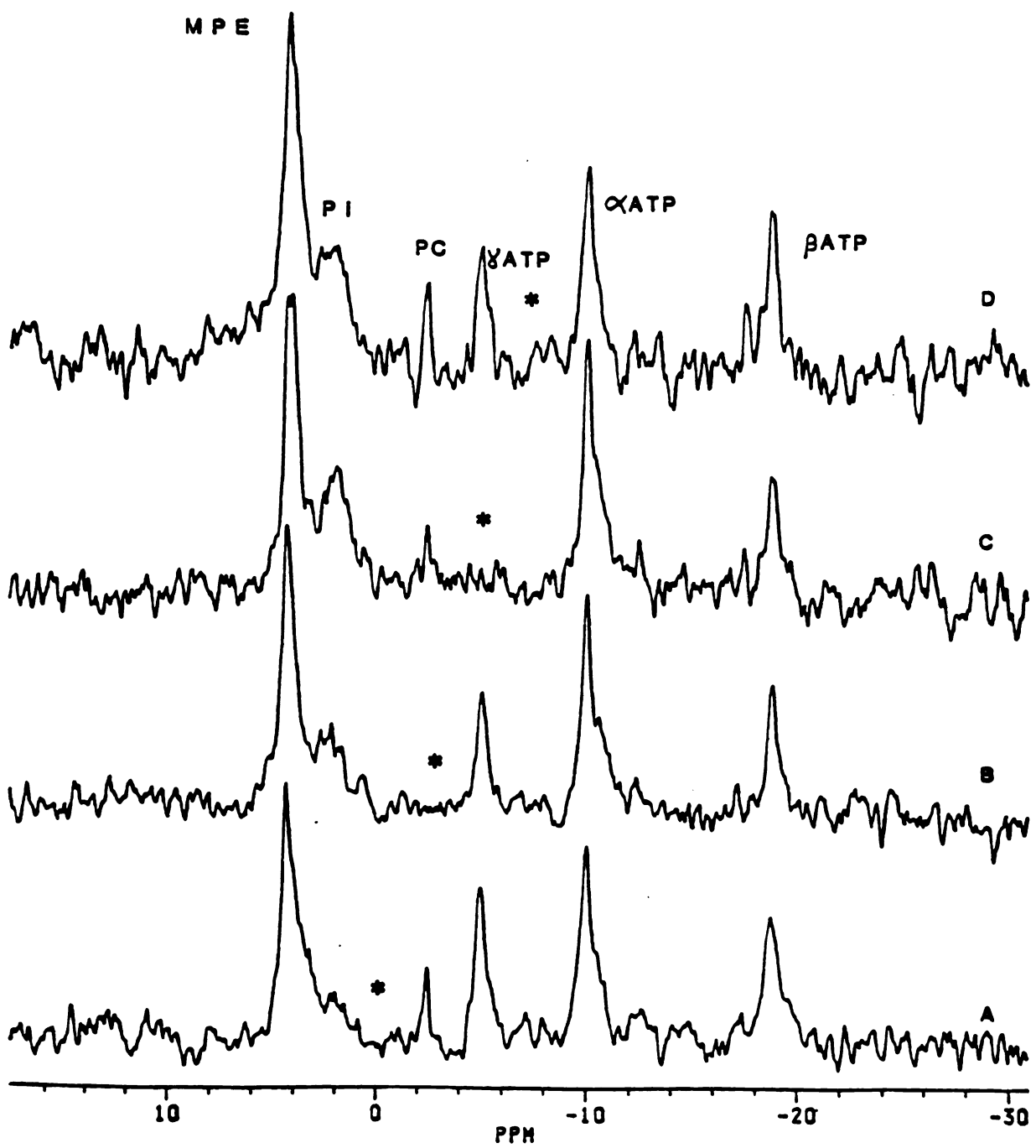
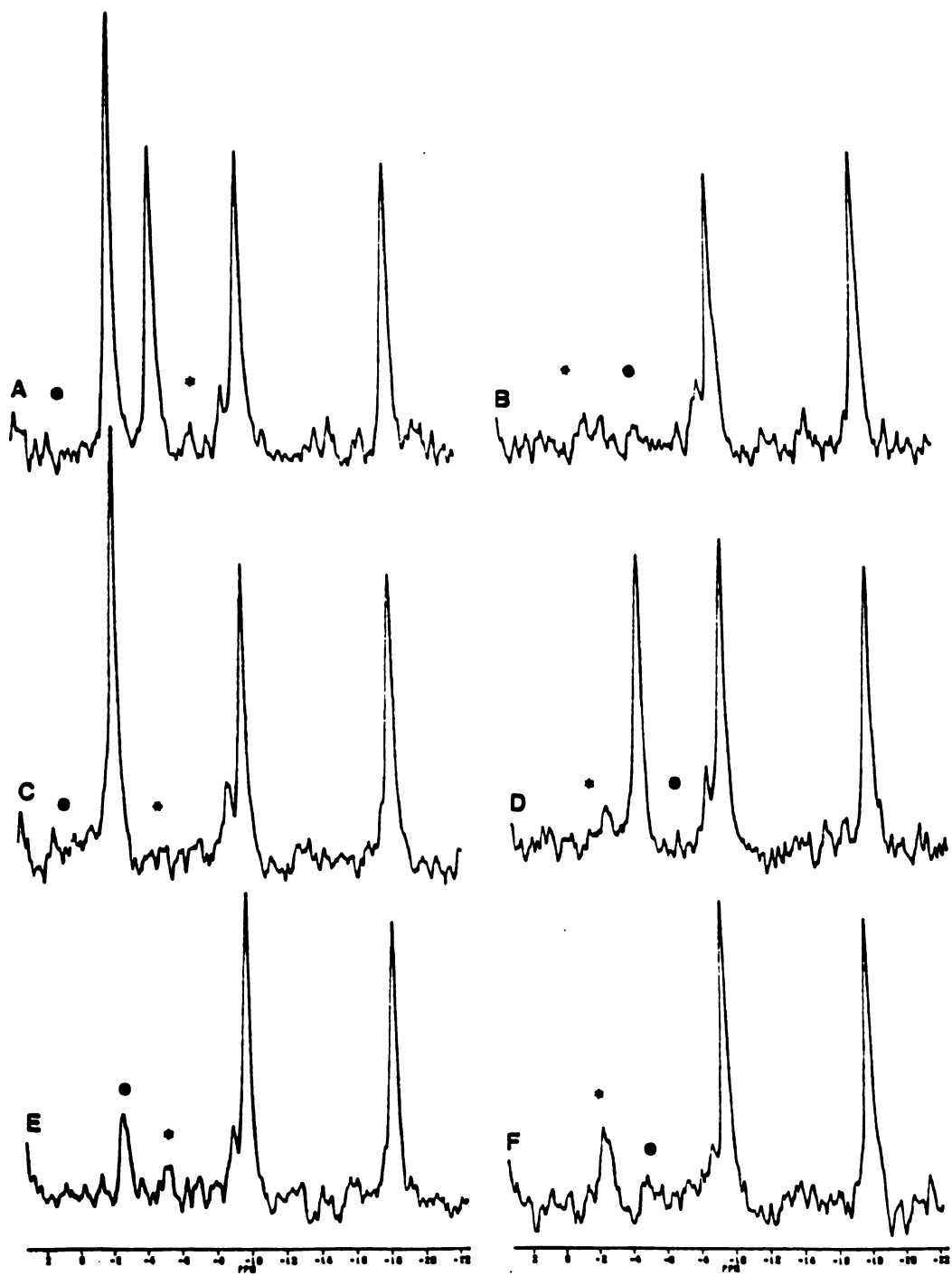


Figure 17. This is a figure of six spectra taken using an ATP, PC solution (see text for concentrations) to demonstrate the effectiveness of the DANTE pulse sequence. Figure 17A is a control spectrum without saturation to any resonance. Figure 17B is a spectrum with PC saturated with DANTE (♣) and γ ATP saturated with CW (●) for 15 seconds. In this case, the DANTE consisted of 50,000 pulses with a pulse width of 0.7 μ seconds and an interpulse delay of 290 milliseconds. Figure 17C is a spectrum which was obtained by saturating γ ATP with DANTE as described for Figure 17B and CW saturation 410 Hz down field of PC. Figure 17D is a spectrum obtained by saturating PC with DANTE similar to Figures 17B and C. CW saturation was applied 410 Hz upfield of γ ATP. Figure 17E was obtained by saturating PC for 3 seconds with CW saturation and γ ATP with 15 seconds of DANTE saturation. Figure 17F was obtained by saturating γ ATP with 15 seconds of CW saturation while PC was saturated with 3 seconds of DANTE saturation. The 3 seconds of DANTE saturation was accomplished by pulsing 10,000 times with a pulse width of 0.7 μ seconds and with an interpulse delay of 290 milliseconds.



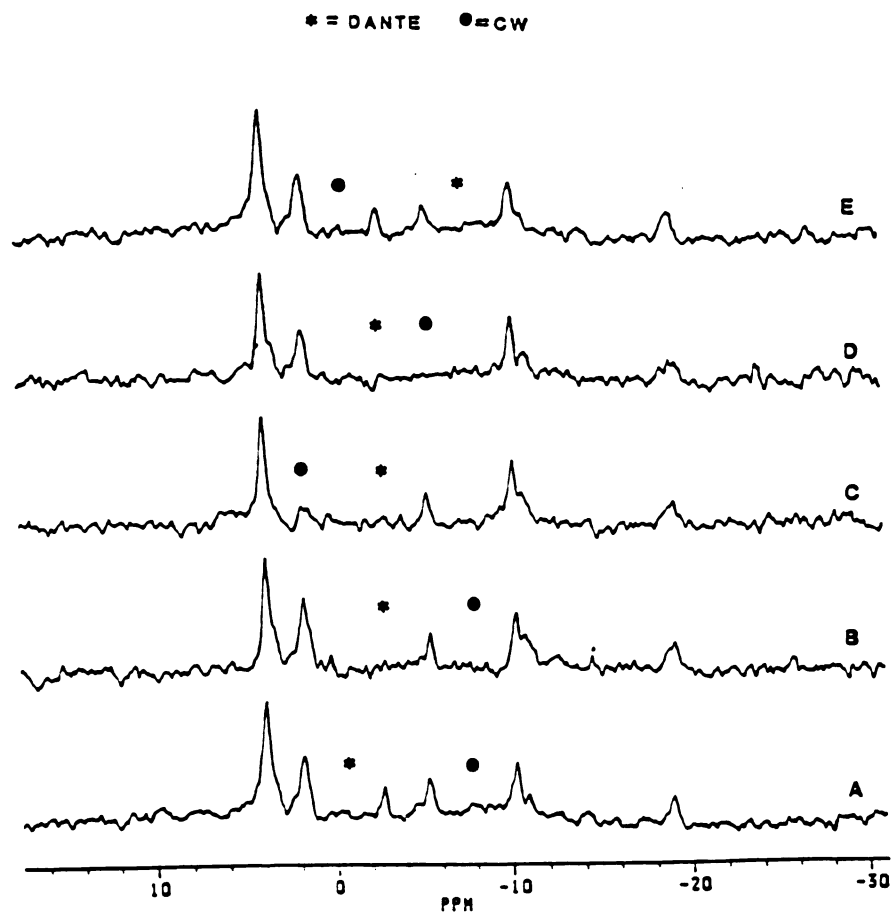


Figure 18. ^{31}P NMR spectra of unstimulated porcine carotid arteries during a sample MST experiment. Spectra 18A and E are control spectra where off resonance saturation has been accomplished with DANTE or CW as indicated by * or ● respectively. Spectra 18B, C, and D demonstrate the ability of DANTE and CW techniques to saturate various peaks and multiple peaks.

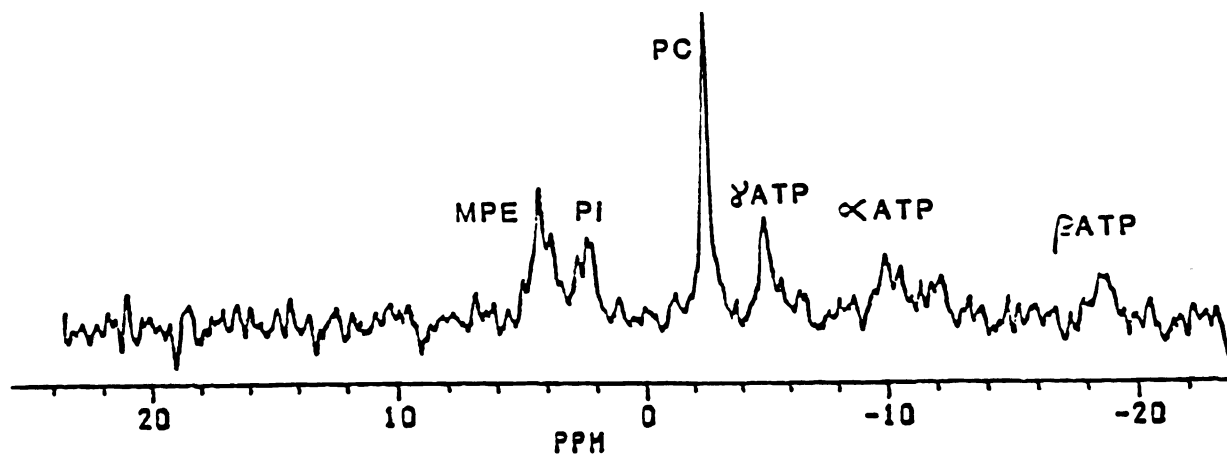


Figure 19. Spectrum of unstimulated carotid artery which has been loaded with 40 mM creatine. Creatine loading and spectra acquisition parameters are described in the text. The increase in the PC resonance represents an increase in tissue concentration of PC which is seen with creatine loading.

DISCUSSION

Purification

BBCK can be purified from porcine carotid arteries separate from the other two cytosolic isoenzymes of CK present in the tissue. During the purification procedure, the BBCK specific activity increases (Table 8). A large drop in total CK activity occurs during the alcohol precipitation. The CK lost during the precipitation may be bound to insoluble proteins or become insoluble itself upon addition of the ethanol. The CK which remains after the precipitation is adsorbed onto the hydroxylapatite column. For adsorption on the column to occur, CK must demonstrate an affinity for the adsorbent (hydroxylapatite). CK is known to be inhibited by Pi (56,95,109) and thus it might be predicted that it may have some form of molecular (e.g., hydrophilic) interaction. For chromatography to be successful, there must be a binding or molecular interaction occurring between the two molecules. This interaction between BBCK and the phosphate of hydroxylapatite results in the enzyme being eluted off of the column by the elution buffer. This concentration of phosphate could significantly inhibit CK if it remained 10 mM (55,95,109). However Wang and Cushman (174) determined that a significant amount of phosphate is dialyzed away from the enzyme solution such that phosphate inhibition is not a concern for BBCK.

Multiple Isoenzymes

Usually smooth muscle tissue is considered to contain a significant amount of BBCK activity (65,71, 123). However, there are variations in the ratio of BBCK to the other forms ranging from 97% BB to 42% BB (Table 3)(71). Such variations may be due to the metabolic differences found in the various smooth muscle tissues. Grossman (52,53) has studied these tissue and isoform differences and these results are summarized in the Background Section of this thesis. Grossman believes that isoenzyme differences may predicate subcellular localization of isoenzymes.

The results from the fractionation experiments demonstrated three cytosolic isoenzymes of CK present in the porcine carotid artery having an activity ratio of approximately 1:1:1. Though variations in the activities of cytosolic CK have been reported for smooth muscle a 1:1:1 activity ratio has yet to be reported. The presence of multiple isoenzymes and their role(s) in the tissue becomes increasingly convoluted in light of the observed differential solubilities of the isoenzymes with ethanol. The possibility of subcellular localization of the isoenzymes due to their differential solubility is a plausible explanation for these data. This explanation however, has not been rigorously investigated.

CK Elution Profile

During the purification procedure it was observed that the alcohol precipitation produced a large shift in the ratios of the cytosolic isoenzymes towards the BBCK isoform and away from the MMCK isoenzyme. Hydroxylapatite chromatography appeared to also shift the activity ratio towards BBCK. The alcohol precipitation produced a loss of approximately 88% of the total CK activity. Much of this lost CK activity may be due to the loss of MM and MB activity which could be as much as 64% of the activity (see Figures 11-13). The remaining loss of CK activity may be due to unrecoverable BBCK but with an increase in specific activity following chromatography.

The hydroxylapatite chromatography resulted in essentially purified BBCK. This purification step also produces a loss of CK activity but there is a seven fold increase in the specific activity. It appears from the results that the hydroxylapatite chromatography step purified the BBCK from residual protein contaminants, MB, and MM isoenzymes. The apparently elevated baseline for protein concentration and CK activity seen in Figure 6 is most probably due to the presence of a mixture of BBCK which is being lost and MBCK and MMCK which has persisted through the purification scheme and/or small amounts of unknown protein impurities.

The elution profile observed in Figure 6 demonstrates two well defined peaks of CK being eluted from the column. Two peaks being eluted off the column could be interpreted as two different proteins

being eluted. However, the results from the isoenzyme fractionation and electrophoresis demonstrated one isoenzyme and one predominating protein. The reason(s) for these purification data may have several different explanations.

First, the two peaks eluted off the hydroxylapatite column may be produced by an elution of two different variants of the BBCK. Variants of the MMCK have been found by Takasawa et al (149,150,151) as well as others (158). However, determination of variants of BBCK within a tissue has not been thoroughly investigated though the results of Grossman (52) and Focant (45) describe BBCK variants between tissues. If there were two variants of BBCK that had 2 different binding constants for hydroxylapatite, the elution profile could demonstrate two peaks. These two BB variants would be observed as BBCK upon fractionation using agarose electrophoresis. The molecular weights of these two variants would have to be similar because the SDS-PAGE demonstrated a single monomeric protein (Figures 10 and 11).

Another possible explanation for the two peaks eluted off the column is the enzyme may be dissociating into the monomeric form during the chromatography. Thus the monomer and dimer might be demonstrating different affinities for hydroxylapatite. Again this would cause two elution peaks as well as producing purified BBCK as observed by isoenzyme fractionation and electrophoresis.

Another explanation for two peaks from the elution is that there could be multiple variants of BBCK produced by two different monomers.

In this case the dimer is 100% dissociated into the monomer and the two forms of the monomer have different binding constants for hydroxylapatite. If this were the appropriate explanation for the two elution peaks then the observed 1:1 peak ratio for the elution profile would be indicative of a 1:1 ratio of the two CKB variants. Again this explanation would also account for two peaks eluted of the column and a single purified enzyme as demonstrated by isoenzyme fractionation and electrophoresis (Figures 6,10 and 11).

A final explanation for two elution peaks is a phosphorylated BBCK form which alters the affinity of the BBCK for the hydroxylapatite column matrix. Phosphorylation of BBCK from rat brain has been found by Mahadevan et al (90a). The phosphorylated BBCK was found by 2-D electrophoresis and was reported as possibly being the cause of BBCK variants that other investigators have reported (151). In this study Mahadevan et al were unable to observe a completely phosphorylated form of BBCK. The two elution peaks observed in Figure 9 could be caused by an alteration in the column retention time, due to phosphorylation of the monomer or dimer. If the dimer were phosphorylated causing a conformational change, the phosphorylation at the corresponding site on the remaining subunit could be inhibited due to some steric interactions. Such a scenario would be consistent with the observation that complete phosphorylation of the monomer could not be found by Mahadevan et al (90a). They did not determine the phosphorylation state of the dimer so the steric actions of phosphorylation are yet to be determined. However, if the dimer has only one phosphorylation site available to it, and if it had been

fully phosphorylated prior to purification, then the 1:1 ratio observed in the results of this thesis would be consistent with these observations.

None of these possibilities is mutually exclusive. Only further investigation will determine the actual reason(s) for the double peaks.

The possible clinical implications of variants of BBCK cannot be assessed from the data described above. CK activity in serum of human patients has been used to evaluate skeletal muscle disease (50,180) myocardial infarction (92,103,105,124,177) and injury (79,148). CK found in human serum retains its kinetic activity and has been correlated to the extent or severity of these disease processes, in differential diagnosis (121,125), and patient assessment (35,153). In spite of the interest in CK as a clinical diagnostic tool there is still dispute among the scientists regarding the significance of the release of CK (3,137,166,177) or the mechanism of the CK release (103). To find a solution to this dispute more work needs to be done on differential roles (if any) of the different isoenzymes, their variants, and their relative release of CK from the cells. In any case, the concentration of CK in vascular smooth muscle is so low that its release is unlikely to effect serum CK measurements in any quantitative manner.

Electrophoresis

Electrophoresis of purified BBCK seen in Figure 10 shows one major band with a molecular weight of 42.5 kD. There are also lighter bands observed above and below the 42.5 kD band of unknown protein impurities. When compared to the lane containing purified BBCK purchased from Sigma Chemical Company it can be seen that the purchased BBCK has more impurities and greater amounts. The relative adequacy of the purified BBCK is further supported by considering the purity (or impurity) of BBCK which was purchased from and purified by Sigma Chemical Company as well as the specific activities (discussed below).

Possible Protein Impurities

Upon examination of the electrophoresis, a protein at approximately 57,000 D is observed. The protein migrating to this point may be the monomeric form of pyruvate kinase (PK). PK is a tetramer whose monomeric molecular weight is 57,000 D. Though the solubility of PK in alcohol is not considered to be significant, unpublished observation by Dillon and Root-Bernstein have shown skeletal muscle CK and PK together to be soluble in ethanol. They used paper chromatography to demonstrate no migration of PK alone in 50 % ethanol and significant migration of MMCK while alone. When the two enzymes are mixed together, they migrate as one predominant species and with an increased migration distance. Dillon and Root-Bernstein suggest a coupling between CK and PK producing a more hydrophobic molecular species.

The interaction of CK with another protein in a hydrophobic environment has been reported by Saks et al (128,129,132), who discussed the role of CK in heart muscle metabolism. They described CK as important in the transfer of high energy phosphates (via PC) from the site of synthesis in the mitochondria to the myofibrils and other key points of energy utilization. It was shown that there exists a close and specific spatial arrangement of mitochondrial CK and adenine nucleotide translocase within the mitochondrial membrane. It was proposed that the two proteins interact within the inner membrane by molecular collision. It has not yet been determined if similar interactions of CK and PK occur or what the physiological implications (if any) are.

These results conclude that PK could exhibit significant solubility in alcohol while in the presence of CK. Because of these observations, it appears plausible that a component of the protein impurities found in the purified BBCK could be due to PK. PK may persist throughout the purification procedure due to its increased solubility when associated with CK. The identity of the other protein impurities (mostly low molecular weight) has yet to be determined. These proteins may bind to CK during the purification process.

Activity of the Purified BBCK

Following the purification of BBCK from porcine carotid artery, a comparison of its specific activity and molecular activity was made. The specific activity found for the purified BBCK was 84 U/mg protein.

One unit will transfer 1 μ mole of phosphate from PC to ADP forming one ATP per minute at pH 7.4 at 30°C. The BBCK which can be purchased from Sigma Chemical Co. has a specific activity range of 10 to 30 U/mg protein. The comparatively high specific activity for the purified BBCK used in this thesis, with regard to Sigma BBCK, is consistent with the electrophoresis data seen in Figures 10 and 11. That is, the purified BBCK from porcine carotid artery has a larger fraction of active CK and fewer protein impurities than Sigma BBCK.

The molecular activity of the purified BBCK was also determined and compared to values found in the literature. The molecular activity or k_{cat} represents the maximum velocity per mole of enzyme ($V_{max}/[E]$) or mole of catalytic sites. Jacobs and Kuby (66) in a study of human CK expressed the similar molecular weight CK isoenzymes as maximum velocity per milligram protein. Using data from Jacobs and Kuby (66) as well as Nihei et al (107) a range for the molecular activity was found from 30 to 1400 μ M/min/mg. The k_{cat} forward for porcine carotid artery BBCK was 27 μ M/min/mg while in the reverse direction it was 509. Jacobs and Kuby consistently found the value for k_{cat} reverse significantly greater than k_{cat} forward (at pH 7). Thus an examination of the specific and catalytic activities of the purified BBCK reveals results not inconsistent with previously published results from other tissue and animal models.

Solution Kinetics

Figure 12 demonstrated that after 20 seconds the reaction had not gone to completion. The 20 second time point is a time where the appearance of ATP is linear with time indicating steady state kinetics. In this part of the curve the product concentrations are low compared to the K_m .

The high K_m of 16 to 43 mM reported in this thesis for ATP is greater than that found by Jacobs and Kuby (66) for human BBCK. This K_m is also greater than the 0.63 mM K_m found for MMCK from skeletal muscle. Such a low affinity for ATP by the BBCK from porcine carotid artery may assist the enzyme in buffering the ATP concentration in the tissue cytoplasm. If the cellular activity increased ATP demand, a low K_m for ATP could hinder the buffering response of CK. The concentration of ATP and PC in the porcine carotid artery has been reported as 0.70 and 0.51 $\mu\text{mol/g}$ tissue wet weight (38). The decreased buffering response would be produced by a decreased propensity of CK to release ATP due to a relatively high affinity for ATP. The low affinity of CK for ATP would thus produce a directionality for the cytosolic BBCK in the direction of ATP release. A high K_m for ATP in porcine carotid artery may be beneficial to the tissue in light of the low PC concentration found in the tissue. A low concentration of PC could be indicative of an inefficient ATP buffering capacity for the enzyme. The relatively high affinity for PC compared to ATP may augment the buffering of ATP by BBCK. This effective buffering of ATP has been characterized in previous experiments (38). Fisher and

Dillon observed effective buffering of ATP in porcine carotid artery, and if the K_m for ATP were not significantly lower than the K_m for PC such buffering may not have been observed (38). Thus in a tissue with a low concentration of PC the K_m of CK enables the tissue to buffer the ATP concentration by favoring the release of ATP from the enzyme.

CST Experiments

The *in vivo* kinetics of the creatine kinase reaction for porcine carotid arteries were studied using conventional saturation transfer. The results indicated that the reaction at rest was near equilibrium while assuming a two site exchange. The rate constants k_f and k_r were $0.17 \pm 0.04 \text{ s}^{-1}$ and $0.12 \pm 0.03 \text{ s}^{-1}$ respectively (SE). These values are lower than the values found in the heart (155) by Ugurbil using saturation transfer. The flux ratio of 0.71 ± 0.11 may be indicative of the CK reaction shifted away from equilibrium in resting porcine carotid artery. The flux ratio is defined as the product of the pseudo first order rate constant ratio and the PC to ATP ratio. However, the value for k_f may be deflated due to underestimation of the PC peak area and thus cause a decreased value for the flux ratio. Therefore, the CK reaction may be at equilibrium in the resting porcine carotid artery.

Were the ATPase reaction to alter the estimation of the CK reaction, the flux ratio would increase above one. The deviation measured cannot be ascribed to ATPase activity in the tissue.

MST Experiment

In Ugurbil's experiments it was determined that the CK reaction was at equilibrium in the heart (155). The result of equilibrium was also found by Spencer et al (146) when multisite saturation transfer was used to determine the kinetics and assuming a three site exchange for CK. As discussed in the Background Section of this thesis, CST assumes a two site exchange for the CK reaction. If the two site exchange assumption is not valid then erroneous rate constants may result. The third site of molecular exchange, which caused the erroneous rate constants mentioned above, was produced by a significant degradation of ATP attributed to ATPase activity.

Several reports have stated a difference in the forward and reverse flux for CK. Similar observations have been made under resting conditions where equilibrium would be expected for CK. To determine if the difference in the net flux is due to the assumption of a two site exchange Ugurbil (77,155,156,157) describes and utilizes a multisite saturation transfer technique (MST). The MST technique assumes a three site exchange:



In these studies, the three site exchange can be made to behave as a two site exchange by continuous irradiation of the Pi resonance.

Irradiating the Pi resonance throughout the NMR experiment while alternating the saturation of PC and γ ATP effectively removes the signal of Pi from the possible measurable exchanges. Now, without Pi's effect on the reaction, the measurement of CK exchange can accurately be determined.

The results of the CK reaction near equilibrium found in porcine carotid artery might be indicative of a high CK relative to ATPase rate. If the ATPase were effecting the equilibrium state of the CK reaction the flux ratio (as written) would be greater than one. Thus, from the data and resulting flux ratio, a contribution by the ATPase reaction on CK equilibrium is not likely. In an attempt to determine the ATPase rate *in vivo* the multisite saturation transfer experiments were performed specifically on the NMR observable ATPase substrates: Pi and γ ATP. The arteries were potassium stimulated to activate ATPase. To prevent a contribution from the ATP \leftrightarrow PC exchange by CK the MST was used. It was demonstrated by Paul (86) that the ATP flux in porcine coronary arteries was 0.71 $\mu\text{mol}/\text{min}/\text{g}$ tissue wet weight during stimulation. Using Paul's data about 0.012 $\mu\text{M}/\text{g}/\text{sec}$ could be the value for the flux due to ATPase. The lowest measurable flux which could be observed with saturation transfer is approximately 0.04 $\mu\text{M}/\text{g}/\text{sec}$. Thus the lack of observable flux due to ATPase is apparently due to limitations of the technique and is consistent with previously reported flux values from Paul (86).

Because of this relatively low exchange rate the arteries were also loaded with 40 mM creatine using the technique described by Scott.

This procedure was found to increase the PC concentration. The results of MST experiments are summarized in Table 12. They show that no detectable ATPase could be observed. These results indicate that when creatine loaded, and under stimulated conditions, the ATPase rate of porcine carotid arteries is not significant enough to be observable by MST. These results also indicate that further CST experiments on porcine carotid arteries could be undertaken and assume a two site exchange because of a relatively insignificant ATPase rate. Absence of observable ATPase activity, relative to the rate of CK exchange, under stimulated conditions and in the presence of measurable CK activity may thus obviate the need for a three site model in vascular smooth muscle.

Physiologically, this low ATPase rate in the carotid artery and the relatively low rate constants, as well as determination of CK equilibrium, lend support to previous observations by Ishida et al. (8). Ishida found that porcine vascular smooth muscle has lower energy costs than gastrointestinal smooth muscle, while others also reported higher values with cardiac muscle (20,23). Paul and Lynch have hypothesized that energy metabolism in the vascular smooth muscle is tuned to meet the needs set by the contractile system (15). If this were the case, a stimulated system not generating tension may not have the same flux as a system generating tension. However, previous studies by Krisanda and Paul (10) and Hai et al. (6) have demonstrated a low cost for tension maintenance in porcine vascular smooth muscle while having a relatively inefficient mechanism for tension generation. Therefore an examination of the metabolic flux in porcine carotid

artery while maintaining tension may yield results similar to those demonstrated above for unloaded porcine vascular smooth muscle. In contrast, the flux observed during tension generation may yield different results. Improved NMR resolution times or utilization of smooth muscle with higher metabolic rates than the carotid must be used to observe such a phenomena.

The ADP concentration for porcine carotid artery has been determined with NMR to be 18-31 $\mu\text{moles/g}$ tissue wet weight at rest (38). The concentration of ADP which can be estimated from K_{eq} from these experiments is 25 $\mu\text{moles/g}$ using the flux ratio of 0.71, the estimate of ADP concentration from kinetic data 18 $\mu\text{moles/g}$ tissue wet weight. The higher estimate assumed all measurable ADP was available for the CK reaction at equilibrium. The latter figure assumes a deviation from equilibrium. In either case, it may be concluded that an ADP value in the vicinity of 20 $\mu\text{moles/g}$ is present in resting porcine carotid artery.

DANTE Discussion

In this thesis it was demonstrated that the modified DANTE sequence could be applied to saturate a selected resonance and effect saturation similar to and simultaneous with the CW saturation. One may then use the two saturation techniques to determine the molecular exchange kinetics of a three-site molecular exchange system, and Ugurbil's MST calculations may be used to determine the rate constants in a tissue.

Saturation transfer has proven to be a useful technique for determining the molecular exchange kinetics of high energy phosphate metabolites in living tissue. Tissues which have a significant ATPase rate may demonstrate a deflated rate of ATP degradation during saturation transfer experiments performed to measure the CK exchange. The multisite saturation transfer technique described by Ugurbil (156) makes it possible to measure the CK exchange without being effected by the ATPase reaction. This technique requires that two sites are irradiated simultaneously. In the event that physical or financial difficulties prohibit the multisite saturation described by Ugurbil a combination of techniques can be utilized to produce equivalent two site saturation. In this thesis the combined techniques of continuous wave saturation and a modified DANTE pulse sequence were utilized to saturate two resonances.

In order to apply the DANTE pulse sequence and have this sequence be equivalent to CW saturation the original pulse sequence of Morris and Freeman (100) had to be modified. The modification of the DANTE pulse sequence did not change the excitation effects of the DANTE pulse sequence described by the Bloch equations and solved by Morris and Freeman. Equation 17 (Background Section) is the same solution to the Bloch equations Morris and Freeman determined. In this way it was clear that the modified DANTE could be applied to saturate a selected resonance and effect saturation similar to the way CW can apply saturation. The two saturation techniques could then be applied simultaneously to determine the molecular exchange kinetics to a three site molecular exchange system and use Ugurbil's MST calculations to

determine the appropriate rate constants.

Rate Constant Introduction

The physical interpretation of the first order rate constant is as an estimation of the fraction of substrate converted to product with respect to time. If $k = 0.1 \text{ s}^{-1}$, then 10% of substrate is converted to product per second. When a reactant is present in excess, a special case of second order kinetics exists. For example, if a hydrolysis reaction is carried out in solution, the consumption of water is considered negligible. The reaction, therefore, appears to follow first order kinetics and is called a pseudo-first order reaction.

The first order rate constant is effected by the enzyme concentration as well as the equilibrium state in the tissue. A change in enzyme content for a reaction system will affect the first order rate constant. Increasing the enzyme concentration will cause an increase in the first order rate constant. Thus a comparison of the first order rate constants between solution and tissue must be done under consistent and accurate enzyme concentration. The solution kinetics have a known enzyme content and a single isoform. Tissue concentration of an enzyme, however, is difficult to determine. Carotid artery has been demonstrated in this thesis to contain three CK isoforms, none of whose cellular locations or concentrations are known. Because of the discovery of the MM and MB forms in vascular smooth muscle, a definitive identification of the major contributor(s) to the tissue CK

activity cannot be made at this time. The tissue kinetics may reflect multiple forms of CK activity.

Kinetics Summary

Solution kinetics may accurately reflect the kinetics occurring in the tissue only if the purification procedure has not caused the enzyme to be damaged or altered such that the kinetics are changed. The vascular smooth muscle cell has a diameter of approximately 5 μm . Soluble CK and its metabolites in the smooth muscle cell would have a relatively small distance to diffuse throughout the cell. This small diffusion distance makes it improbable for the compartmentalization of metabolites in the smooth muscle cell, although the three different CK isoforms may have particular locations. It is possible that the different solubilities of CK isoforms as well as other uncharacterized physical properties, such as protein-protein binding, may allow certain isoenzymes of CK to be coupled to discrete locations within the cell. Paul has found CK activity in the membrane fraction of porcine carotid artery but did not determine the isoenzyme involved (178a). From the data presented in this thesis, the isoenzyme predicted to be found in the membrane fraction would be BBCK due to its greater solubility in ethanol than the MM or MB forms. There is no direct evidence for a membrane specific BBCK (as opposed to membrane specific MMCK or MBCK) at this time.

A discussion of the CK isoenzymes can be found in the Background Section of this thesis and from the available data it is difficult to

assess the relative kinetic differences present in the different isoenzymes. Therefore, the kinetics observed by NMR in tissue may be reflecting the sum of the kinetic activity possible in the tissue. The contribution of the MM and MB isoforms cannot be determined because a detailed analysis of their kinetic properties from porcine carotid artery has not been determined. For the observable tissue kinetics to be dominated by the BBCK kinetics in the presence of known potential MB or MM activity, the overall activity of BBCK would have to be greater than the MB and MM activity. Therefore, MB and MM isoform activities would have to be significantly attenuated relative to the activity of the BB form in the tissue. The results presented in this thesis (1:1:1 activity ratio) cannot determine a contribution from multiple (or single) CK isoforms in the porcine carotid artery.

The observation of multiple forms of CK present in the smooth muscle cell may indicate specialization of CK within the cell (e.g., coupled to myofilaments or in the membrane). This observation may be supportive of localization of discrete isoforms of CK in particular subcellular sites. As stated above, the results obtained from the kinetic determinations of porcine carotid artery CK are inconclusive with regard to this localization, although their differential solubilities may provide clues as to tissue localization.

Conclusions

There are several conclusions which can be drawn from this thesis. It has been found that porcine carotid artery contains three

isoenzymes of CK in approximately a 1:1:1 ratio. Future estimates of smooth muscle CK activity must take into account potential MM and MB isoform contributions. The BBCK from porcine carotid artery can be purified using alcohol precipitation and adsorption chromatography. Differential isoform solubility may provide clues to the subcellular locations of the different isoforms. BBCK isolated from porcine carotid artery has a relatively high K_m for ATP relative to CK from other tissues. Thus, even the relatively low PC concentration of vascular smooth muscle will be able to effectively buffer the ATP pool. Using NMR saturation transfer techniques, it was demonstrated that the CK rate in porcine carotid artery is high relative to the ATPase rate. Thus conventional saturation transfer is sufficient to determine the CK kinetics of porcine carotid artery. Finally, multi-site saturation transfer can be accomplished using a combined technique of DANTE and CW.

Future Directions

There are several questions which remain unanswered or have been raised through this work. The behavior and function of the other cytosolic isoenzymes in the porcine carotid artery has yet to be determined. Their kinetics may be producing a significant contribution to the kinetics observed in the tissue. By determining their kinetics, a more accurate estimation of the contribution of the different isoenzymes and their specific metabolic processes in the tissue can be found. The unique kinetics (e.g.: high K_m) of the BBCK from porcine carotid artery also warrants a further study of its kinetics.

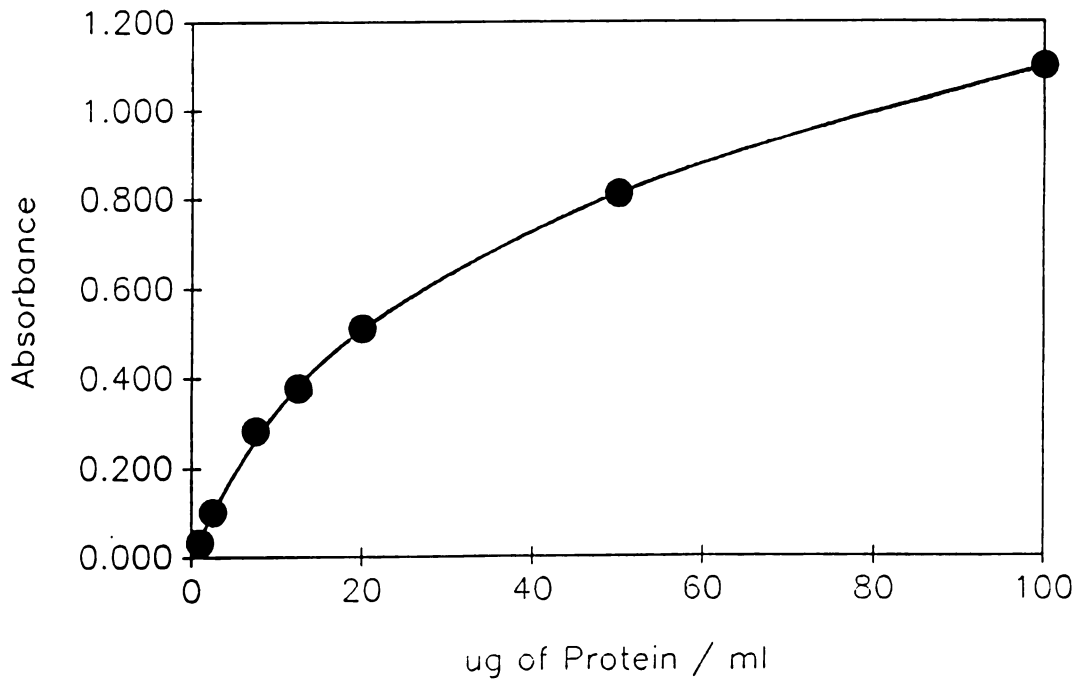
An investigation of the protein impurities associated with the purification process should be performed to determine if there may be any protein coupling involving BBCK and other proteins. The possible causes (e.g., phosphorylation or other modification) for the two elution peaks of BBCK should be examined. A more detailed analysis of the tissue kinetics using saturation transfer should be undertaken using varying metabolic conditions to determine if such conditions might enable dissociation of the different isoform activities. A study determining the number and characteristics of possible variants of BBCK should also be undertaken.

APPENDICES

APPENDIX I

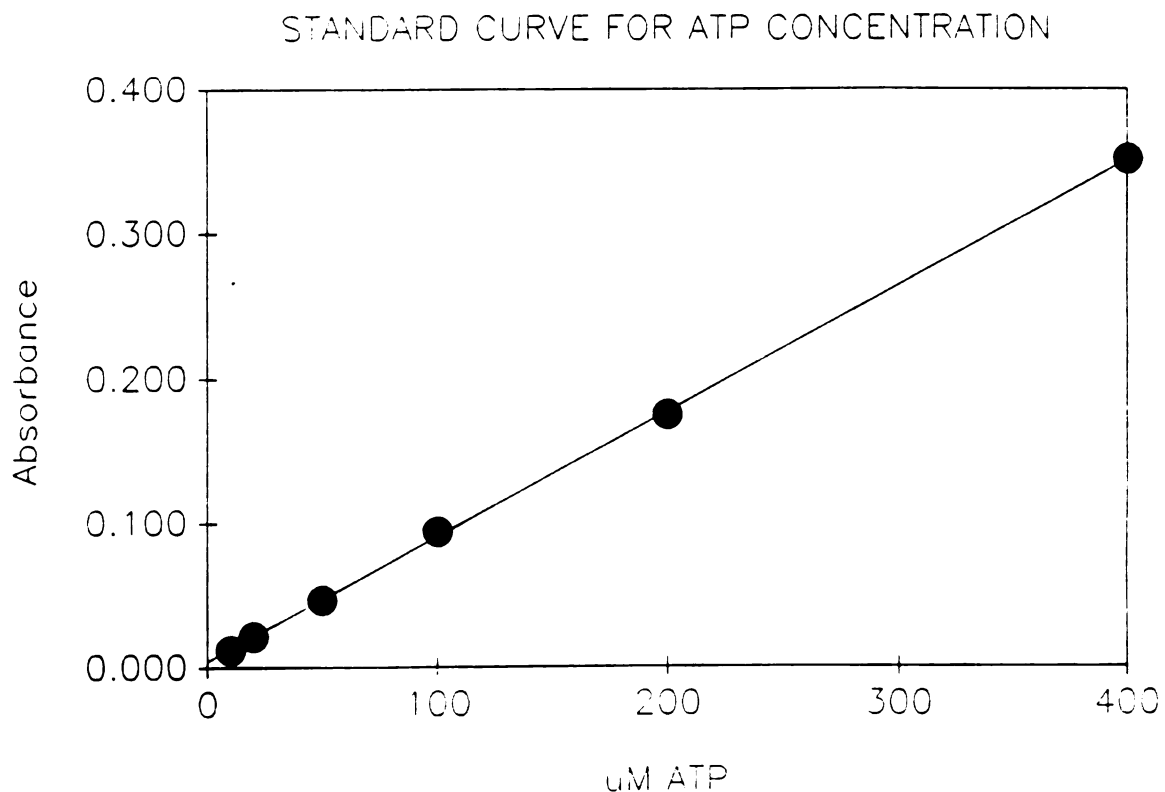
Standard curve obtained for the Biorad Micro-Protein Assay. Absorbance is determined spectrophotometrically at 595 nm. Protein concentration is μg of bovine serum albumin per ml. Assay was performed by combining 0.2 ml of Biorad reagent and 0.8 ml of sample. For assay procedure see methods section.

STANDARD CURVE FOR PROTEIN CONCENTRATION
BIORAD PROTEIN ASSAY



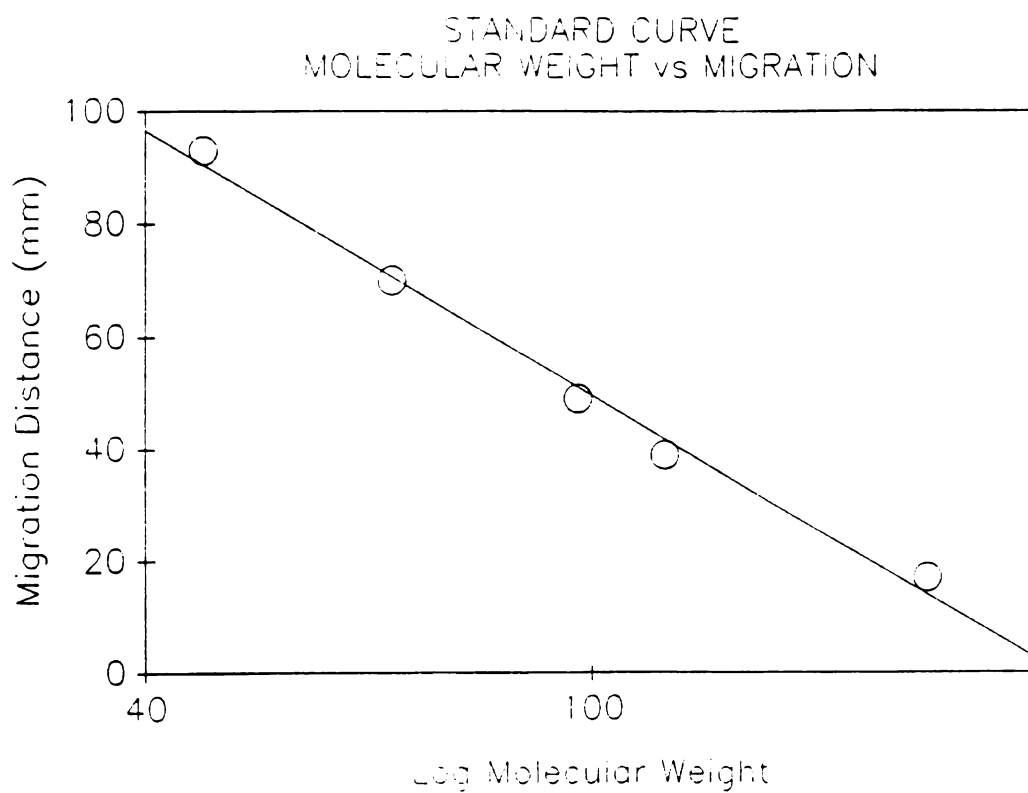
APPENDIX II

Standard curve obtained for the production of NADPH measured at 340 nm. NADPH production was correlated to the concentration of ATP present in the system in μmoles . The reaction system consisted of: hexokinase, G6PDH, NADPH, glucose, MgCl_2 , tris, at a pH of 8.0. For assay procedures see methods section.



APPENDIX III

Standard curve obtained for molecular weight determination. Molecular weight standards were obtained from Biorad Heavy Molecular Weight Standard. Log of molecular weight graphed vs migration distance in mm. See methods section for determination of molecular weight.



LIST OF REFERENCES

LIST OF REFERENCES

- 1 Anosike EO, Moreland BH, Watts DC. Evolutionary Variation Between a Monomer and a Dimer Arginine Kinase. Biochem. J. 1975;145:535-543.
- 2 Anosike EO, Watts DC. Effects of Arginine and Some Analogues on the Partial Adenosine Triphosphate-Adenosine Diphosphate Exchange Reaction Catalysed by Arginine Kinase. Biochem. J. 1976;155:689-693.
- 3 Armstrong PW, Watts DG, Hamilton DC, Chiong MA, Parker JO. Quantification of Myocardial Infarction: Template Model for Serial Creatine Kinase Analysis. Circulation. 1979;60,4:856-865.
- 4 Arner A, Hellstrand P, Ruegg JC. Influence of ATP, ADP and AMPPNP on the Energetics of Contraction in Skinned Smooth Muscle. Regulation and Contraction of Smooth Muscle. 1987;43-57.
- 5 Atta-ur-Rahman. Nuclear Magnetic Resonance. 1986. Springer-Verlag.
- 6 Ault A. Techniques and Experiments for Organic Chemistry. 1979. Allyn and Bacon Inc.
- 7 Bernhard SA. The Intracellular Equilibrium Thermodynamic and Steady-State Concentrations of Metabolites. Cell Biophysics. 1988;12:119-132.
- 8 Bessman SP. The Physiological Significance of the Creatine Phosphate Shuttle. Myocardial and Skeletal Muscle Bioenergetics. 1986;194:1. Plenum Press.
- 9 Bessman SP. The Origin of the Creatine-Creatine Phosphate Energy Shuttle. Heart Creatine Kinase. 1980;Chapter 7. Williams & Wilkins.
- 10 Bessman SP, Geiger PJ. Transport of Energy in Muscle: The Phosphorylcreatine Shuttle. Science. 1981;211:448-452.
- 11 Bialojan C, Ruegg JC, DiSalvo J. A Myosin Phosphatase Modulates Contractility in Skinned Smooth Muscle. Pflugers Arch. 1987;410:304-312.
- 12 Bing RJ, Sasaki Y, Chemnitius M, Burger W. Compartmentation and Functional Mechanisms in Myocardial Failure and Myocardial Infarction. Myocardial and Skeletal Muscle Bioenergetics.

- 1986;194:283. Plenum Press.
- 13 Bittl JA, DeLayre J, Ingwall JS. Rate Equation for Creatine Kinase Predicts the in vivo Reaction Velocity: ^{31}P NMR Surface Coil Studies in Brain, Heart, and Skeletal Muscle of the Living Rat. Biochemistry. 1987;26:6083-6090.
 - 14 Bittl JA, Ingwall JS. Reaction Rates of Creatine Kinase and ATP Synthesis in the Isolated Rat Heart. Journal of Biological Chemistry. 1985;260,6:3512-3517.
 - 15 Bose D. Mechanical Changes in Smooth Muscle During Rigor. Smooth Muscle Contraction. 1984;199.
 - 16 Brindle KM. NMR Methods for Measuring Enzyme Kinetics in Vivo. Progress in NMR Spectroscopy. 1988;20:257-293.
 - 17 Brindle KM, Blackledge MJ, Challiss AJ, Radda GK. ^{31}P NMR Magnetization-Transfer Measurements of ATP Turnover During Steady-State Isometric Muscle Contraction in the Rat Hind Limb in Vivo. Biochemistry. 1989;28:4887-4893.
 - 18 Brown TR. Saturation Transfer in Living Systems. Philos. Trans. R. Soc. London. 1980;289:441-444.
 - 19 Brown TR, Gadian DG, Garlick PB, Radda GK, Seeley PJ, Styles P. Creatine Kinase Activities in Skeletal and Cardiac Muscle Measured by Saturation. Frontiers of Biological Energetics. 1978;Vol. 2;1341-1349. Academic Press Inc.
 - 20 Butler TM, Davies RE. High-Energy Phosphates in Smooth Muscle. Hand Book of Physiology Section 2: The Cardiovascular System, Vascular Smooth Muscle. 1980;Vol. II:237-252. American Physiology Society.
 - 21 Butler TM, Pacifico DS, Siegman MJ. ADP Release from Myosin in Permeabilized Smooth Muscle. Am. J. Physiol. 256 (Cell Physiol. 25). 1989;C59-C66.
 - 22 Cain DF, Davies RE. Breakdown of Adenosine Triphosphate During a Single Contraction of Working Muscle. Biochemical and Biophysical Research Communications. 1962;8,5:361-366.
 - 23 Cande WZ, McDonald K, Meeusen RL. A Permeabilized Cell Model for Studying Cell Division: A Comparison of Anaphase Chromosome Movement and Cleavage Furrow Constriction in Lysed PtK₁ Cells. Journal of Cell Biology. 1981;Vol. 88:618-629.
 - 24 Chatterjee M, Hai C, Murphy RA. Dependence of Stress and Velocity on CA^{2+} and Myosin Phosphorylation in the Skinned Swine Carotid Media. Regulation and Contraction of Smooth Muscle. 1987;399-410.
 - 25 Chegwiddden WR, Watts DC. Kinetic Studies and Effects of

- Anions on Creatine Phosphokinase from Skeletal Muscle of Rhesus Monkey. Biochimica et Biophysica Acta. 1975;410:99-114.
- 26 Chevli R, Fitch CD. β -Guanidinopropionate and Phosphorylated β -Guanidinopropionate as Substrates for Creatine Kinase. Biochemical Medicine. 1979;21:162-167.
- 27 Cohn M. NMR Studies of Phosphoryl Transfer Reactions. Current Topics in Cellular Regulation. 1984;24:Chapter 1. Academic Press, Inc.
- 28 Connett RJ. Analysis of Metabolic Control: New Insights Using Scaled Creatine Kinase Model. American Physiological Society. 1988;88:R949-R959.
- 29 Corea M, Klob R, Stober T, Schimrigk K, Keller HE. Elevated Serum CK-BB Levels in Patients with Cerebral Transtentorial Herniation After Ischemic Stroke. Clin. Biochem. 1989;22:131-134.
- 30 Davuluri SP, Hird FJR, McLean RM. A Re-Appraisal of the Function and Synthesis of Phosphoarginine and Phosphocreatine in Muscle. Comp. Biochem. Physiol. 1981;69B:329-336.
- 31 Dawson DM, Eppenberger HM, Kaplan NO. The Comparative Enzymology of Creatine Kinase, II. Journal of Biological Chemistry. 1967;242,2:210-217.
- 32 Dawson DM, Fine IH. Creatine Kinase in Human Tissues. Arch. Neurol. 1967;16:175-180.
- 33 Dawson MJ, Wray S. The Effects of Pregnancy and Parturition on Phosphorus Metabolites in Rat Uterus Studied by ^{31}P Nuclear Magnetic Resonance. J. Physiol. 1985;368:19-31.
- 34 Dillon PF, Aksoy MO, Driska SP, Murphy RA. Myosin Phosphorylation and the Cross-Bridge Cycle in Arterial Smooth Muscle. Science. 1981;211:495-497.
- 35 Eisenberg PR, Shaw D, Schaab C, Jaffe AS. Concordance of Creatine Kinase-MB Activity and Mass. Clin. Chem. 1989;35,3:440-443.
- 36 Eldin ES, Gercken G, Harm K, Voigt KD. The Isoelectric Focusing of Creatine Kinase Variants: I. The Heterogeneity of Creatine Kinase in Human Heart Cytosol and Mitochondria. J. Clin. Chem. Clin. Biochem. 1986;24:283-292.
- 37 Eppenberger HM, Dawson DM, Kaplan NO. The Comparative Enzymology of Creatine Kinase, I. Journal of Biological Chemistry. 1967;242,2:204-209.
- 38 Fisher MJ, Dillon PF. Direct Determination of ADP in Hypoxic

- Porcine Carotid Artery Using ^{31}P NMR. NMR in Biomedicine. 1988;1,3:121-126.
- 39 Fisher MJ, Dillon PF. Phenylphosphonate: A ^{31}P -NMR Indicator of Extracellular pH and Volume in the Isolated Perfused Rabbit Bladder. Circulation Research. 1987;60:472-477.
- 40 Fitch CD, Jellinek M, Fitts RH, Baldwin KM, Holloszy JO. Phosphorylated β -Guanidinopropionate as a Substitute for Phosphocreatine in Rat Muscle. American Journal of Physiology. 1975;228,4:1123-1125.
- 41 Fitch CD, Jellinek M, Mueller EJ. Experimental Depletion of Creatine and Phosphocreatine from Skeletal Muscle. Journal of Biological Chemistry. 1974;249,4:1060-1063.
- 42 Fitch CD, Shields RP. Creatine Metabolism in Skeletal Muscle. Journal of Biological Chemistry. 1966;241,15:3611-3614.
- 43 Fitch CD, Shields RP, Payne WF, Dacus JM. Creatine Metabolism in Skeletal Muscle. Journal of Biological Chemistry. 1968;243,8:2024-2027.
- 44 Focant B. Isolement et Proprietes de la Creatine-Kinase de Muscle Lisse de Boeuf. FEBS Letters. 1970;10,1:57-61.
- 45 Focant B. Purification et comportement a l'electrophorese sur gel d'amidon de la creatine kinase de carotides de bovide. Arch. Intern. Physiol. Biochim. 1968;76:373-374.
- 46 Focant B, Watts DC. Properties and Mechanism of Action of Creatine Kinase From Ox Smooth Muscle. Biochem. J. 1973;135:265-276.
- 47 Gadian DG. Nuclear Magnetic Resonance and Its Applications to Living Systems. 1982. Oxford University Press.
- 48 Gadian DG, Radda GK, Brown TR, Chance EM, Dawson MJ, Wilkie DR. The Activity of Creatine Kinase in Frog Skeletal Muscle Studied by Saturation-Transfer Nuclear Magnetic Resonance. Biochem. J. 1981;194:215-228.
- 49 Geng JG, Cheng HZ, Yang YF, Qian ZH, Jiang CY. Isolation of Creatine Kinase BB Isoenzyme with High Specific Activity and Adequate Purity for Radioimmunoassay from Human Placenta on Preparative Polyacrylamide Gel Electrophoresis. Clinica Chimica Acta. 1989;181:1-10.
- 50 Goto I, Peters HA, Reese HH. Creatine Phosphokinase in Neuromuscular Disease. Arch. Neurol. 1967;16:529-535.
- 51 Grosse R, Spitzer E, Kupriyanov VV, Saks VA, Repke KRH. Coordinate Interplay Between $(\text{Na}^+ + \text{K}^+)\text{-ATPase}$ and Creatine Phosphokinase Optimizes $(\text{Na}^+/\text{K}^+)\text{-Antiport}$ Across the Membrane

- of Vesicles Formed From the Plasma Membrane of Cardiac Muscle Cell. Biochimica et Biophysica Acta. 1980;603:142-156.
- 52 Grossman SH. Interaction of Creatine Kinase from Monkey Brain with Substrate: Analysis of Kinetics and Fluorescence Polarization. Journal of Neurochemistry. 1983;41:729-736.
- 53 Grossman SH. Resonance Energy Transfer Between the Active Sites of Rabbit Muscle Creatine Kinase: Analysis by Steady-State and Time-Resolved Fluorescence. Biochemistry. 1989;28:4894-4902.
- 54 Hai CM, Murphy RA. Cross-Bridge Phosphorylation and Regulation of Latch State in Smooth Muscle. Am. J. Physiol. 254 (Cell Physiol. 23). 1988;C99-C106.
- 55 Hai CM, Murphy RA. Regulation of Shortening Velocity by Cross-Bridge Phosphorylation in Smooth Muscle. Am. J. Physiol. 255 (Cell Physiol. 24). 1988;C86-C94.
- 56 Hall N, Deluca M. The Effect of Inorganic Phosphate on Mitochondrial Creatine Kinase. Myocardial and Skeletal Muscle Bioenergetics. 1986;194:71. Plenum Press.
- 57 Harris RK. Nuclear Magnetic Resonance Spectroscopy. 1983. Pitman Publishing Inc.
- 58 Hellstrand P, Arheden H, Sjolín L, Arner A. Stiffness and the Energetics of Active Shortening in Chemically Skinned Smooth Muscle. Regulation and Contraction of Smooth Muscle. 1987;333-345.
- 59 Henry PD, Roberts R, Sobel BE. Rapid Separation of Plasma Creatine Kinase Isoenzymes by Batch Adsorption on Glass Beads. Clin. Chem. 1975;21,7:844-849.
- 60 Herlihy JT, Murphy RA. Length-Tension Relationship of Smooth Muscle of the Hog Carotid Artery. Circ. Res. 1973;33:275-283
- 61 Hoar PE, Pato MD, Kerrick WGL. Myosin Light Chain Phosphatase: Effect on the Activation and Relaxation of Gizzard Smooth Muscle Skinned Fibers. Journal Biol. Chem. 1985;260:8760-8764.
- 62 Ingwall JS. Phosphorus Nuclear Magnetic Resonance Spectroscopy of Cardiac and Skeletal Muscles. American Journal of Physiology 242 (Heart Circ. Physiol. 11.) 1982;H729-H744.
- 63 Ishida Y, Hashimoto M, Paul RJ. Does a Limitation of Energy Supply to the Contractile Apparatus Underlie the Relaxation Induced by Hypoxia in Smooth Muscle? Regulation and Contraction of Smooth Muscle. 1987;463-464.
- 64 Iyengar MR. Creatine Kinase as an Intracellular Regulator.

- Journal of Muscle Research and Cell Motility. 1984;5:527-534.
- 65 Iyengar MR, Fluellen CE, Iyengar C. Creatine Kinase From the Bovine Myometrium: Purification and Characterization. Journal of Muscle Research and Cell Motility. 1982;3:231-246.
- 66 Jacobs HK, Kuby SA. Studies on Muscular Dystrophy. Journal of Biological Chemistry. 1980;255,18:8477-8482.
- 67 Jacobus WE. General Introduction. Myocardial Energy Transport: Current Concepts of the Problem. Heart Creatine Kinase. 1980;Chapter 1. Williams & Wilkins.
- 68 Jacobus WE. Respiratory Control and the Integration of Heart High-Energy Phosphate Metabolism by Mitochondrial Creatine Kinase. Ann. Rev. Physiol. 1985;47:707-725.
- 69 Jacobus WE, Saks VA. Creatine Kinase of Heart Mitochondria: Changes in Its Kinetic Properties Induced by Coupling to Oxidative Phosphorylation. Archives of Biochemistry and Biophysics. 1982;219,1:167-178.
- 70 Jacobus WE, Vandegaer KM, Moreadith RW. Aspects of Heart Respiratory Control by the Mitochondrial Isozyme Creatine Kinase. Myocardial and Skeletal Muscle Bioenergetics. 1986;194:169. Plenum Press.
- 71 Jockers-Wretou E, Pflleiderer G. Quantitation of Creatine Kinase Isoenzymes in Human Tissues and Sera By An Immunological Method. Clinica Chimica Acta. 1975;58:223-232.
- 72 Kannan MS, Davis C, Ladenius ARC, Kannan L. Agonist interactions at the Calcium pools in skinned and unskinned canine tracheal smooth muscle. Can. J. Physiol. Pharmacol. 1987;65:1780-1787.
- 73 Kargacin GJ, Fay FS. Physiological and Structural Properties of Saponin-skinned Single Smooth Muscle Cells. J. Gen. Physiol. 1987;90:49-73.
- 74 Kato K, Shimizu A. Highly Sensitive Enzyme Immunoassay for Human Creatine Kinase MM and MB Isozymes. Clinica Chimica Acta. 1986;158:99-108.
- 75 Kerrick WGL, Bridenbaugh RI, Cassidy PS, Hoar PE. Myosin Light Chain Kinase/Phosphatase Dependent Regulation in Skinned Smooth Muscle Fibers. Smooth Muscle Contraction. 1984;373-390.
- 76 Kerrick WGL, Hoar PE. Non-Ca²⁺-Activated Contraction in Smooth Muscle. Regulation and Contraction of Smooth Muscle. 1987;473-448.
- 77 Kingsley-Hickman PB, Sako EY, Mohanakrishnan P, Robitaille

- PML, From AHL, Foker JE, Ugurbil K. ^{31}P NMR Studies of ATP Synthesis and Hydrolysis Kinetics in the Intact Myocardium. Biochemistry. 1987;26:7501-7510.
- 78 Kitchin SE, Watts DC. Comparison of the Turnover Patterns of Total and Individual Muscle Proteins in Normal Mice and those with Hereditary Muscular Dystrophy. Biochem. J. 1973;136:1017-1028.
- 79 Klein MS, Shell WE, Sobel BE. Serum Creatine Phosphokinase (CPK) Isoenzymes After Intramuscular Injections, Surgery, and Myocardial Infarction. Cardiovascular Research. 1973;7:412-418.
- 80 Koretsky AP, Basus VJ, James TL, Klein MP, Weiner MW. Detection of Exchange Reactions Involving Small Metabolite Pools Using NMR Magnetization Transfer Techniques: Relevance to Subcellular Compartmentation of Creatine Kinase. Magnetic Resonance in Medicine. 1985;2:586-594.
- 81 Kossmann T, Furst D, Small JV. Structural and Biochemical Analysis of Skinned Smooth Muscle Preparations. Journal of Muscle Research and Cell Motility. 1987;8:135-144.
- 82 Krisanda JM, Paul RJ. Dependence of Force, Velocity, and O_2 Consumption on $[\text{Ca}^{2+}]$ in Porcine Carotid Artery. Am. J. Physiol. 255 (Cell Physiol 24). 1988;C393-C400.
- 83 Kuby SA, Keutel HJ, Okabe K, Jacobs HK, Ziter F, Gerber D, Tyler FH. Isolation of the Human ATP-Creatine Transphosphorylases (Creatine Phosphokinases) from Tissues of Patients with Duchenne Muscular Dystrophy. Journal of Biological Chemistry. 1977;252,23:8382-8390.
- 84 Kuby SA, Noda L, Lardy HA. Adenosinetriphosphate-Creatine Transphosphorylase. Journal of Biochemistry. 1954;209:191-201.
- 85 Kupriyanov VV, Steinschneider AY, Ruuge EK, Kapel'ko VI, Zueva MY, Lakomkin VL, Smirnov VN, Saks VA. Regulation of Energy Flux Through the Creatine Kinase Reaction in Vitro and in Perfused Rat Heart. Biochimica et Biophysica Acta. 1984;805:319-331.
- 86 Kushmerick MJ, Dillon PF, Meyer RA, Brown TR, Krisanda JM, Sweeney HL. ^{31}P NMR Spectroscopy, Chemical Analysis, and Free Mg^{2+} of Rabbit Bladder and Uterine Smooth Muscle. Journal of Biological Chemistry. 1986;261,31:14420-14429.
- 87 Laemmli UK. Cleavage of Structural Proteins During the Assembly of the Head of Bacteriophage T4. Nature. 1970;227:680-685
- 88 Lang H. Creatine Kinase Isoenzymes. 1981. Springer-Verlag.

- 89 Lipskaya TY, Rybina IV. Properties of Mitochondrial Creatine Kinase from Skeletal Muscle. Biochimiya. 1987;52,4:690-700.
- 90 Ljungdahl L, Gerhardt W. Creatine Kinase Isoenzyme Variants in Human Serum. Clin. Chem. 1978;24,5:832-834.
- 90a Mahadevan LC, Whatley A, Leung TKC, Lim L. The Brain Isoform of a Key ATP-Regulating Enzyme, Creatine Kinase, is a Phosphoprotein. Biochem. J. 1984;222:139-144
- 91 Mani RS, Kay CM. Physicochemical Studies on the Creatine Kinase M-Line Protein and Its Interaction with Myosin and Myosin Fragments. Biochimica et Biophysica Acta. 1976;453:391-399.
- 92 Matsui Y, Hashimoto H, Tsukamoto H, Okumura K, Ito T, Ogawa K, Satake T. Disappearance and Appearance of Isoenzymes of Creatine Kinase, Lactate Dehydrogenase and Aspartate Aminotransferase in the Myocardium Undergoing Infarction. Cardiovascular Research. 1989;23:249-253.
- 93 Matthews PM, Bland JL, Gadian DG, Radda GK. A ^{31}P -NMR Saturation Transfer Study of the Regulation of Creatine Kinase in the Rat Heart. Biochimica et Biophysica Acta. 1982;721:312-320.
- 94 McClellan G, Weisberg A, Winegrad S. Energy Transport From Mitochondria to Myofibril by a Creatine Phosphate Shuttle in Cardiac Cells. Am. J. Physiology 245 (Cell Physiol. 14). 1983;C423-C427.
- 95 Mekhfi H, Ventura-Clapier R. Dependence Upon High-Energy Phosphates of the Effects of Inorganic Phosphate on Contractile Properties in Chemically Skinned Rat Cardiac Fibres. Pflugers Arch. 1988;411:378-385.
- 96 Meyer RA. A Linear Model of Muscle Respiration Explains Monoexponential Phosphocreatine Changes. Am. J. Physiol. 254 (Cell Physiol. 23). 1988;C548-C553.
- 96a Meyer RA, Brown TR, Krilowicz BL, Kushmerick MJ. Phosphagen and Intracellular pH Changes During Contraction of Creatine-Depleted Rat Muscle. Am. J. Physiol. 250 (Cell Physiol. 19). 1986;C264-274.
- 96b Meyer RA, Fisher MJ, Nelson SJ, Brown TR. Evaluation of Manual Methods for Integration of in vivo Phosphorous NMR Spectra. NMR in Biomedicine 1988;1:131-135
- 97 Meyer RA, Kushmerick MJ, Brown TR. Application of ^{31}P -NMR Spectroscopy to the Study of Striated Muscle Metabolism. Am. J. Physiol. 242 (Cell Physiol. 11). 1982;C1-C11.

- 98 Meyer RA, Sweeney HL, Kushmerick MJ. A Simple Analysis of the "Phosphocreatine Shuttle." Am. J. Physiol. 246 (Cell Physiol. 15). 1984;C365-C377.
- 99 Miller J, Johnson M, Wei R. Preparation of Creatine Kinase-MM Isoenzymes From Canine and Human Tissues. Clinica Chimica Acta. 1982;118:67-76.
- 100 Morris GA, Freeman R. Selective Excitation in Fourier Transform Nuclear Magnetic Resonance. Journal of Magnetic Resonance. 1978;29:433-462.
- 101 Morris PG. Nuclear Magnetic Resonance Imaging in Medicine and Biology. 1986. Oxford University Press.
- 102 Morrison JF, Uhr ML. The Function of Bivalent Metal Ions in the Reaction Catalysed by ATP:Creatine Phosphotransferase. Biochimica et Biophysica Acta. 1966;57-74.
- 103 Muller-Hansen S, Mathey DG, Bliefeld W, Voigt K. Isoelectric Focusing of Creatine Kinase MM Isoforms and its Application for Diagnosis of Acute Myocardial Infarction. Clinical Biochemistry. 1989;22:125-130
- 104 Murphy RA. Mechanics of Vascular Smooth Muscle. Hand Book of Physiology Section 2; The Cardiovascular System, Vascular Smooth Muscle. 1980;Vol. II:325-351. American Physiology Society.
- 105 Mutru O, Laakso M, Isomaki H, Koota K. Cardiovascular Mortality in Patients with Rheumatoid Arthritis. Cardiology. 1989;76:71-77.
- 106 Nayler RA, Sparrow MP. Inhibition of Cycling and Nonsycline Crossbridges in Chemically Skinned Smooth Muscle by Vanadate. Regulation and Contraction of Smooth Muscle. 1987;475-476.
- 107 Nihei T, Noda L, Morales MF. Kinetic Properties and Equilibrium Constant of the Adenosine Triphosphate-Creatine Transphosphorylase-catalyzed Reaction. Journal of Biological Chemistry. 1961;235,12:3203-3209.
- 108 Noda L, Kuby SA, Lardy HA. Adenosinetriphosphate-Creatine Transphosphorylase. Journal of Biological Chemistry. 1953;83-95.
- 109 Noda L, Nihei T, Morales MF. The Enzymatic Activity and Inhibition of Adenosine 5'-Triphosphate-Creatine Transphosphorylase. Journal of Biological Chemistry. 1960;235,10:2830-2834.
- 110 Norwood WI, Ingwall JS, Norwood CR, Fossel ET. Developmental Changes of Creatine Kinase Metabolism in Rat Brain. Am. J. Physiol. 244 (Cell Physiol. 13.) 1983;C205-C210.

- 111 Obara K, Ito Y, Yabu H. Ca^{2+} Release in Skinned Single Smooth Muscle Cells Isolated From Guinea-Pig Taenia Caeci. Compl. Biochem. Physiol. 1987;86A,4:703-708.
- 112 Ogunro EA, Peters TJ, Wells G, Hearse DJ. Sub-mitochondrial and Sub-microsomal Distribution of Creatine Kinase in Guinea Pig Myocardium. Cardiovascular Research. 1979;13:562-567.
- 113 Olson EN, Lathrop BK, Glaser L. Purification and Cell-Free Translation of a Unique High Molecular Weight Form of the Brain Isozyme of Creatine Phosphokinase from Mouse. Biochemical and Biophysical Research Communications. 1982;108,2:715-723.
- 114 Paul RJ. Chemical Energetics of Vascular Smooth Muscle. Handbook of Physiology Section 2: The Cardiovascular System. Vascular Smooth Muscle. 1980;201-234.
- 115 Paul RJ. Functional Compartmentalization of Oxidative and Glycolytic Metabolism in Vascular Smooth Muscle. Am. J. Physiol. 244 (Cell Physiol. 13). 1983;C399-C409.
- 116 Paul RJ, Krisanda JM, Hellstrand P. Relations Among Oxygen Consumption, Phosphagen and Contractility in Vascular Smooth Muscle. Smooth Muscle Contractility. 1984;245-257. Marcell-Dekker Inc.
- 117 Perriard JC, Achtnich U, Cerny L, Eppenberger HM, Grove BK, Hossle HP, Schafer B. Expression of M-Band Proteins During Myogenesis. Molecular Biology of Muscle Development. 1986;693-707.
- 118 Perry SB, McAuliffe J, Balschi JA, Hickey PR, Ingwall JS. Velocity of the Creatine Kinase Reaction in the Neonatal Rabbit Heart: Role of Mitochondrial Creatine Kinase. Biochemistry. 1988;27:2165-2172.
- 119 Pfitzer G, Merkel L, Ruegg JC, Hofmann F. Cyclic GMP-Dependent Protein Kinase Relaxes Skinned Fibers from Guinea Pig Taenia Coli but Not From Chicken Gizzard. Pflugers Arch. 1986;407:87-91.
- 120 Portman MA, James S, Heineman FW, Bajaban RS. Simultaneous Monitoring of Coronary Blood Flow and ^{31}P NMR Detected Myocardial Metabolites. Magnetic Resonance in Medicine. 1988;7:243-247.
- 121 Prior TW, Blasco PA, Dove JL, Leshner RT, Gruemer HD. Use of DNA Probes in Detecting Carriers of Duchenne Muscular Dystrophy: Selected Case Studies. Clin. Chem. 1989;35,4:679-683.
- 122 Rees D, Smith MB, Harley J, Radda GK. In Vivo Functioning of

- Creatine Phosphokinase in Human Forearm Muscle, Studied by ^{31}P NMR Saturation Transfer. Magnetic Resonance in Medicine. 1989;9:39-52.
- 123 Reiss NA, Kaye AM. Identification of the Major Component of the Estrogen-Induced Protein of Rat Uterus as the BB Isozyme of Creatine Kinase. Journal of Biological Chemistry. 1981;256,11:5741-5749.
- 124 Roberts R, Gowda KS, Ludbrook PA, Sobel BE. Specificity of Elevated Serum MB Creatine Phosphokinase Activity in the Diagnosis of Acute Myocardial Infarction. American Journal of Cardiology. 1975;36:433-437.
- 125 Roberts R, Henry PD, Witteveen SAGJ, Sobel BE. Quantification of Serum Creatine Phosphokinase Isoenzyme Activity. American Journal of Radiology. 1974;33:650-654.
- 126 Ruegg JC, Sparrow MP, Mrwa U, Schneider M, Pfitzer G. Calcium and Calmodulin Dependent Regulatory Mechanisms in Chemically Skinned Smooth Muscle. Smooth Muscle Contraction. 1984;361.
- 127 Saks VA. Creatine Kinase Isozymes and the Control of Cardiac Contraction. Heart Creatine Kinase. 1980;Chapter 10. Williams & Wilkins.
- 128 Saks VA, Khuchua ZA, Kuznetsov AV. Specific Inhibition of ATP-ADP Translocase in Cardiac Mitoplasts by Antibodies Against Mitochondrial Creatine Kinase. Biochimica et Biophysica Acta. 1987;891:138-144.
- 129 Saks VA, Kuznetsov AV, Kupriyanov VV, Miceli MV, Jacobus WE. Creatine Kinase of Rat Heart Mitochondria. Journal of Biological Chemistry. 1985;260,12:7757-7764.
- 130 Saks VA, Lipina NV, Sharov VG, Smirnov VN, Chazov E, Grosse R. The Localization of the MM Isozyme of Creatine Phosphokinase on the Surface Membrane of Myocardial Cells and Its Functional Coupling to Ouabain-Inhibited (Na^+, K^+)-ATPase. Biochimica et Biophysica Acta. 1977;465:550-558.
- 131 Saks VA, Rosenshtraukh LV, Smirnov VN, Chazov EI. Role of Creatine Phosphokinase in Cellular Function and Metabolism. Can. J. Physiol. Pharmacol. 1978;56:691-706.
- 132 Saks VA, Ventura-Clapier R, Huchua ZA, Preobrazhensky AN, Emelin IV. Creatine Kinase in Regulation of Heart Function and Metabolism. Biochimica et Biophysica Acta. 1984;803:254-264.
- 133 Scholte HR. On the Triple Localization of Creatine Kinase in Heart and Skeletal Muscle Cells of the Rat: Evidence for the Existence of Myofibrillar and Mitochondrial Isoenzymes. Biochimica et Biophysica Acta. 1973;305:413-427.

- 134 Schwartz JG, Brown RW, McMahan CA, Gage CL, Herber SA. Clinical and Analytical Evaluation of Different Methods for Measurement of Creatine Kinase Isoenzyme MB. Clinical Chemistry. 1989;35,1:130-134.
- 135 Scott DP, Davidheiser S, Coburn RF. Effects of Elevation of Phosphocreatine on Force and Metabolism in Rabbit Aorta. Am. J. Physiol. 253 (Heart Circ. Physiol. 22). 1987;H461-H465.
- 136 Segel IH. Enzyme Kinetics. 1975;18-34. John Wiley & Sons, Inc.
- 137 Semenovskiy ML, Shumakov VI, Sharov VG, Mogilevskiy GM, Asmolovskiy AV, Makhotina LA, Saks VA. Protection of Ischemic Myocardium by Exogenous Phosphocreatine. Journal of Thoracic and Cardiovascular Surgery. 1987;94,5:762-769.
- 138 Seraydarian MW. The Correlation of Creatine Phosphate with Muscle Function. Heart Creatine Kinase. 1980;Chapter 8. Williams & Wilkins.
- 139 Seraydarian MW, Artaza L, Abbott BC. The Effect of Adenosine on Cardiac Cells in Culture. Journal of Molecular and Cellular Cardiology. 1972;4:477-484.
- 140 Seraydarian MW, Harary I, Sato E. In Vitro Studies of Beating-Heart Cells in Culture XI. The ATP Level and Contractions of the Heart Cells. Biochimica et Biophysica Acta. 1968;162:414-423.
- 141 Seraydarian MW, Sato E, Savageau M, Harary I. In Vitro Studies of Beating Heart Cells in Culture XII. The Utilization of ATP and Phosphocreatine in Oligomycin and 2-Deoxyglucose Inhibited Cells. Biochimica et Biophysica Acta. 1969;180:264-270.
- 142 Seraydarian MW, Yamada T. Isozymes of Creatine Kinase in Mammalian Myocardial Cell Culture. Myocardial and Skeletal Muscle Bioenergetics. 1986;194:41. Plenum Press.
- 143 Sharov VG, Saks VA, Kupriyanov VV, Lakomkin VL, Kapelko VI, Steinschneider AY, Javadov SA. Protection of Ischemic Myocardium by Exogenous Phosphocreatine I. Morphologic and Phosphorus 31-Nuclear Magnetic Resonance Studies. Journal of Thoracic and Cardiovascular Surgery. 1987;94,5:749-761.
- 144 Shoubridge EA, Briggs RW, Radda GK. ³¹P NMR Saturation Transfer Measurements of the Steady State Rates of Creatine Kinase and ATP Synthetase in the Rat Brain. FEBS Letters. 1982;140,2:288-292.
- 145 Smith EL, Hill RL, Lehman IR, Lefkowitz RJ, Handler P, White A. Principles of Biochemistry: Mammalian Biochemistry.

1983;Seventh Edition:198-202. McGraw-Hill Book Co.

- 146 Spencer RGS, Balschi JA, Leigh JS, Ingwall JS. ATP Synthesis and Degradation Rates in the Perfused Rat Heart. Bioophysical Journal. 1988;54:921-929.
- 147 Suelter CH. A Practical Guide to Enzymology. 1985. John Wiley & Sons.
- 148 Svendsen O, Rasmussen F, Nielsen P, Steiness E. The Loss of Creatine Phosphokinase (CK) from Intramuscular Injection Sites in Rabbits. A Predictive Tool for Local Toxicity. Acta Pharmacol. et Toxicol. 1979;44:324-328.
- 149 Takasawa T, Onodera M, Shiokawa H. Properties of Three Creatine Kinases MM From Porcine Skeletal Muscle. J. Biochem. 1983;93:389-395.
- 150 Takasawa T, Shiokawa H. Dimer Structure of Three Creatine Kinases MM From Porcine Skeletal Muscle. J. Biochem. 1983;93:383-388.
- 151 Takasawa T, Shiokawa H. Isolation of Three Creatine Kinases MM From Porcine Skeletal Muscle. J. Biochem. 1983;93:375-382.
- 152 Tombes RM, Shapiro BM. Enzyme Termini of a Phosphocreatine Shuttle. Journal of Biological Chemistry. 1987;262,33:16011-16019.
- 153 Trainer TD, Gruenig D. A Rapid Method for the Analysis of Creatine Phosphokinase Isoenzymes. Clinica Chimica Acta. 1968;21:151-154.
- 154 Tsung SH. Creatine Kinase Isoenzyme Patterns in Human Tissue Obtained at Surgery. Clin. Chem. 1976;22,2:173-175.
- 155 Ugurbil K. Magnetization Transfer Measurement of Creatine Kinase and ATPase Rates in Intact Hearts. Circulation. 1985;72,IV:94-96.
- 156 Ugurbil K. Magnetization-Transfer Measurements of Individual Rate Constants in the Presence of Multiple Reactions. Journal of Magnetic Resonance. 1985;64:207-219.
- 157 Ugurbil K, Petain M, Maida R, Michurski S, From AHL. Measurement of an Individual Rate Constant in the Presence of Multiple Exchanges: Application to Myocardial Creatine Kinase Reaction. Biochemistry. 1986;25:100-107.
- 158 Vaidya H, Dietzler DN, Leykam JF, Ladenson JH. Purification of Five Creatine Kinase-MM Variants From Human Heart and Skeletal Muscle. Biochemica et Biophysica Acta. 1984;790:230-237.

- 159 Veksler VI, Kapelko VI. Creatine Kinase in Regulation of Heart Function and Metabolism. Biochimica et Biophysica Acta. 1984;803:265-270.
- 160 Veksler VI, Ventura-Clapier R, Lechene P, Vassort G. Functional State of Myofibrils, Mitochondria and Bound Creatine Kinase in Skinned Ventricular Fibers of Cardiomyopathic Hamsters. J. Mol. Cell Cardiol. 1988;20:329-342.
- 161 Ventura-Clapier R. Localization and Function of M-Line-Bound Creatine Kinase. Cell and Muscle Motility. 1985;6:239.
- 162 Ventura-Clapier R, Mekhfi H, Vassort G. Role of Creatine Kinase in Force Development in Chemically Skinned Rat Cardiac Muscle. J. Gen. Physiol. 1987;89:815-837.
- 163 Ventura-Clapier R, Saks VA, Vassort G, Lauer C, Elizarova GV. Reversible MM-Creatine Kinase Binding to Cardiac Myofibrils. Am. J. Physiol. 253 (Cell Physiol. 22). 1987;C444-C455.
- 164 Ventura-Clapier R, Vassort G. Rigor Tension During Metabolic and Ionic Rises in Resting Tension in Rat Heart. Journal of Molecular and Cellular Cardiology. 1981;13:551-561.
- 165 Ventura-Clapier R, Veksler VK, Elizarova GV, Mekhfi H, Levitskaya EL, Saks VA. Contractile Properties and Creatine Kinase Activity of Myofilaments Following Ischemia and Reperfusion of the Rat Heart. Biochemical Medicine and Metabolic Biology. 1987;38:300-310.
- 166 Vladutiu AO, Shachner A, Schaefer PA, Schimert G, Lajos TZ, Lee AB, Siegal JH. Detection of Creatin Kinase BB Isoenzyme in Sera of Patients Undergoing Aortocoronary Bypass Surgery. Clinica Chimica Acta. 1977;75:467-473
- 167 Wagner J, Pfitzer G, Ruegg JC. Calcium/Calmodulin Activation of Gizzard Skinned Fibers at Low Levels of Myosin Phosphorylation. Regulation and Contraction of Smooth Muscle. 1987;427-436.
- 168 Wagner J, Ruegg JC. Skinned Smooth Muscle: Calcium-Calmodulin Activation Independent of Myosin Phosphorylation. Pflugers Arch. 1986;407:569-571.
- 169 Walker JB. Creatine: Biosynthesis, Regulation, and Function. Advances in Enzymology. 1979;50:177-243. John Wiley & Sons.
- 170 Wallimann T, Eppenberger HM. Localization and Function of M-Line-Bound Creatine Kinase. Cell and Muscle Motility. 1985;6:239-285.
- 171 Wallimann T, Kuhn HJ, Pelloni G, Turner DC, Eppenberger HM. Localization of Creatine Kinase Isoenzymes in Myofibrils, II.

- Journal of Cell Biology. 1977;75:318-325.**
- 172 Wallimann T, Schnyder T, Schlegel J, Quest A. Ultrastructural Compartmentation, Regulation, Structure and Function of Creatine Kinase (CK) Isoenzymes in Tissues of Sudden High Energy Demand. Abstract for the **III International Congress on Muscle Energetics.** 1988
- 173 Wallimann T, Turner DC, Eppenberger HM. Localization of Creatine Kinase Isoenzymes in Myofibrils, I. **Journal of Cell Biology.** 1977;75:297-317.
- 174 Wang FL, Cushman DW. A Simplified Method for Purification of the Creatine Kinase Isoenzyme of Human Brain (BB). **Clinica Chimica Acta.** 1980;106:339-345.
- 175 Watts DC. Creatine Kinase (Adenosine 5-Triphosphate-Creatine Phosphotransferase). **The Enzymes.** 1975;Third Edition,8:383-455. Academic Press, NY.
- 176 Watts DC, Kumudavalli I. Further Evidence for the Role of the Essential Thiol Groups in Adenosine Triphosphate-Creatine Phosphotransferase from a Comparison of the Human and Rabbit Enzymes. **Biochemistry Journal.** 1970;118,2:22P-23P.
- 177 Weinberger I, Fuchs J, Rotenberg Z, Davidson E, Haral D, Agmon J. Changes in CK Activity in the Course of Acute MI. **Clin. Chem.** 1989;35,3:414-416.
- 178 Wendland MF, White RD, Derugin N, Finkbeiner WE, McNamara MT, Moseley ME, Lipton MJ, Higgins CB. Characterization of High-Energy Phosphate Compounds During Reperfusion of the Irreversibly Injured Myocardium Using ³¹P MRS. **Magnetic Resonance in Medicine.** 1988;7:172-183.
- 178a Wuytack, F. Casteels R., Paul R.J. Comparison of Endogenous and Exogenous Sources of ATP in Supporting Ca²⁺ Uptake in Isolated Smooth Muscle Plasma Membrane Vesicles. **Biophys. J.** 1988;53:347.
- 179 Yoshizaki K, Radda GK, Inubushi T, Chance B. ¹H- and ³¹P-NMR Studies on Smooth Muscle of Bullfrog Stomach. **Biochimica et Biophysics Acta.** 1987;928:36-44.
- 180 Zsigmond EK, Starkweather WH, Duboff GS, Flynn KA. Abnormal Creatine-Phosphokinase Isoenzyme Pattern in Families with Malignant Hyperpyrexia. **Anesthesia and Analgesia.** 1972;51,5:827-840.

MICHIGAN STATE UNIV. LIBRARIES



31293005923721